

Effect of Coexisting Minerals  
on Graphitization of Carbon  
under Pressure

Shin-ichi Hirano

Faculty of Engineering  
Nagoya University

1970

Thesis

Presented by Shin-ichi Hirano  
to  
Faculty of Engineering  
Nagoya University  
for  
the Degree of Doctor of Engineering

January, 1970

## Preface

The present thesis submitted to the Faculty of Engineering, Nagoya University, is the record of the research works which have been carried out at Nagoya University under the guidance of Professor Tokiti Noda for the period of 1965-1967 and Professor Hajime Saito for the period of 1967-1970.

The studies on the effect of coexisting minerals on graphitization of carbon under pressure are involved in the present thesis. The possible mechanisms for the accelerating effect of coexisting minerals and some considerations on the application to industrial techniques are discussed under taking into account of the geological occurrence of natural graphite.

The author is greatly indebted to Professor Hajime Saito (Nagoya University) and Dr. Tokiti Noda (President of Mie University) for their valuable discussions and extends his gratitude to all members of laboratory which he has been belonging.

The author also wishes to thank his parents for their continual encouragements.

Shin-ichi Hirano

Department of Applied Chemistry  
Faculty of Engineering  
Nagoya University

## Table of Contents

1. Introduction	1
a. General aspects on carbon	1
b. Structure of graphite and graphitization of carbon	1
c. View on geological occurrence of natural graphite	4
d. Survey of earlier investigations on catalytic graphitization and on graphitization under pressure	7
e. Purpose of the present study	11
2. Experimental—sample, heat treatment under pressure and X-ray diffraction	12
a. Carbon sample used	12
b. High pressure apparatus and arrangements of pressure cell	12
c. Calibration of pressure	14
(1) Principle of the method	14
(2) Experimental	15
(3) Results	18
(a) Calibration of pressure in the present high pressure apparatus	18
(b) Measurement of flow of pyrophyllite in the pressure cell	20
(4) Discussion	20
d. Measurement of temperature and temperature gradient in pressure cell	24
e. Procedure for heat treatments of carbon under pressure	26
f. Method for determination of a measure of graphitization	27
(1) X-ray diffraction method	27
(2) Determination of a degree of graphitization	28
3. Accelerating effect of calcium compounds on graphitization of carbon under pressure	32
a. Heat treatments of carbon under pressure in the presence of limestone	32
(1) Introduction	32
(2) Experimental and results	32

b.	Heat treatments of carbon under pressure in the presence of calcium carbonate	36
(1)	Introduction	36
(2)	Experimental	39
(3)	Results	40
(a)	Observation of heat-treated specimens	40
(b)	Changes of profile of (002) diffraction line	42
(c)	Electron microscopic observation	46
c.	Accelerating effect of calcium hydroxide	51
(1)	Introduction	51
(2)	Experimental and results	51
d.	Discussion and summary	54
4.	Effect of reactivity of coexisting calcium oxide on the graphitization of carbon under pressure	58
a.	Accelerating effect of calcium oxide	58
(1)	Introduction	58
(2)	Experimental	59
(3)	Results	60
b.	Distribution of calcium and graphitic component in heat-treated specimens	63
(1)	Introduction	63
(2)	Experimental and results	66
c.	Heat treatments of calcium carbide under pressure	70
(1)	Introduction	70
(2)	Experimental and results	74
d.	Discussion	75
5.	Accelerating effect of some metal oxides on graphitization of carbon under pressure	80
a.	Introduction	80
b.	Experimental and results	80
(1)	Heat treatments of carbon under pressure in the presence of sodium carbonate	80
(2)	Heat treatments of carbon under pressure in the presence of alumina and silica	81
(3)	Heat treatments of carbon in the presence of magnesia	83
c.	Discussion and summary	87

6.	Accelerating effect of water vapor on graphitization of carbon under pressure in the presence of coexisting minerals	93
a.	Introduction	93
b.	Experimental and results	93
	(1) Heat treatments of carbon in the presence of calcium fluoride	93
	(2) Heat treatments of carbon under pressure in the presence of magnesium fluoride	99
	(3) Heat treatments of carbon under pressure in the presence of calcium carbonate absorbed water	101
c.	Discussion	101
7.	Effect of nitrogen gas on graphitization of carbon in the presence of calcium carbonate	107
a.	Introduction	107
b.	Experimental	107
	(1) Heat treatments of carbon in the presence of calcium carbonate	107
	(2) Heat treatment of calcium carbide	108
c.	Results	111
	(1) Heat treatments of carbon in the presence of calcium carbonate under the flows of nitrogen and argon	111
	(2) Heat treatments of calcium carbide under the flows of nitrogen and argon	115
d.	Discussion	115
8.	Mechanism of accelerating effect of coexisting minerals on graphitization of carbon under pressure	120
a.	Possible processes of graphitization of carbon under pressure in the presence of coexisting minerals	120
b.	Additional effect of surrounding atmosphere on formation of graphitic component	125
c.	Effect of pressure on graphitization of carbon in the presence of coexisting minerals	129
9.	Summary	132

## Tables

Table 1. Properties of calcium oxide used	59
Table 2. Measurement of carbon isotope	126

## Illustrations

Fig. 1. Hexagonal structure of graphite	2
Fig. 2. Rhombohedral structure of graphite	2
Fig. 3. Schema of simple piston-sylinder type high pressure apparatus	13
Fig. 4. Arrangements of pressure cell	13
Fig. 5. Arrangement of pressure cell for calibration of pressure	16
Fig. 6. High frequency circuit diagram for detection of inductance change	17
Fig. 7. Capacity changes induced by volume change of $\text{KNO}_3$ and AgI with applied load	19
Fig. 8. Relation between applied load and pressure	19
Fig. 9. Capacity change with load for arrangement used calcined pyrophyllite disk	21
Fig.10. Capacity changes with time after compression of $\text{KNO}_3$ to various pressures of 1, 2 or 3kbar	22
Fig.11. Capacity changes with time after compressing to 3kbar for three kinds of pressure cells	22
Fig.12. Relation between temperature and input power	25
Fig.13. Schema of different parts in heat-treated carbon specimen	25
Fig.14. Schema of separation of composite profile	29
Fig.15. Growth of grain of recrystallized limestone in contact with carbon sample heat-treated at $1120^\circ\text{C}$ for 60min under 3.2kbar (under polarized light)	34
Fig.16. Change of profile of (002) diffraction line of carbon specimen heat-treated in the presence of limestone with HTT	35
Fig.17. Variation of $c_0$ -spacing of two components of $G_M$ and $A_M$ with HTT	37

Fig.18.	Change of content of the component $G_M$ with HTT	37
Fig.19.	Representative change of (002) diffraction line with HTT without any minerals	38
Fig.20.	Polarization micrograph of thin section of calcium carbonate disk heat-treated at 1360°C for 60min under 3.2kbar	41
Fig.21.	Change of profile of (002) diffraction line with HTT	43
Fig.22.	Change of profile of (002) diffraction line with residence time at the constant temperature of 1280°C	43
Fig.23.	Change of profile of (002) diffraction line with HTT without any coexisting minerals	44
Fig.24.	Change of profile of (002) diffraction line with HTT under flow of nitrogen	44
Fig.25.	Variation of $c_0$ -spacing with HTT	45
Fig.26.	Variation of crystallite size $L_c$ with HTT	45
Fig.27.	Change of content of component $G_M$ with HTT	47
Fig.28.	Relation between thickness of recrystallized part of disk of calcium carbonate and content of component $G_M$	47
Fig.29.	Particle showing diffraction pattern of six-fold symmetry of graphite single crystal overlapping on reflection ring	49
Fig.30.	Bright-field micrographs and selected area diffraction patterns taken on carbon specimen heat-treated at 1070°C for 60min with calcium carbonate under 3.2kbar	50
	(a) particle having turbostratic structure	
	(b) particle having graphitic structure	
Fig.31.	Change of observed profile of (002) diffraction line with heat treatment	53
Fig.32.	Bright-field micrograph and selected area diffraction pattern of graphitic particle in carbon specimen heat-treated at 600°C for 60min under 3.2kbar	55



Fig.33.	Bright-field micrograph and selected area diffraction pattern of turbostratic particle in carbon specimen heat-treated at 600°C for 60min under 3.2kbar	55
Fig.34.	Change of profile of (002) diffraction line with HTT	61
	(a) in the presence of CaO-9	
	(b) in the presence of CaO-10	
	(c) in the presence of CaO-15	
Fig.35.	Variation of content of graphitic component $G_M$ with HTT	62
Fig.36.	(a) Change of $c_0$ -spacing with HTT	
	(b) Change of crystallite size $L_c$ with HTT	64
Fig.37.	Bright-field micrograph and selected area diffraction pattern of graphitic particle in carbon specimen heat-treated at 1100°C with CaO-9	65
Fig.38.	Bright-field micrograph and selected area diffraction pattern of turbostratic particle in carbon specimen heat-treated at 1100°C with CaO-9	65
Fig.39.	Direction of scanning of electron beam on polished section of caked carbon specimen	67
Fig.40.	Schema of part from which sample for X-ray diffraction analysis was taken	67
Fig.41.	Profiles of (002) diffraction line for different parts of carbon specimen	68
	(a) heat-treated under 3.2kbar at 1280°C in the presence of $CaCO_3$	
	(b) heat-treated under 3.2kbar at 1300°C in the presence of CaO-9	
Fig.42.	Distribution of calcium obtained with electron beam width of 100 $\mu$ on carbon specimen heat-treated at 1360°C under 3.2kbar in the presence of $CaCO_3$	69
Fig.43.	Distribution of calcium obtained with electron beam width of 100 $\mu$ on carbon specimen heat-treated at 1100°C under 3.2kbar in the presence of CaO-9	69
Fig.44.	Distribution of calcium obtained with electron beam width of 10 $\mu$ on carbon specimen heat-treated at 1090°C and 1360°C under 3.2kbar in the presence of $CaCO_3$	

Fig.45.	Distribution of calcium obtained with electron beam width of $10\mu$ on carbon specimen heat-treated at 1100, 1400 and 1500°C under 3.2kbar in the presence of CaO-9	71
Fig.46.	X-ray fluorescence photographs for carbon and calcium in the central area of carbon specimen heat-treated at 1360°C under 3.2kbar in the presence of CaCO <sub>3</sub>	72
Fig.47.	X-ray fluorescence photographs for carbon and calcium in the central area of carbon specimen heat-treated at 1100°C under 3.2kbar in the presence of CaO-9	73
Fig.48.	Arrangement of pressure cell for heat treatment of calcium carbide under 3.2kbar	76
Fig.49.	Dependence on HTT of content of graphitic component formed by decomposition of calcium carbide under 3.2kbar	76
Fig.50.	Bright-field micrograph and selected area diffraction pattern of graphitic component formed by decomposition of calcium carbide at 1200°C	77
Fig.51.	Bright-field micrograph and selected area diffraction pattern of graphitic particle in carbon specimen heat-treated at 500°C for 60min under 3.2kbar in the presence of sodium carbonate	82
	(a) Bright-field micrograph	
	(b) Selected area diffraction pattern	
Fig.52.	Change of content of graphitic component $G_M$ with HTT in the presence of alumina and magnesia	84
Fig.53.	Bright-field micrograph and selected area electron diffraction pattern on carbon specimen heat-treated at 1200°C with alumina	84
Fig.54.	Arrangement used for heat treatment of carbon under flow of nitrogen in the presence of magnesia	86
Fig.55.	Weight loss of carbon specimen by heat treatment under flow of nitrogen in the presence of magnesia	86
Fig.56.	(a) Change of $c_0$ -spacing with heat treatment (b) Change of crystallite size $L_c$ with heat treatment	88

Fig.57.	Bright-field micrograph and selected area diffraction pattern of graphitic particle in carbon specimen heat-treated at 1400°C for 60min under 3.2kbar in the presence of magnesia	89
Fig.58.	Arrangements of pressure cell for three kinds of heat treatment	95
Fig.59.	Photograph of disk of calcium fluoride in contact with carbon specimen heat-treated at 1300°C for 60min under 3.2kbar	97
Fig.60.	Change of profile of (002) diffraction line with HTT in heat treatment of carbon under 3.2kbar for 60min with cell arrangement A	97
Fig.61.	Bright-field micrograph and selected area electron diffraction pattern of graphitic particle in carbon specimen heat-treated at 1300°C for 60min under 3.2kbar with cell arrangement A in the presence of calcium fluoride	98
Fig.62.	Bright-field micrograph and selected area electron diffraction pattern of particle in carbon specimen heat-treated at 1500°C for 60min under 3.2kbar with cell arrangement B in the presence of calcium fluoride	98
Fig.63.	Changes of $c_0$ -spacing with HTT	100
Fig.64.	Changes of content of graphitic component $G_M$ with HTT	100
Fig.65.	Bright-field micrograph and selected area diffraction pattern of graphitic particle in carbon specimen heat-treated at 1400°C for 60min under 3.2kbar in the presence of magnesium fluoride	102
Fig.66.	Change of content of graphitic component $G_M$ with HTT	103
Fig.67.	Isobaric equilibrium diagram for join $CaCO_3-H_2O$ at 100bar	106
Fig.68.	Cell arrangement for heat treatment under flow of nitrogen or argon	109
Fig.69.	Chemical analysis for measurement of content of graphitic component	110

Fig.70.	Electron micrograph and selected area diffraction pattern of particle having singular discoidal appearance in carbon specimen heat-treated at 1730°C for 60min under flow of nitrogen in the presence of calcium carbonate	112
Fig.71.	Bright-field micrographs and selected area electron diffraction patterns of graphitic particle in carbon specimen heat-treated (a) at 1850°C under flow of nitrogen (b) at 1930°C under flow of argon	113
Fig.72.	Change of content of graphitic component $G_M$ with HTT	114
Fig.73.	Change of content of graphitic component produced from calcium carbide with HTT	116
Fig.74.	Bright-field micrographs and selected area electron diffraction patterns of graphitic particles produced from calcium carbide heat-treated at 1850°C (a) under flow of nitrogen (b) under flow of argon	117
Fig.75.	Free energy diagram of amorphous carbon and graphite	124

## 1. Introduction.

### a. General Aspects on Carbon.

The carbon element, C (atomic number 6) occurs as a diamond and graphite and in a variety of so-called amorphous forms. Owing to the structural variety of carbon, the electrical conductivity covers a wide range between  $10^5$ - $10^6 \Omega$ -cm (near semiconductor) and  $10^{-4} \Omega$ -cm (comparable to metal), and the thermal conductivity also extends from the value of metals to that of insulator. Chemically the resistivity to corrosion is remarkable except under oxidizing conditions. The mechanical properties are also excellent particularly at high temperature above  $1500^\circ\text{C}$  because of low vapor pressure at high temperature and high melting point (about  $3700^\circ\text{C}$  under about 100 atm).

In the past 20 years, major improvements have been in the properties of carbons which are used in their 'old' applications, such as electrodes for electric arc furnace, and have resulted in developments of 'new' applications, such as pyrolytic carbon, synthetic diamonds, carbon fibers and so on. Due to noted physical and chemical properties, "carbon materials" recently appear before the footlights in "the age of materials". Carbon, therefore, is truly worthy of calling as an "old but new material".

### b. Structure of Graphite and Graphitization of Carbon.

The crystal structure of graphite is shown in Fig. 1. In the hexagonal net of carbon atom (usually called "layer plane"), carbon atoms are bound to three neighbours by strong covalent bond of  $sp^2$  hybrid orbital. One of four electrons in the outermost shell,  $\pi$ -electron, is equally resonated in the layer plane. Therefore, the order of the carbon-carbon bond in the plane is  $4/3$  and its length is  $1.415\text{\AA}$  which is a little longer than that in benzene. The interaction force between layer planes is so weak that it has been said van der Waals force. The ABAB... sequence of parallel stacking of layer planes is the most common one in natural graphite. This crystal belongs to the hexagonal system and

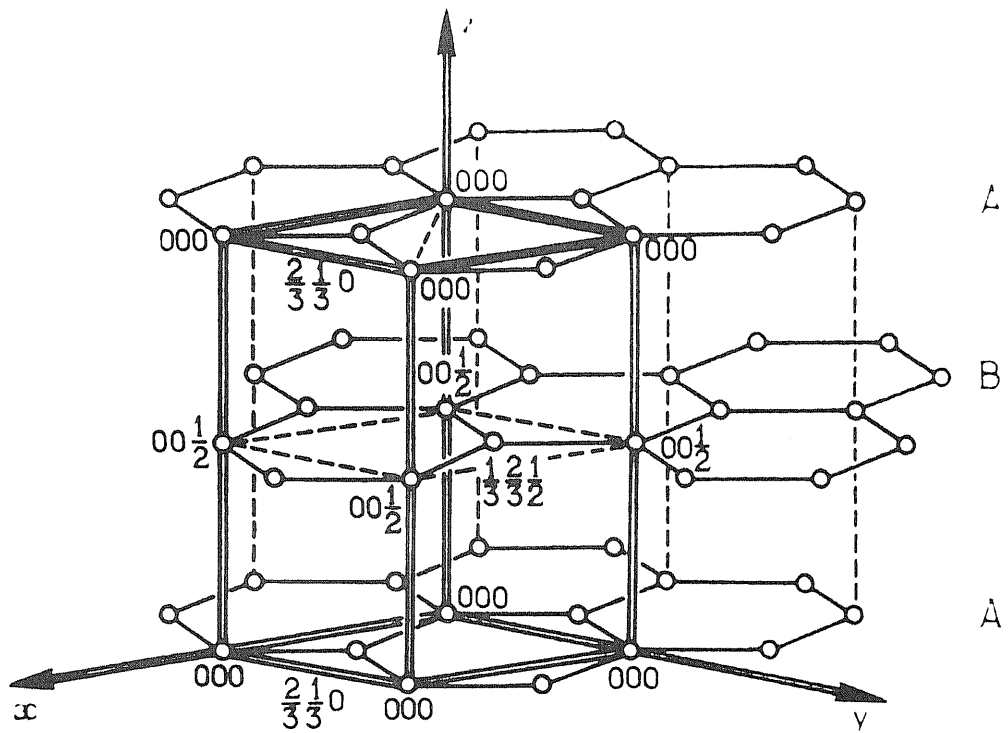


Fig. 1 Hexagonal structure of graphite

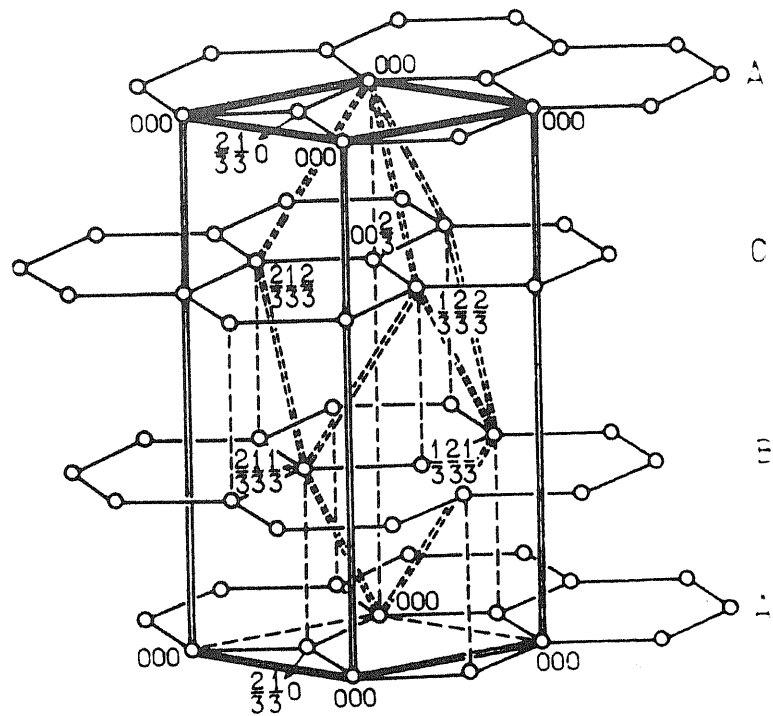


Fig. 2 Rhombohedral structure of graphite

its unit cell is shown in Fig. 1 by dotted line. The  $a_0$ -spacing of the cell is  $2.456\text{\AA}$  and the  $c_0$ -spacing is  $6.708\text{\AA}$  which is twice of the spacing of layer planes stacked parallel,  $3.3538\text{\AA}$ . A small amount of another sequence of layer stacking, that is ABCABC.... sequence, has also been found in natural graphite. This is the rhombohedral modification of graphite of which unit cell is shown in Fig. 2. In carbon, graphite-like layer planes stack only parallel and rotate about the normal of the layer plane in random. We call such a structure as turbostratic one.<sup>1)</sup>

According to Houska and Warren<sup>2)</sup>, prior to the beginning of graphitization, the layers of a parallel layer group have random orientations about the normal of layer planes and a spacing of  $3.44\text{\AA}$ . Presumably, there is no incentive for neighbouring layers to take on the ordered relation until the layer diameter  $L_a$  exceeds a value of the order of  $100\text{\AA}$ <sup>3)</sup>. In the stages of graphitization, some of the pairs of neighbouring layers assume the graphite relation<sup>2)3)</sup>, and the spacing decreases to approximately that of graphite  $3.354\text{\AA}$ .

By suitable heat treatments, carbons having the turbostratic structure show a gradual change in structure towards the three-dimensional ordering of crystalline graphite and the growth of crystallite occurs. The process of such a transformation from the turbostratic structure to the graphitic one seems to be roughly divided in two stages<sup>4)~6)</sup>. In the first stage, any evidence of the existence of the three-dimensional ordering of layer planes in the carbon cannot be detected, while the small decrease in the mean interlayer spacing  $\bar{c}_0/2$  and the increase in layer plane size occur. This stage is called as pregraphitization. The second stage is characterized by the appearance of the three-dimensional ordering of layer planes. The graphitization in the second stage can be followed phenomenally by the modulation of the (hk) diffraction bands of X-ray and electron and by the decrease in interlayer spacing.

Carbons prepared by the carbonization of organic substances differ strongly in the degree of graphitization even when the carbons are heat-treated up to  $3000^\circ\text{C}$ , in other words,

differ in graphitizability. Some carbons show, on heating to temperatures up to 3000°C, a continuous and homogeneous evolution from the turbostratic to the graphitic structure. These are referred to graphitizing carbon<sup>7)</sup> or soft carbons<sup>8)</sup>. Other carbons show no trace of homogeneous development of the graphitic structure even after heating to 3000°C and are referred to nongraphitizing carbons<sup>7)</sup> or hard carbons<sup>8)</sup>.

### c. View on Geological Occurrence of Natural Graphite.

Graphite is one of the chief representatives of elementary substances among rock-forming minerals. It is widely distributed geographically in the world. Geologically, it is mostly limited to areas where older rocks, such as Precambrian and lower Paleozoic, are exposed. This is particularly true for disseminated flaky graphite and for vein graphite. Some of the so-called amorphous graphites occur with younger rocks.

The vein graphite deposits are only believed to have been formed by reduction, at high temperatures and pressures, of carbon dioxide liberated during the assimilation of limestone and dolomite by charnockitic and related igneous magmas. Calcite, quartz, pyrite and augite are the minerals most commonly associated with graphite; others include scapolite, wollastonite, forsterite, tremolite and phlogopite.

Disseminated flaky graphite is associated with older rocks subjected to a high degree of regional metamorphism. Occurrence is therefore mostly limited to regions in which such rocks as marble, gneisses, schists, slate and quartzites exist. The genesis theory of flaky graphite is not so well known because the original form of the mother rock is conjectural, the original composition and structure having been obliterated by shearing stresses and high temperatures during metamorphosis.

By considering phenomena of occurrences of graphite deposits, it seems to be able to classify these geneses into the following types of mineralogical background<sup>9)</sup>: (1) This first type of mineralogy is that expected in the geologically



older rocks such as Precambrian and lower Paleozoic, which have been subjected to diastrophic forces, perhaps even several periods of them, resulting in the production of recrystallized rock such as marbles, gneisses, shists, quartzites and slates, together with the structure and mineral associations, and alterations expected in them such as biotite and muscovite. The Madagascar deposits are outstanding examples of such mineralogic association with graphite in a large scale. (2) The second type of mineralogic background is the so-called pneumatolytic suite of minerals accompanying mainly calcite. By far the best example of this occurrence are the Ceylon deposits which have been given the most attention. Dana<sup>(10)</sup> supposed that graphite might have resulted from the metamorphism of carbonaceous material entrapped in sediments, the assimilation and reduction of carbon compounds by hydrothermal solutions or magmatic fluids, and possibly the crystallization of original magmatic carbon. However, there is no general agreement as to the physical and chemical conditions leading to the formation of large bodies of graphite. In Japan, it is seemed that Chinotani Mine in Toyama pref. and Kamioka Mine in Gifu pref. are typical examples of this type. (3) The third type of mineralogical background is the contact or thermal metamorphism of coal beds to produce the end products such as anthracites and graphite. The Sonora, Mexico, deposits are examples of this type.

In all these examples, the mineral originating as a result of secondary processes such as weathering and the effect of circulating waters are also to be expected. As mentioned above, a wide range of accompanying minerals and resulting complicacy make it difficult to explain the general mechanism of the occurrence of natural graphite. According to Craig's data of isotopic analyses of a large number of natural graphites<sup>(11)</sup>, however, it seems likely that most graphite deposits are driven from organic matter and calcium carbonate, which interpretes wide variation in isotopic composition.

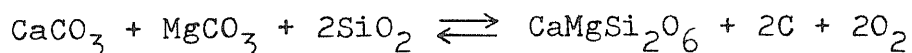
Unfortunately on account of the lack of experimental data on the mineralogical formation of graphite, it appears very doubtful that geological data will cast much light on the mechanism of the formation of graphite. Only a few

literatures are available to discuss the mechanism of the formation of graphite.

On the formation of carbon from the decomposition of siderite ( $\text{FeCO}_3$ ) to magnetite, French and Rosenberg<sup>12)</sup> studied with externally-heated cold seal pressure vessels of Tuttle-type and found that small but significant amount of black carbonaceous material, which proved later to be disordered carbon<sup>13)</sup>, were formed in the sealed tube at the temperatures of  $455^\circ\text{--}465^\circ\text{C}$  under moderate pressures (500 to 2000 bars). These temperatures and pressures are consistent, at least in part, with those suggested by Wyllie and Tuttle<sup>14)~16)</sup>. Gellatly<sup>17)</sup> suggested later that the graphite in carbonate and other alkaline igneous rocks might have also been formed by the decomposition of siderite or iron-rich carbonates on the basis of their results<sup>12)~16)</sup>.

Giardini and Salotti<sup>18)</sup> investigated the reaction of calcite with hydrogen in a cold seal pressure vessel over a range of pressure from 7 to 800 atm, temperature from  $420$  to  $970^\circ\text{C}$  and duration from a few minutes to 64 hours. They reported the following observations concerning with the hydrogen-calcite reaction; (1) the reaction initiated at about  $500^\circ\text{C}$ , (2) the reaction rate was strongly temperature-dependent and, within the range investigated, secondarily pressure- and time-dependent, (3) methane and water are ubiquitous reaction products; ethane and carbon monoxide appeared under certain conditions; carbon dioxide was not observed, (4) carbon having graphitic structure, and possibly solid hydrocarbons were formed by some reactions, (5) the reaction rate was crystallographically anisotropic. From these observations and the equilibrium calculations that hydrogen can be an important species in a gas phase in equilibrium with rock material at elevated temperature, they suggested that hydrocarbons and graphite in igneous rock could have formed by this hydrogen-carbonaceous solid reaction process, and that the enigmatic graphite veins might have formed by similar reaction, and some graphite in graphitic marbles and schists also may have an abiotic origin.

On the other hand, Mueller and Condie<sup>19)</sup> proposed the derivation of graphite on the basis of thermodynamic analysis of the carbon-mineral assemblages to be as follows:



As mentioned above, there have been few reports concerning the genesis of graphite on geological aspects. However, it would appear that the mechanisms presented have been the subject of speculation rather than detailed experimental analysis.

d. Survey of earlier Investigations on Catalytic Graphitization and on Graphitization under Pressure.

Acheson (1896) found deposits of graphite at the area of the highest temperature in silicon carbide furnace and supposed the graphite deposit might result from the decomposition of silicon carbide. In this experiment, however, he could not detect such an effect in the case of lithium carbonate, calcium oxide, manganese dioxide and nickel oxide. Almost the same time, Moissan (1896) obtained well-crystallized graphite flakes during cooling of molten iron. Seven years later, Bockers (1903) observed the accelerating effect of alumina and metallic aluminum on graphitization. In Japan, Ishikawa<sup>20)</sup> first reported the accelerating effect on graphitization resulting from the additions of metallic silicon, aluminum, iron and tungsten and also their oxides. On the basis of his experimental facts that graphite was formed even below temperatures at which no amount of carbide could be detectable<sup>21)</sup>, however, he assumed a critical attitude to Acheson's explanation for graphite formation.

For the purpose of manufacturing of artificial graphite and understanding of the genesis of natural graphite, phenomena of catalytic graphitization have been devoted attention of many investigators.

Foster et al<sup>22)</sup> obtained well crystallized graphite flakes by thermal decomposition of aluminum carbide at 2400°C. Noda and Tanaka<sup>23)</sup> heat-treated a carbon rod, which

consisted of carbon black and binder pitch, embedding in aluminum powder under pressure and found a remarkable acceleration of graphitization. For the carbon heat-treated above 2400°C, the same  $c_0$ -spacing as that of natural graphite, 6.708Å, was obtained. Taoka et al<sup>24)</sup> also obtained the graphite flakes of single crystal on the inside wall of the lid of graphite crucible by thermal decomposition of aluminum carbide. The possible mechanism of the formation of graphite single crystal was assumed to be a chemical transport of carbon atoms through vapor of some compounds of aluminum and carbon. Ishikawa et al<sup>25)</sup> observed the catalytic actions of sericite and kaolinite on graphitization around the temperatures of 1800°-2000°C. They suggested the intermediate formation of various carbides as the catalytic mechanism. Silicon was found to accelerate the graphitization of carbon by heat-treating carbon black with small amount of silicon.<sup>27)~29)</sup>

Badami<sup>26)</sup> demonstrated a definite relationship between the structure of carbon pseudomorphs, which was formed by the thermal decomposition of silicon carbide, and the structure of the parent crystalline carbide.

Shwartz and Bokros<sup>30)</sup> showed that the graphitization of pyrolytic carbons made in fluidized bed could be accelerated by titanium. Irving and Walker<sup>31)</sup> found the catalytic effects of tungsten, tantalum, titanium, platinum and molybdenum on graphitization. They suggested the carbide formation as the mechanism except for molybdenum. For molybdenum, diffusion mechanism of carbon was suspected. Miura et al<sup>32)</sup> investigated the catalytic action of iron and nickel on graphitization. Transition metals, such as iron, cobalt and nickel, are known to show the excellent catalysts for the thermal decomposition of carbon monoxide and hydrocarbons to give flaky graphite at low temperature of pyrolysis.<sup>33)~39)</sup> The precipitation of well-crystallized graphite flakes from a carbon saturated melt of metals and carbides, for instances Fe, Ni, TiC, ZrC, VC<sup>33)~44)</sup>, has been observed by slight deviation from equilibrium conditions. Graphite flakes were also reported to have been separated from boron carbide melt in

a graphite crucible<sup>45)</sup>. It was reported that highly crystalline graphite was precipitated from melts of hexaborides of rare earth elements when the melts were kept in contact with carbon heat-treated above 2000°C. The interlayer spacing of these graphite crystals was from 3.462 to 3.377Å and small amount of boron and rare earth metals were detected in it.<sup>46)</sup>

Kotlensky<sup>47)</sup> observed on boron-doped pyrolytic graphite prepared by co-deposition technique at 2000°C that the  $c_0$ -spacing of the pyrolytic graphite heat-treated decreased with the increase in boron level up to 1.0wt% of carbon, but decreased with further increase in boron level. Lowell<sup>48)</sup> found that boron dissolved substitutionally in carbon up to 2.35wt% at 2350°C and that the  $c_0$ -spacing of carbon decreased and  $a_0$ -spacing increased with increase in the content of boron.

According to Yokogawa et al<sup>49)</sup>, graphitizing carbons were obtained from the resins and other organic compounds, which gave nongraphitizing carbons by usual treatments, if some compounds of copper, nickel, cobalt and manganese, such as chloride or oxide, were added to them before their carbonization, whereas no detectable effect was observed by the addition of copper compounds to pitches or other compounds which had been known to give graphitizing carbons. Carbons prepared from humic acids and carbon black also changed their graphitization behavior by the addition of copper compounds. Some intermediate compounds between copper and carbonized resins were suggested to be responsible for the accelerating effect of metals, and carbon-carbon linkages between condensed aromatic clusters in carbonized resins were assumed to be broken by the metal atoms. The rate-determining step of the graphitization process should be the decomposition of the intermediate compounds. Sulfur has been known to be a negative catalyst for graphitization. When sulfur was added to pitches or resins which gave graphitizing carbons by pyrolysis, the graphitizability of the resulting carbons was lowered, decreasing to that of nongraphitizing carbon. Kippling et al<sup>50)</sup> reported that sulfur acts as an agent both for cross-linking of graphite-like

layers and for dehydrogenation.

According to Noda<sup>51)</sup>, many works on the effect of foreign minerals can be classified in four categories by their possible mechanisms;

- (1) formation and subsequent decomposition of carbide,
- (2) solution of carbon in metals or metallic compounds and subsequent deposition as graphite,
- (3) substitutional solid solution of foreign element in carbon,
- (4) chemical reaction during carbonization causing structural change in resulting carbon.

Pearce and Heintz<sup>52)</sup> explained the effects of ambient atmospheres and several additives on the graphitization process of carbons by using kinetic and chemical mechanisms. The effect of catalysts was explained by reducing the energy barriers which oppose the graphitization through intermediate state.

Although there are so many works on catalytic graphitization of carbon, as mentioned above, the discussions on mechanism of the accelerating effect of foreign minerals are still mere guess-work because of some singularities of carbon.

On the other hand, the density of carbon increases and the atomic volume of carbon decreases when amorphous carbon transforms to graphite. This means that the pressure favors the graphitization of carbon. Ubbelohde et al<sup>53)</sup> hot-pressed pyrolytic carbon by applying uniaxial pressures of about 400-500kg/cm<sup>2</sup> at temperatures above 2800°C and obtained graphite blocks of which the c-axes were orientated perfectly, comparable with those of natural graphite. However, the orientation of a-axes of each crystallite in the graphite blocks was still random. When carbons were heat-treated under 10kbar, a very abrupt change of the c<sub>0</sub>-spacing was observed with heat treatment around 1500°C<sup>54)</sup>. Noda et al<sup>55)56)</sup> investigated the effect of pressure on graphitization of carbon in detail. They suggested that the graphitization of carbon under pressure without any coexisting minerals could be classified into the following two stages. In the first stage, the graphitization corresponds to the same homogeneous one as that in the heat treatments of carbon under normal pressure and in this

stage, the  $c_0$ -spacing decreased gradually to about  $6.85\text{\AA}$  and the crystallite size  $L_c$  increased, but no graphitic component could be detected by X-ray diffraction method. In the second stage, the graphitization is so-called "heterogeneous one" and the profile of (00 $l$ ) diffraction line was the composite one, consisting of the graphitic component and the turbostratic component, after the  $c_0$ -spacing had reached to  $6.85\text{\AA}$ .

e. Purpose of the Present Study.

although the extent of the occurrence of natural graphite has inspired much study by earth science authorities, little is known about the origin, due to varieties of the principal country rocks and the lack of experimental data of systematic and synthetic works.

In the nature, a good quality of graphite crystals has been found in beds of metamorphic rocks, such as limestone. The temperature-pressure condition for the graphite formation was estimated geologically as the temperature of several hundreds degrees and the pressure of several kilobars. However, the conditions reported for the formation of the graphite were still more severe than that of natural graphite in spite of some investigations which might have been directed to obtained the well-crystallized graphite at low temperature. Taking hints from the geological phenomena, one can expect to reproduce the phenomena of the occurrence of natural graphite on a laboratory scale.

The purposes of the present study are to examine the effect of coexisting minerals on graphitization of carbon under pressure and to elucidate its mechanism. The results of the present study are expected to give important and useful informations on the understanding of complicated graphitization phenomena, which has been reported by others, and may develop new industrial techniques to make artificial graphite. The results of the present study are also expected to give the substantial laboratory data for the formation mechanism of natural graphite.

## 2. Experimental— Sample, Heat Treatment under Pressure and X-ray Diffraction.

In this chapter, the carbon sample, the apparatus for heat treatments under pressure and the conditions for X-ray diffraction are described. New technique was developed to know the real pressure on the small specimen in high pressure cell. The procedure of graphical separation of the composite profiles of X-ray diffraction, which has been observed on the carbons heat-treated under pressure, is explained in detail.

### a. Carbon Sample used.

The carbon sample used was a coke (PV-7) prepared by carbonization of polyvinylchloride and consequently heated up to 680°C. This coke is well known to be a typical graphitizing carbon. The grain size of the sample was limited in the range between 0.1 and 0.4mm because of the suitability for heat treatment under pressure.

### b. High Pressure Apparatus and Arrangements of Pressure Cell.

A high pressure apparatus used was a simple piston-cylinder type one shown in Fig. 3, which was made from a tool steel SKH-4A<sup>57)</sup>. The bore and outer diameter of the cylinder were 24 and 50mm, respectively, and the cylinder was protected by a soft steel guard ring. The diameter of the pistons is 23.6mm.

The arrangements of pressure cell used are shown in Fig. 4. The carbon sample was placed between disks of coexisting minerals. The pressure was transmitted through pyrophyllite. The arrangement A in Fig. 4 was mostly used in the present study. The arrangement B in Fig. 4 was used only in the experiments which were performed in order to examine the influence of water vapor on graphitization. In order to eliminate the effect of adulteration through water vapor caused by the decomposition of pyrophyllite during



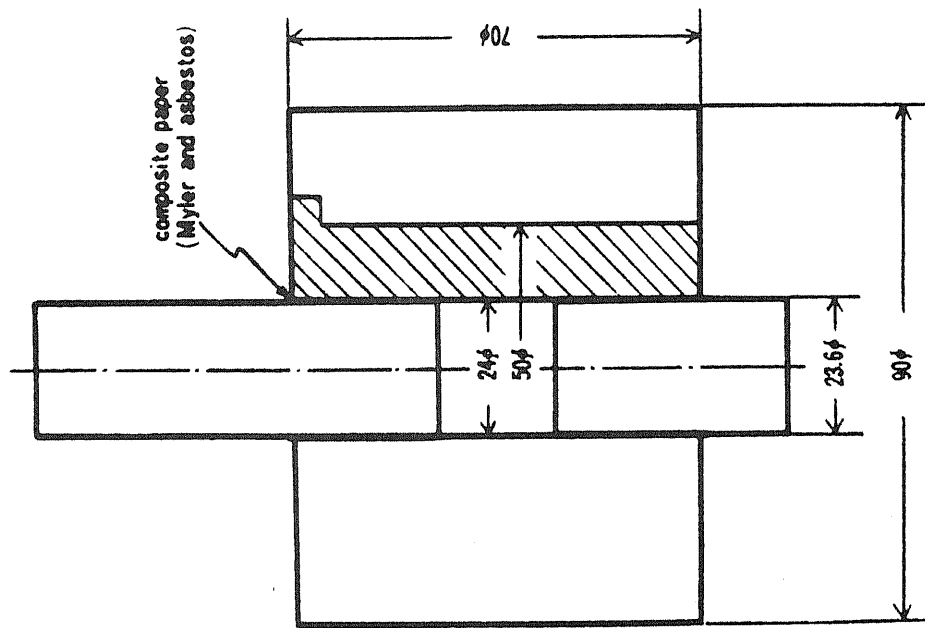
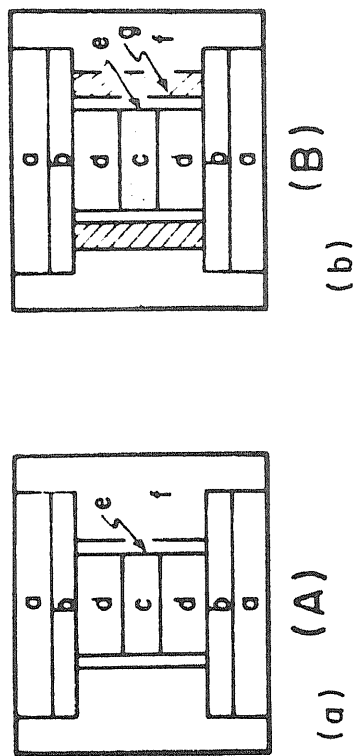


Fig. 3 Simple piston-cylinder type high pressure apparatus



- a : steel disk
- b : graphite disk
- c : carbon sample
- d : coexisting mineral
- e : graphite holder
- f : pyrophyllite sleeve
- g : pyrophyllite sleeve calcined at 970°C

Fig. 4 Arrangements of pressure cell

heat treatments under pressure, a part of raw pyrophyllite holder close to the graphite heater was replaced with the pyrophyllite tube (2.1mm thick) which was calcined at 970°C for 60min to be dehydrated. Even if the calcined pyrophyllite was partly used in the holder (the arrangement B), the relation between real pressure applied on the specimen and applied load was found not to be different from the arrangement A (without calcined pyrophyllite). The heat treatments at temperatures up to 1500°C under 3kbar were able to be carried out with such arrangements without any technical troubles.

The heating of the carbon sample was performed with the graphite heater through which the alternating current was passed via the upper and lower pistons. The electrical insulation between cylinder and pistons was assured by a Myler-asbestos composite paper of 0.1mm thick on each piston. The whole pressure apparatus was cooled in the flowing water.

### c. Calibration of Pressure.

#### (1) Principle of the Method.

Calibration of pressure in a high pressure range of above 25kbar has been usually performed by detecting the discontinuity in electrical resistance changes associated with the phase transition of metals, such as Bi, Tl, Cs and Ba<sup>58)</sup>. Below 25kbar, however, most of calibrations has been accomplished by detection of discontinuity in volume change at the phase transition points of standard substances<sup>59) 60)</sup>. On carrying out high pressure experiments with the high pressure cell in which a furnace assembly is placed, the volume fraction of the specimen to the whole volume of the pressure cell is considerably small. In such a case, one can hardly detect the phase transition of a standard substance placed in the sample room by detecting the abrupt movement of piston.

Since the volume fraction of specimen was as small as about 8.7% of the total volume of pressure cell in the present study, it was difficult to use the usual method in which resistance discontinuity and piston movement were

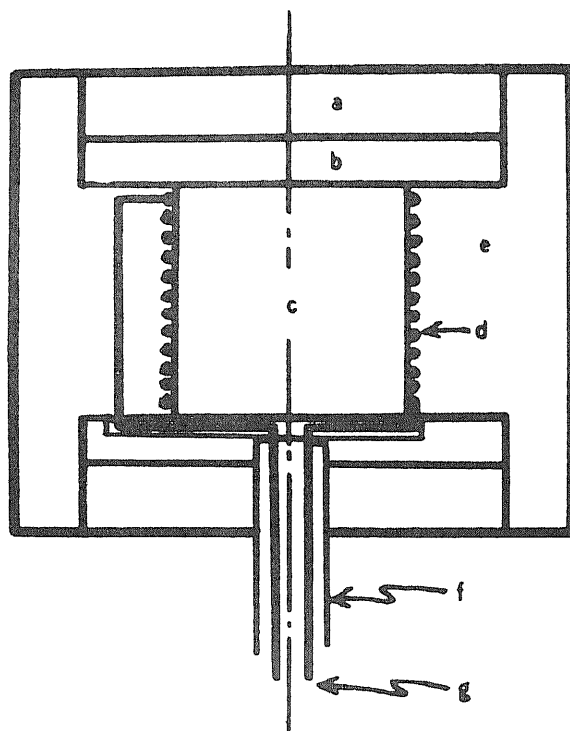
detected, for the calibration of pressure. In the present study, therefore, a new method for detecting of small volume change of standard substances was developed. The principle of the new method is the detection of the volume change of standard substance by measuring the change in inductance of high frequency coil which is wound on the standard substance. The flow of pressure transmitter of pyrophyllite was also examined by means of the same method.

## (2) Experimental.

The standard substances used were  $\text{KNO}_3$  and AgI which are known to transform at room temperature at the pressure of 3.6kbar from II-phase to IV-phase associating with the volume change of 9% and at the pressure of 3.0kbar from II-phase to III-phase associating with the volume change of 16%, respectively.<sup>(1)(2)</sup>

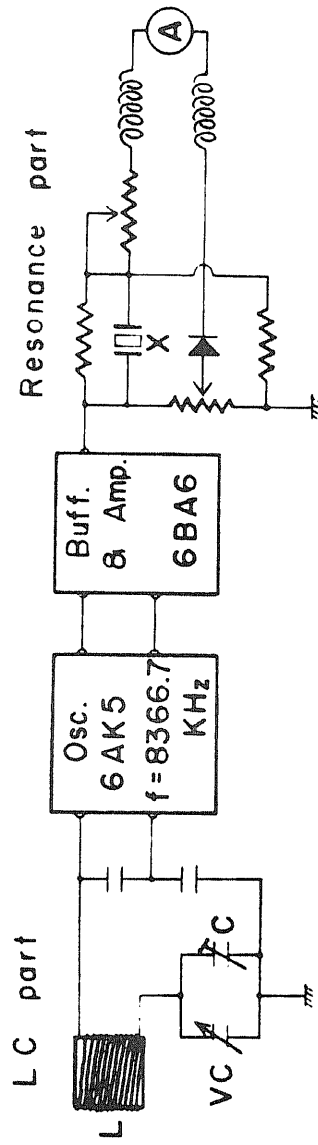
Specimen of  $\text{KNO}_3$  was prepared in the form of rod of the diameter of 10mm by melting and subsequently solidifying the powder of the chemical reagent grade in a glass tube. Specimen of AgI was obtained in the form of rod by compressing the powder of the chemical reagent grade. After wound by an enameled copper wire of 0.35mm in diameter, the specimen of standard substances was set into the pressure cell as shown in Fig. 5. The volume occupied by the specimen was about 8.7% of the whole volume of the pressure cell. Wire leads of the coil was drawn out of the pressure cell through a insulation tube inserted in the lower piston. This arrangement is exactly the same as that used in the heat treatment of carbon under pressure if the specimen of the standard substances is replaced with a furnace assembly.

The measurement of inductance changes was done with the stabilized high frequency circuit shown in Fig. 6 which consists of an oscillation, buffer, amplifier and resonance parts. The inductance change was followed by recording the capacity change of the variable condenser in the oscillation circuit which is necessary to resonate with the frequency of a crystal oscillator (8366.7KHz) in the resonance part. Thus the phase transition of the specimen could be found by



- a : steel disk (18  $\phi$   $\times$  3)    b : graphite disk (18  $\phi$   $\times$  2)**  
**c : specimen (10  $\phi$   $\times$  10)    d : enameled copper coil**  
**e : pyrophyllite holder (24  $\phi$   $\times$  20)    f : insulator tube (3  $\phi$ )**  
**g : enameled copper wire lead (0.35  $\phi$ )**

**Fig.5 Arrangement of pressure cell.**



$L$  : 10 mm  $\phi$ . 11 ~ 15 turns

$VC$  : variable condenser

$C$  : setting condenser

$X$  : crystal oscillator, 8366.7 KHz.

Fig.6 High frequency circuit diagram for detection of inductance change

searching for the discontinuity of the changes in the capacities of the variable condenser. The accuracy of the reading of capacity was within 0.1pF. Therefore the decrease of capacity means the increase in inductance of the coil.

### (3) Results.

#### (a) Calibration of Pressure in the Present High Pressure Apparatus.

Figure 7 shows the capacity changes induced by volume changes of  $\text{KNO}_3$  and AgI with the applied loads in the pressure cell shown in Fig. 5. One can observe the abrupt inductance changes corresponding to the volume change associated with phase transition. Gradual capacity decrease before and after phase transition seemed to be due to the densification of the specimen. The transition points of the standard substances were detected with good accuracy and reproducibility. The loads necessary to start the transition were  $16.4 \pm 0.2t$  and  $13.8 \pm 0.2t$  for  $\text{KNO}_3$  and AgI, respectively. Standard substance  $\text{KNO}_3$  showed a relatively larger inductance change at its transition point than AgI, although  $\text{KNO}_3$  had smaller volume change than AgI at the transition point. This seems to be caused from that dielectric constant of  $\text{KNO}_3$  changes at its transition point. No abrupt inductance change but only monotonous increase of inductance was found if a pyrophyllite rod was used instead of standard substances.

The resulting relation between applied load and pressure is shown in Fig. 8. A linear extrapolation of these two experimental points were found to pass the origin of the coordinates. The pressure loss was known to be as small as about 3% in the present arrangement. Usually the pressure loss in the same type of piston-cylinder apparatus is known to be about 10%.

In order to understand the role of the steel disks in the pressure cell, further experiments were carried out by replacing a set of steel and graphite disks with a raw pyrophyllite or a calcined pyrophyllite disks. For an example the inductance change with load for the arrangement used

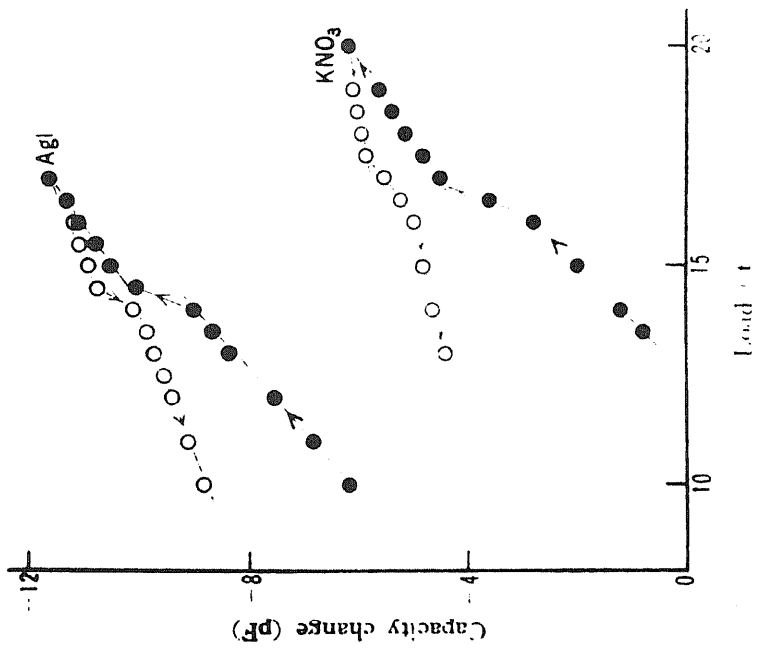


Fig. 7 Capacity changes induced by volume changes of KNO<sub>3</sub> and AgI with applied loads

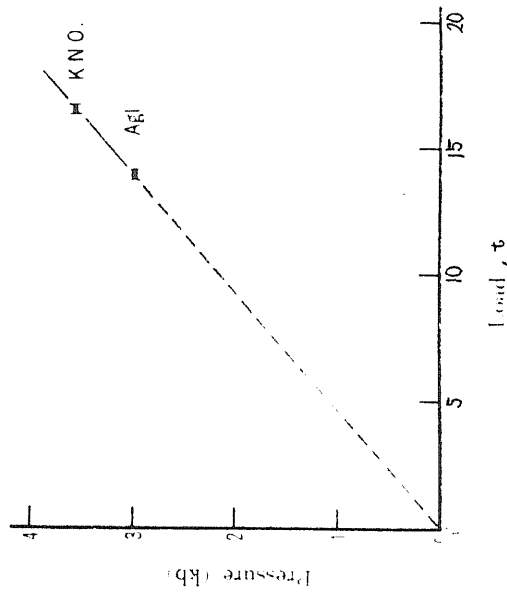


Fig. 8 Relation between applied load and pressure

calcined pyrophyllite disks is shown in Fig. 9. In comparison with Fig. 7, it was found that the transformation of  $\text{KNO}_3$  started to occur from a little higher load and took place over relatively wider range of load. Conclusively, if steel, calcined pyrophyllite and raw pyrophyllite disks are used in the pressure cell, the phase transition of  $\text{KNO}_3$  starts to occur from  $16.4 \pm 0.2$ ,  $16.9 \pm 0.3$  and  $17.8 \pm 0.3$  tons, respectively and spreads in a range of 1, 2 and 3 tons, respectively.

(b) Measurement of Flow of Pyrophyllite in the Pressure Cell.

The flow of pressure transmitter of pyrophyllite during compression was studied by following the inductance change of  $\text{KNO}_3$  in the arrangement shown in Fig. 5. In Fig. 10, the capacity changes with time are shown after compression of  $\text{KNO}_3$  to various pressures of 1, 2 or 3kbar. In the present experiments, pressure was increased with the rate of 0.2kb/min. At the moment when pressure was reached 3kbar, the flow of pyrophyllite was found to be completed. At 1kbar, however, it required about further 5min to complete the flow of pyrophyllite. Capacity changes with time after compressing to 3kbar for the three kinds of pressure cells are shown in Fig. 11. In the arrangement of pressure cell used steel disks, the flow of pyrophyllite was completed at the moment when pressure was reached 3kbar. On the other hand, time intervals required to complete the flow of pyrophyllite were about 5min for the pressure cell used the raw pyrophyllite disks and about 2min for that used the calcined pyrophyllite.

(4) Discussion.

The pressure in the simple piston-cylinder type apparatus used was calibrated with good accuracy and reproducibility by detecting the volume change associated with polymorphic transitions of  $\text{KNO}_3$  and AgI as the change of inductance of high frequency coil wound on the specimen. The present method is expected to be used for detecting the transition associated with the change in dielectric constant or magnetic



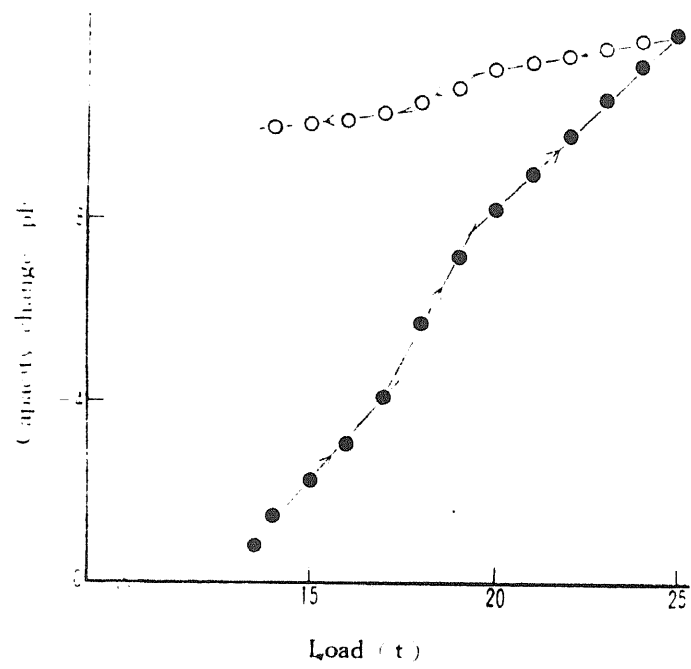


Fig.9 Capacity change with load for arrangement used calcined pyrophyllite disks

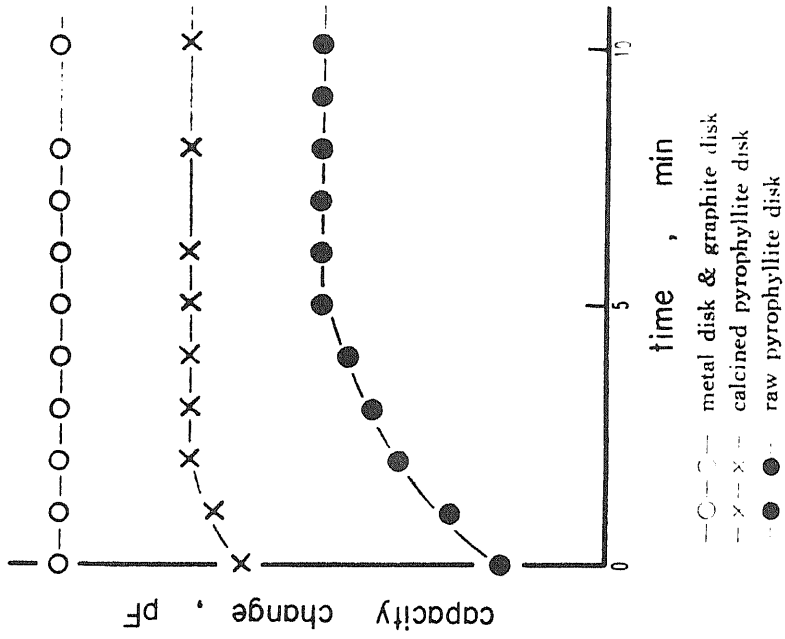


Fig.11 Capacity changes with time after compression to 3kbar for three kinds of pressure cells

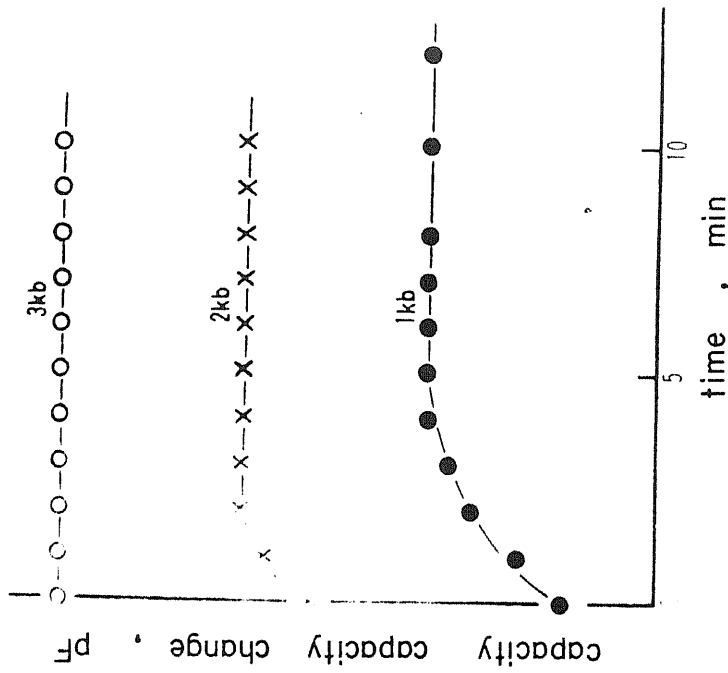


Fig.10 Capacity changes with time after compression of KNO<sub>3</sub> to various pressures of 1, 2 or 3kbar

susceptibility.

The inductance L of high frequency coil is related to its diameter D, winding width  $\ell$  and turn numbers N as follows;

$$L \propto \frac{N^2 \cdot D^2}{\ell}$$

and the resonance frequency f is combined with the capacity C according to the following equation;

$$f = \frac{1}{2\pi\sqrt{L \cdot C}}$$

Therefore it is essential to search for a suitable value of D,  $\ell$ , and N, in order to obtain Q value as high as possible (Q value is one of the measures of the quality of high frequency coil). Thus it is necessary to determine the spacing of wire not to contact with each other by densification of the specimen during compression. For instance, it is difficult to detect the transition of the specimen smaller than 4mm in diameter and 10mm in height with 8366.7KHz used. However, if higher frequency can be used, the measurement of the transition may be able to use a smaller specimen than that used in the present work.

It was found that the flow of pyrophyllite is greatly affected by the arrangement of pressure cell. As the arrangement of pressure cell used in the heat treatments of carbon under 3.2kbar is the one used the steel disks as shown in Fig. 4, it is sure that the flow of pyrophyllite may be completed in a moment when pressure is reached 3.2kbar. Since the pressure gradient was observed at the transition point of the standard substances because of the use of solid pressure transmitter of pyrophyllite, the pressure applied on the specimen is considered to be not hydrostatic but quasi-hydrostatic.

The pressure loss in the present high pressure apparatus with the arrangement A in Fig. 4 was as small as 3% if one compared with that of 10% reported previously in the same type of a simple piston-cylinder apparatus. This result seems to be caused from the reduction of frictions between cylinder and piston by using a Myler-asbestos composite paper and from

the pressure multiplication with the steel disks used. The pressure multiplication by using the steel disk was understood from the experimental fact that the larger load was required to start the transition of standard substances in the arrangement with steel disk than that with pyrophyllite.

In the present study, the heat treatments were performed always at the constant applied load of 14.9 tons, that is the constant pressure of 3.2 kbar which was evaluated from the obtained relation shown in Fig. 8.

#### d. Measurement of Temperature and Temperature Gradient in Pressure Cell.

The heat treatment temperature (HTT) was estimated from input power using the relation between temperature and input power, which was determined beforehand using a chromel-alumel thermocouple inserted in the carbon specimen. The arrangement used for the measurement of this relation was exactly the same as that used for the actual heat treatments of carbon, except that the thermocouple was inserted through lower piston, metal and graphite disks.

The measurement of temperature was carried out as follows; under the pressure of 3.2 kbar, electrical input power was increased and after 2 min the temperature was measured by using the thermocouple, and then input power was increased again. Such a measurement was repeated at least three times using different pressure cell. Though the chromel-alumel thermocouple contact directly with carbon, no error seemed to result from the contamination of the thermocouple. The thermocouple showed the same e.m.f. before and after exposed to the temperature up to 1200°C in contact with carbon. The obtained relation between temperature and input power was shown in Fig. 12. Above 1250°C, the obtained relation was extrapolated up to 1500°C.

The reproducibility of the relation between input power and temperature in three runs of temperature measurement was excellent as shown in Fig. 12 and so the temperature could be estimated from input power with the accuracy of about 20°C. This deviation in the relation between temperature and input

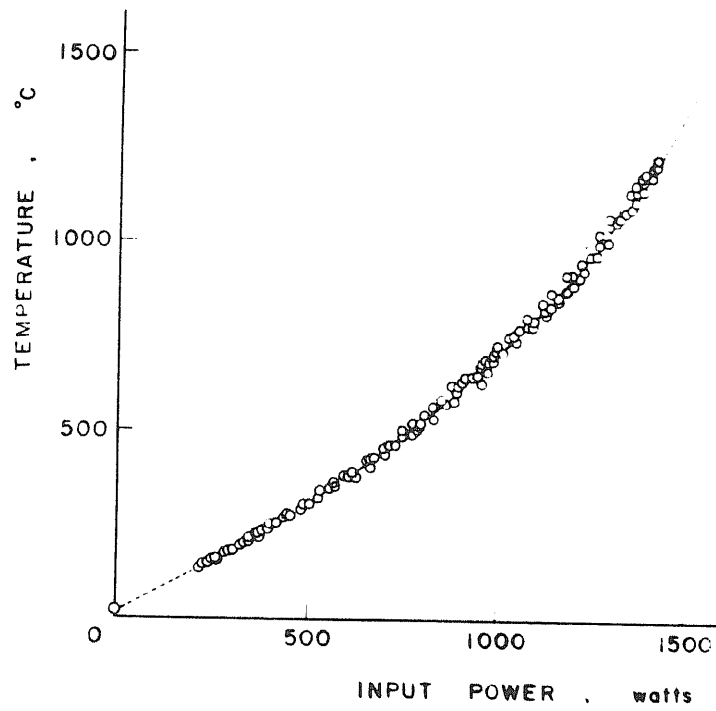


Fig.12 Relation between temperature and input power

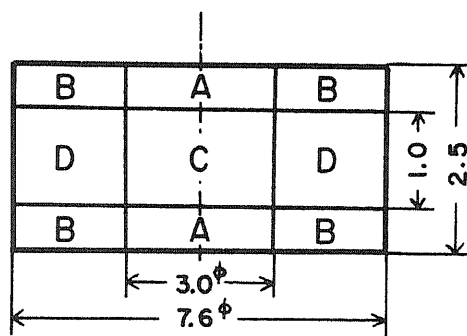


Fig.13 Schema of different parts in heat-treated carbon specimen

power seemed to result from the fluctuation of input power, errors in dimension of pressure cell assemblies and mainly from the displacement of the junction of thermocouple from the center of carbon specimen.

Relations between temperature and input power varied, beyond the observed deviation ( $20^{\circ}\text{C}$ ), with the change in the kind of coexisting minerals and the arrangement of pressure cell. Therefore the temperature-input power relation was determined whenever either the kind of coexisting minerals or the arrangement of pressure cell was changed.

A few of experiments were done in purpose of detecting the temperature gradient in the carbon specimen heat-treated. The junction of the chromel-alumel thermocouple was placed individually at the central part (C part in Fig. 13), at the part close to a disk of the coexisting mineral (A part in Fig. 13) and at the part close to the graphite heater in carbon specimen (D in Fig. 13). It was found that the temperature of the part close to a disk of the coexisting mineral was lower by about  $50^{\circ}\text{C}$  and the temperature at the part close to the graphite heater was higher by about  $30^{\circ}\text{C}$  than that of the central part which was heated at  $1200^{\circ}\text{C}$ .

e. Procedure for Heat Treatments of Carbon under Pressure.

The carbon sample of 180mg was placed between two disks of coexisting mineral (8.0mm in diameter and 3.5mm thick) so as to make a sandwich-type specimen as shown in Fig. 4. The pressure cell was set in the cylinder and then put between pistons on which the composite of Myler-asbestos were wound.

After pressure of 3.2kbar was applied on the carbon sample, water for cooling was led into the water jacket. Then a given electric power was put in the graphite heater at once in order to attain a given temperature within 2min. The temperature was controlled by adjusting manually the input power during heat treatment. The accuracy of the control of temperature was within  $20^{\circ}\text{C}$ . After heat treatment for a given time, the electric input power was cut off and the pressure apparatus was still held in the water jacket. Only a few minutes were required to cool the carbon specimen down

to room temperature.

f. Method for Determination of a Measure of Graphitization.

(1) X-ray Diffraction Method.

Most of the heat-treated carbon specimens were obtained as caked tablets. Thus the sample for X-ray diffraction was taken from the different parts of the specimens as shown in Fig. 12.

If one measures the diffraction profile with a recording X-ray diffractometer, the observed diffracted intensity is known to be affected strongly by some factors, such as Lorentz-polarization factor, atomic scattering factor and geometrical factor of X-ray diffractometer used<sup>63)</sup>. In order to perform corrections of the profile for these factors, one must carry out the deconvolution procedure by means of Fourier analysis.<sup>64) 65)</sup> However such a procedure is tremendously troublesome. Due to some approximations introduced in the process of estimation, the questions on the symmetry of the profile still remain after the correction.

The thickness of the sample for X-ray diffraction measurement was limited to 0.2mm so as to reduce the effect of X-ray absorption. Moreover the observed diffracted intensity was corrected for Lorentz-polarization, atomic scattering and absorption factors by conventional methods<sup>65)</sup>.

The profiles of (00 $\bar{L}$ ) diffraction line of the heat-treated carbon specimens were measured by a recording X-ray diffractometer with Geigercounter using Ni-filtered CuK $\alpha$  radiation. The conditions used were as follows;

Voltage; 30kV

Current; 15mA

Slit system; 1 $^{\circ}$ -1 $^{\circ}$ -0.2mm (Rigaku Denki type)

0.5-C.1-1.0mm (Shimazu type)

Scanning speed; 1 $^{\circ}$ /4min

Recording system

Scale factor; 4~8 (Rigaku Denki type)

Multiplier; 1.0 (Rigaku Denki type)

Full scale; 200~1000 (Shimazu type)

Time constant; 2sec

Chart speed; 1cm/min

The internal standard used was silicon of 99.99% purity, which was pulverized until it passed through 325 mesh sieve and then annealed in the oil bath at temperature of  $260^{\circ}\text{C}$ . The silicon mixed into carbon sample was 20wt%.

(2) Determination of a Degree of Graphitization.

Two kinds of profiles of (002) diffraction line were observed on the carbon heat-treated under pressure. One is almost symmetrical profile. The carbon specimen showing such a profile seemed to consist of only one structural component. The other is so-called composite profile which seemed to consist of at least two different kinds of component profiles. The carbon specimen showing such a composite profile seemed to be composed of at least two structural components. In order to investigate the process of graphitization by following the changes of the profiles of (002) diffraction line, it was necessary to analyse these composite profiles.

The observed single profiles were corrected for the Lorentz-polarization, atomic scattering and absorption factors by the conventional method<sup>65)</sup>. The  $c_0$ -spacing and the thickness of crystallite  $L_c$  were measured from the diffraction angle  $2\theta$  and the half width of the corrected profile, respectively.

The composite profiles were graphically separated into two symmetrical component profiles. The schema of the separation is shown in Fig. 14. After the observed composite profile (profile 1 in Fig. 14) is corrected for the Lorentz-polarization, atomic scattering and absorption factors by the conventional method<sup>65)</sup> (the profile (2)), the high angle side of the sharp profile is folded to the low angle side and the profile (3) is obtained. Subtracting the profile (3) from the composite one (2), the balanced profile (4) is obtained. Since the profile (4) is not symmetrical, however, the profile (5) for the broad component by folding the low angle side of the profile (4) at the angle of the maximum intensity. Finally, the profile (6) for the sharp component is obtained by subtracting the profile (5) from the profile (2). By a few



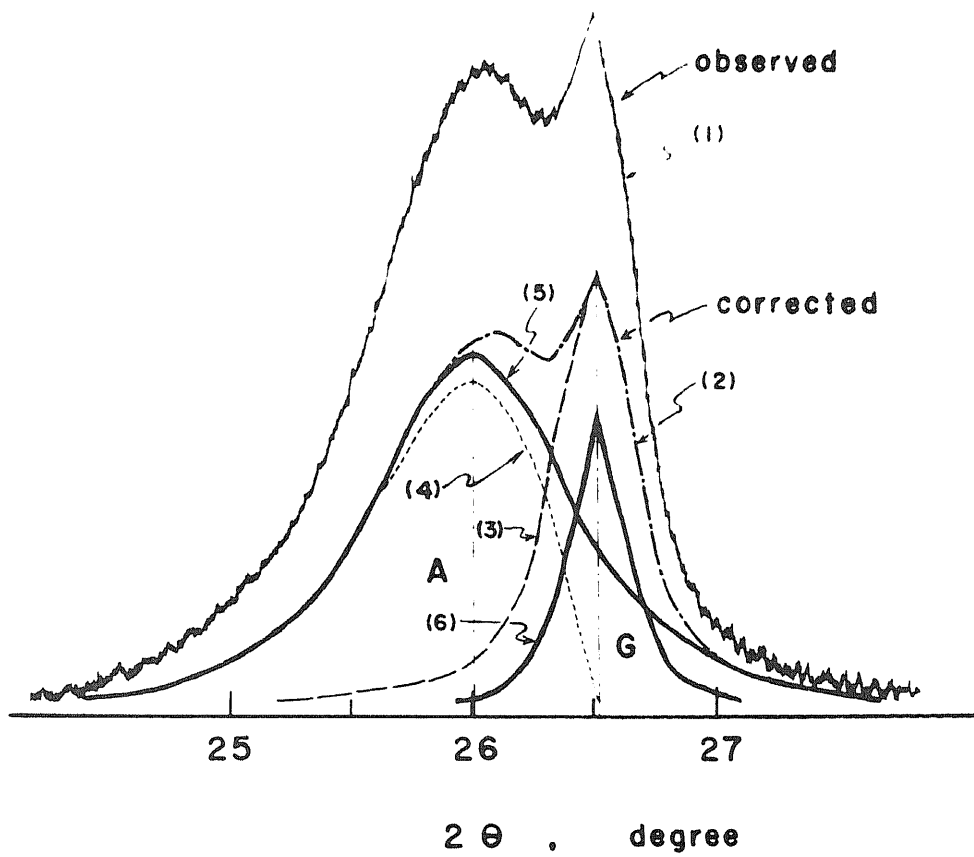


Fig.14 Schema of separation of composite profile

times of trial and error adjustments, two symmetrical component profiles are obtained. The structural components which correspond to the sharp (high angle side in the present work) and broad (low angle side) component profiles are designated as  $G_M$  and  $A_M$ , respectively in the present study.

The  $c_0$ -spacing of the two components were measured from the each separated component profile. As will be described in following chapters, the component  $G_M$  is considered to have the graphitic structure, because it has the  $c_0$ -spacing of  $6.72\text{\AA}$  and the same diffraction pattern of six-fold symmetry as that of graphite single crystal. Therefore, the content of the component  $G_M$  was used as a measure of graphitization of the specimen. The content of the component  $G_M$  was obtained from the ratio of the area under the profile for the component  $G_M$  to the total area under the composite profile. The ratio of areas was measured by using a planimeter and then corrected for the preferred orientation of crystallite in the samples for X-ray diffraction.

The correction for preferred orientation of crystallite in the sample was done as follows; When the sample for X-ray diffraction is mounted on the sample holder, the c-axis of crystallites tends to orient parallel to the normal of the surface of the sample holder. This tendency is emphasized as the structure of carbon develops and is well graphitized. In order to estimate the real content of the component  $G_M$ , one should eliminate such a effect of the preferred orientation of crystallite. However, in the present work a degree of orientation of crystallite in the mounted sample for X-ray diffraction could not be measured directly. Therefore, the conventional method of correction for the preferred orientation of crystallite was employed. The composite profiles of (002) diffraction line similar to those of carbons heat-treated under pressure were obtained by mixing two kinds of carbons which were different in a degree of graphitization; one is a petroleum coke heat-treated at  $1600^\circ\text{C}$  ( $c_0=6.85\text{\AA}$ ) and the other petroleum coke heat-treated at  $3200^\circ\text{C}$  ( $c_0=6.72\text{\AA}$ ). The obtained composite profiles were separated and then the ratio of areas of component profiles was

measured in the same way as that mentioned before. Figure 14 shows the relation between the weight percentage  $x$  of the coke heat-treated at  $3200^{\circ}\text{C}$  in the mixture and the observed ratio  $y$  of the area of the profile for the component  $G_M$  to total area. The general formula for the relation between  $x$  and  $y$  is written as follows;

$$y = \frac{\gamma \cdot x}{1 + (\gamma - 1) \cdot x} \quad (1)$$

The constant  $\gamma$  in Eq. (1) was estimated to be 2.1 for the experimental result of Fig. 14. Thus the content  $x$  of the graphitic component  $G_M$  in the sample can be calculated from the area ratio  $y$  of the profile for the graphitic component  $G_M$  to the composite profile by using the following equation,

$$\begin{array}{l} \text{the content of} \\ \text{the graphitic component } G_M \end{array} = \frac{y}{(2.1 - 1.1y)} \quad (2)$$

### 3. Accelerating Effect of Calcium Compounds on Graphitization of Carbon under Pressure.

In this chapter, the experimental results of the heat treatment of carbon under the pressure of 3.2kbar in the presence of calcium compounds, such as limestone, calcium carbonate and calcium hydroxide, were described and the effect of co-existing calcium compounds on graphitization of carbon was discussed.

#### a. Heat Treatments of Carbon under Pressure in the Presence of Limestone.

##### (1) Introduction.

In the nature, a good quality of graphite crystals has been found in the beds of metamorphic rocks, such as limestone, as described in the section 1.c. The temperature-pressure condition for the graphite formation was estimated geologically at the temperatures of several hundreds degrees and the pressures of several kilobars. On the other hand, it has been found that the carbon is graphitized very rapidly at around  $1500^{\circ}\text{C}$  under the pressure of 10kbar<sup>54)</sup> and under 5 and 3kbar<sup>55)</sup>. However, any indication of the presence of graphite structure could not be found by X-ray diffraction at temperatures lower than  $1300^{\circ}\text{C}$ . Therefore, the limestone might have some effect on graphitization, like the pressure and the temperature had.

The purpose of the present work is to understand the effect of the coexistence of limestone on the graphitization of carbon under pressure.

##### (2) Experimental and Results.

The carbon sample used was a polyvinylchloride coke PV-7 (see section 2.a.). Limestone disks of 3.5mm thick and 8.0mm in diameter were cut out from Fusulina limestone from Akasaka, Gifu Pref., Japan. The bulk density of limestone was about  $2.6\text{g/cm}^3$ .

The arrangement A of pressure cell (see Fig. 4) was used.

The carbon sample used was 180mg. The heat treatments were performed at various temperatures between  $800^{\circ}$  and  $1300^{\circ}$ C for 20 - 240min under the quasi-hydrostatic pressure of 3.2kbar by means of exactly the same method as described in the chapter 2.

Above  $1000^{\circ}$ C, the carbon specimens heat-treated with limestone were obtained as caked tablets. In the tablets, appreciable amounts of calcium carbonate were detected by X-ray diffraction method and the amounts increased with HTT. Limestone disks themselves were found to have recrystallized when carbon specimen was heat-treated above  $1000^{\circ}$ C. The thickness of recrystallized part of limestone increased with the increase in HTT and residence time. The grains of recrystallized limestone was found to grow along the temperature gradient, that is, parallel to the axial direction of the heater (Fig. 15). Limestone was found to have melted above  $1250^{\circ}$ C. Above  $1250^{\circ}$ C, a small amount of calcium oxide was detected by X-ray diffraction method not only in the disks of limestone but in the carbon specimen.

The profile of (002) diffraction line of the heat-treated specimens was measured by a recording X-ray diffractometer using Ni-filtered  $\text{CuK}\alpha$  radiation (see the section 2.f.). Samples for X-ray diffraction were taken from the central part of heat-treated carbon specimens.

The profiles of (002) diffraction line of the carbon specimens heat-treated in the presence of limestone above  $1000^{\circ}$ C were found to be composite, a relatively sharp profile at  $26.5^{\circ}$  in  $2\theta$  overlapping on a broad profile at an angle lower than  $26.2^{\circ}$ . The former seemed to correspond to the profile of the graphitic component  $G_M$  because its  $c_0$ -spacing is almost  $6.72\text{\AA}$ , and the later corresponds to the profile of the turbostratic component  $A_M$ . With the increase in HTT and residence time, the sharp profile of the graphitic component  $G_M$  became stronger and narrower, and the broad band profile of the turbostratic component  $A_M$  shifted to higher angle side. The representative change of the profile with HTT is shown in Fig. 16.

high temperature side  
carbon specimen



graphite plate  
low temperature side

Fig.15 Growth of grain of recrystallized limestone in contact with carbon sample heat-treated at 1120°C for 60min under 3.2 kbar ( under polarized light )

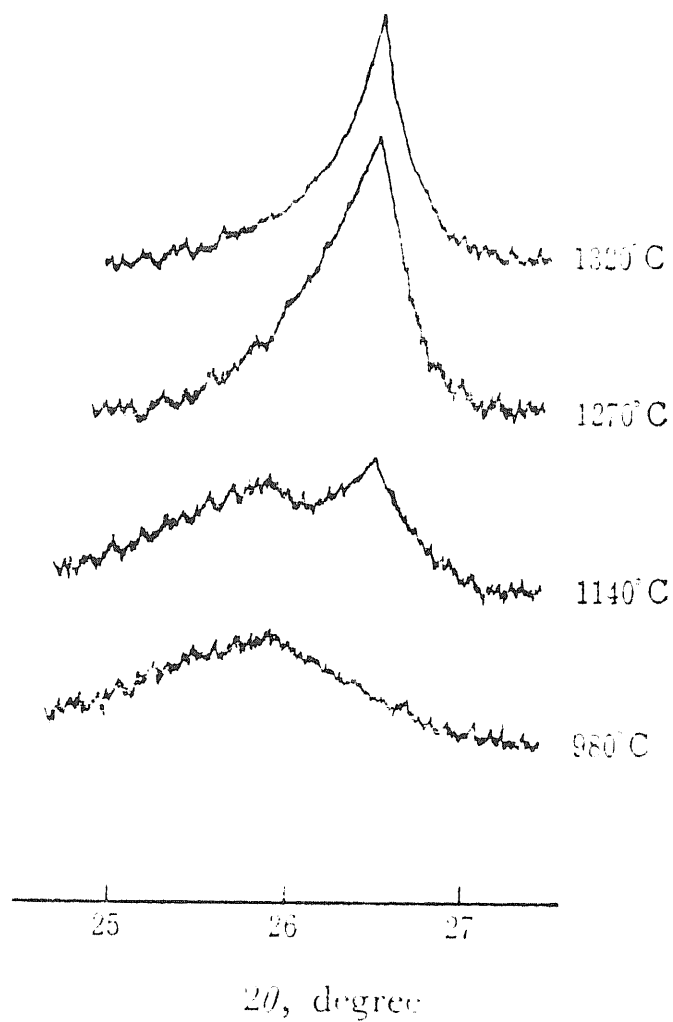


**Fig.16 Change of profile of (002) diffraction line of carbon specimen heat-treated in the presence of limestone with HTT**

According to the same methods described, the composite profile was separated graphically into two component profiles (see the section 2.f.) and the  $c_o$ -spacing and the content of the graphitic component  $G_M$  were measured (see the section 2.f.). The variation of the  $c_o$ -spacing with HTT is shown in Fig. 17. The  $c_o$ -spacing of the component  $G_M$  was almost constant and around  $6.72\text{\AA}$ , while the  $c_o$ -spacing of the component  $A_M$  decreased gradually from  $6.91$  to  $6.80\text{\AA}$ . Changes of the content of the component  $G_M$  with HTT are shown in Fig. 18 for several residence times. The content of the component  $G_M$  increased very rapidly with the increase in HTT. The content attained about 45% with the heat treatment at  $1300^\circ\text{C}$  for 60 min. However, with a longer treatment as 240min, only a small increase in the content was observed.

In comparison, the carbon sample was heat-treated under the same pressure of 3.2kbar without limestone, replacing limestone disks by glassy carbon plates and pyrophyllite disks. Glassy carbon plates were used to prevent the direct contact of carbon specimen with pyrophyllite disks. In this case, the profile of (002) diffraction line of the carbon specimen heat-treated even above  $1300^\circ\text{C}$  had only a hump at about  $26.5^\circ$  in  $2\theta$ . The representative change of the profiles with HTT is shown in Fig. 19.

From the present result, it can be concluded that the graphitization of carbon was accelerated in the presence of limestone. The graphitization of carbon occurred already at  $1100^\circ\text{C}$  with an appreciable amount.

#### b. Heat Treatments of Carbon under 3.2kbar in the Presence of Calcium Carbonate.

##### (1) Introduction.

It was found in the previous work that the graphitization of carbon under pressure was evidently accelerated in the presence of limestone. In order to elucidate the mechanism of the effect of coexisting mineral on graphitization of carbon, similar experiments with various kinds of coexisting minerals should be carried out. However, it is difficult to find out



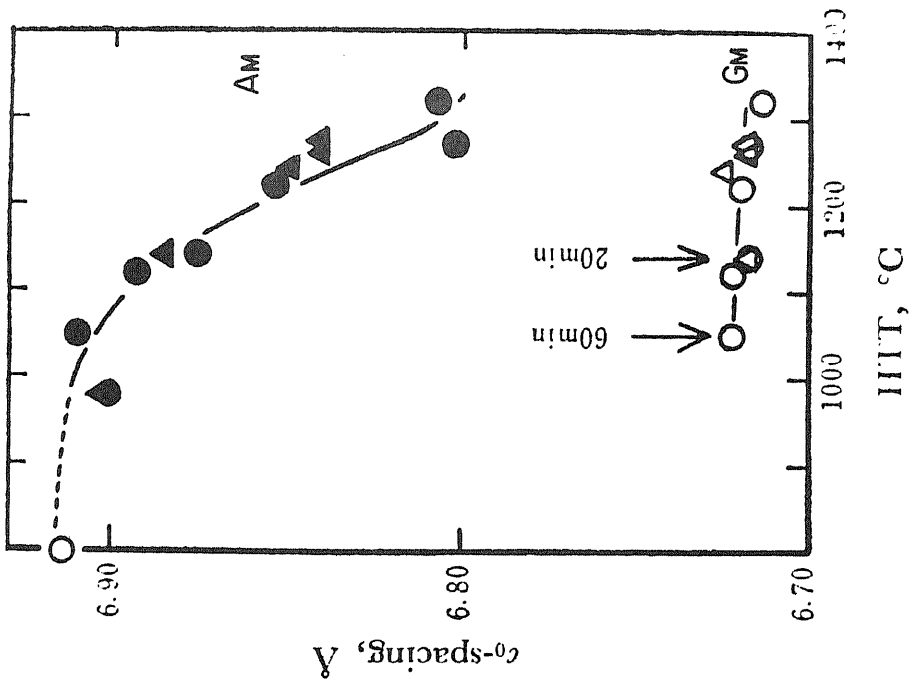


Fig.17 Variation of co-spacing of two components of GM and AM with HTT

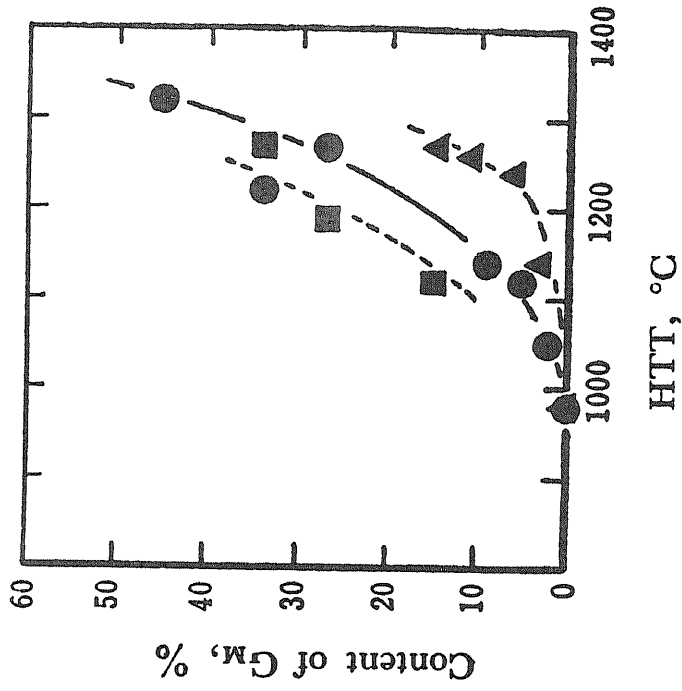
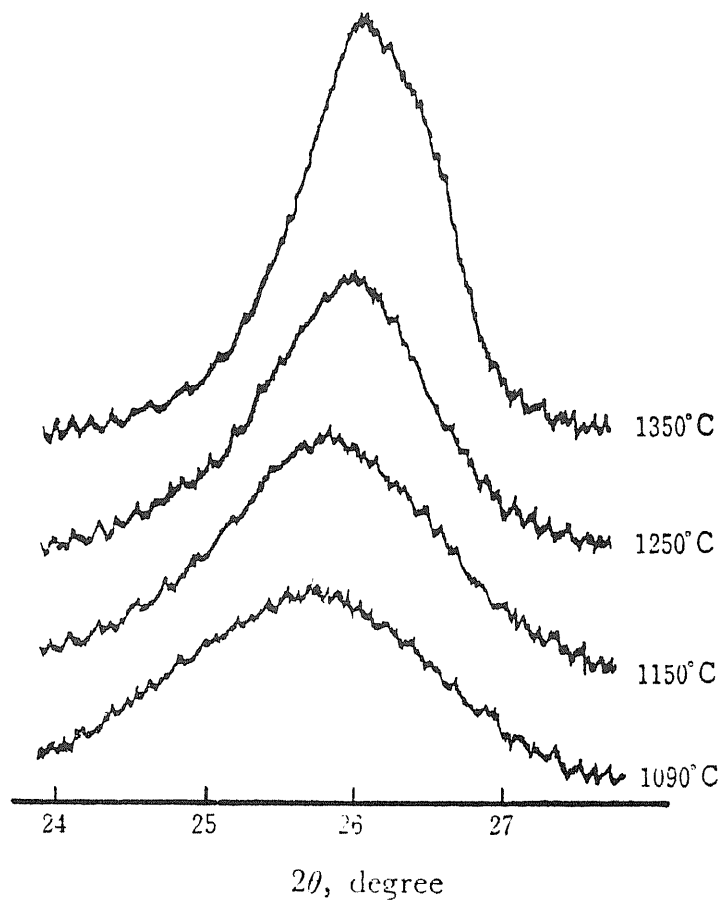


Fig.18 Change of content of component GM with HTT

- ▲ : 20 min
- : 60
- : 240



**Fig.19** Representative change of (002) diffraction line with HTT without any minerals

all kinds of minerals of high purity in the nature. Therefore, the powder of chemical reagent grade should be used in a series of the present study so as to exclude the additional actions of impurities on graphitization and to obtain the further detailed data of the accelerating effects. On the heat treatment of carbon sample placed between two disks of coexisting minerals under pressure, one should also play due regard to the effect of the physical properties of coexisting minerals, such as the porosity and crystallite size etc, on the experimental results.

In the present work, the heat treatments of the coke PV-7 were carried out under quasi-hydrostatic pressure of 3.2kbar and under nitrogen gas flow at atmospheric pressure by sandwiching between disks of calcium carbonate. The coke was also heat-treated under 3.2kbar in the absence of any minerals.

## (2) Experimental.

The disks of calcium carbonate, 8.0mm in diameter and 3.5mm thick, were prepared by compressing calcium carbonate powder (chemical reagent grade, 99% purity, calcite type) under 3.5kbar. The bulk density of the disks was about  $2.2\text{g/cm}^3$  (ca. 20% porosity).

The arrangement A of pressure cell used and the procedure for the heat treatments of carbon under 3.2kbar were described before (see section 2.b. and 2.e.). The heat treatments of carbon under the same pressure of 3.2kbar without any minerals were carried out by replacing the disk of calcium carbonate with a set of a graphite plate of 1.0mm thick and a disk of calcium fluoride of 2.5mm thick. The graphite plate served for avoiding the direct contact of calcium fluoride with the carbon sample.

In order to examine the effect of pressure on graphitization of carbon in the presence of calcium carbonate, the carbon sample pressed moderately with two disks of calcium carbonate was heat-treated in a graphite resistance furnace under a flow of nitrogen gas at ordinary pressure.

The profiles of (002) and (004) diffraction lines of the

heat-treated specimens were measured by using Ni-filtered  $\text{CuK}\alpha$  radiation (see section 2.f.).

The heat-treated specimens were also observed with an electron microscope. The sample for electron microscopy was dispersed in trichloroethylene by ultrasonic vibration, then supported on an evaporated carbon film. Bright-field and dark-field micrographs and selected area diffraction patterns of the particles of the sample were observed with transmission electron microscope (JEM-T7).

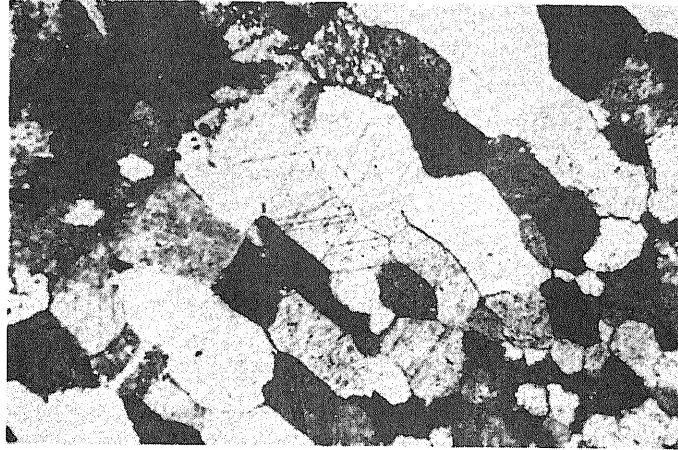
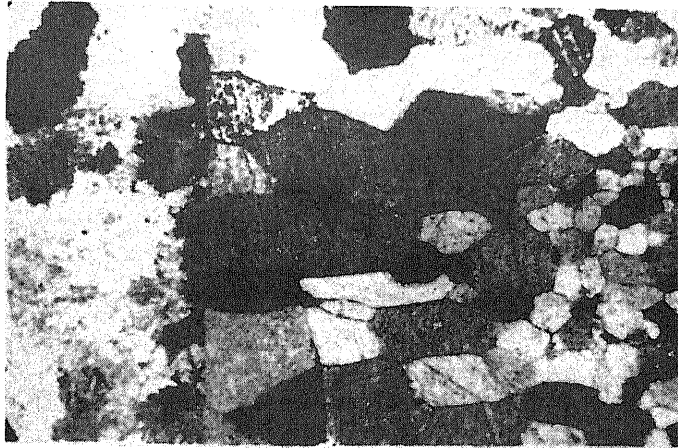
### (3) Results.

#### (a) Observation of Heat-treated Specimens.

The carbon specimens heat-treated above the temperature of  $980^{\circ}\text{C}$  under 3.2kbar in the presence of calcium carbonate were obtained as sintered cakes. The obtained cakes were roughly classified into two; one has the thickness of about 2.5mm and the other of about 3.1mm. The cakes of about 2.5mm thick contained only small amount of calcium carbonate so that it was detected only by X-ray diffraction method. On the other hand, in the cakes of about 3.1mm calcium carbonate existed visibly in the form of stratum. Disks of calcium carbonate, obtained when carbon specimen was heat-treated above  $1070^{\circ}\text{C}$  for 60min under 3.2kbar, have recrystallized and those heat-treated above  $1360^{\circ}\text{C}$  were found to melt at the part in contact with carbon specimen. Above  $1360^{\circ}\text{C}$ , calcium oxide was detected by X-ray diffraction method in the carbon specimen. Figure 20 shows the polarization micrograph of a thin section of the calcium carbonate disk heat-treated at  $1360^{\circ}\text{C}$  for 60min under 3.2kbar. The grains of recrystallized calcium carbonate was found to grow along the direction of temperature gradient, that is parallel to the axial direction of the heater. The thickness of recrystallized part increased with the increase in HTT and residence time. This result is very similar to that obtained for limestone. However the rate of increase in the thickness of recrystallized part with heat treatment was slower than that in the disks of limestone.

In the case of heat treatments of the carbon sample under

high temperature side  
carbon specimen



graphite plate  
low temperature side

Fig.20 Polarization micrograph of thin section of calcium carbonate disk heat-treated at 1360 °C for 60 min under 3.2 kbar

3.2kbar without any minerals, the carbon specimens heat-treated above 1300°C were obtained as sintered cakes whose bulk densities were about 1.5g/cm<sup>3</sup>.

In the heat treatments of carbon under a flow of nitrogen in the presence of calcium carbonate, even the carbon specimen heat-treated at 1550°C for 60min could not be caked and showed no difference in appearance from the original carbon sample. Disks of calcium carbonate heat-treated above 1000°C were completely decomposed to change into disks of calcium oxide. In this case, no amount of calcium carbonate or calcium oxide was detected in the carbon specimen.

(b) Changes of Profile of (002) Diffraction Line.

Figure 21 shows the change of profile of (002) diffraction line with HTT for the central part of the carbon specimens heat-treated under pressure in the presence of calcium carbonate. The profiles of (002) line were found to be composite above 1070°C for 60min consisting of a sharp profile for the graphitic component G<sub>M</sub> and a broad profile for the turbostratic component A<sub>M</sub>. With the increase in HTT, the sharp profile for the component G<sub>M</sub> became stronger and narrower, being fixed at almost constant diffraction angle, while the broad profile of the component A<sub>M</sub> shifted to higher angle side and became slightly narrower. Similar change of profile with residence time was also observed at the constant temperature of 1280°C (Fig. 22).

In heat treatment of carbon under pressure without any minerals, the change of profile of (002) diffraction line with HTT was considerably different from that in the case of the presence of calcium carbonate. Any composite profiles could not be observed up to 1500°C as shown in Fig. 23. Also in the heat treatments of carbon with calcium carbonate under a flow of nitrogen, any component G<sub>M</sub> could not be found below 1550°C as shown in Fig. 24. The profile of (002) diffraction line became slightly stronger with shifting to higher angle side.

The variations of c<sub>0</sub>-spacing and crystallite size L<sub>c</sub> with HTT are shown in Fig 25 and Fig. 26, respectively. The

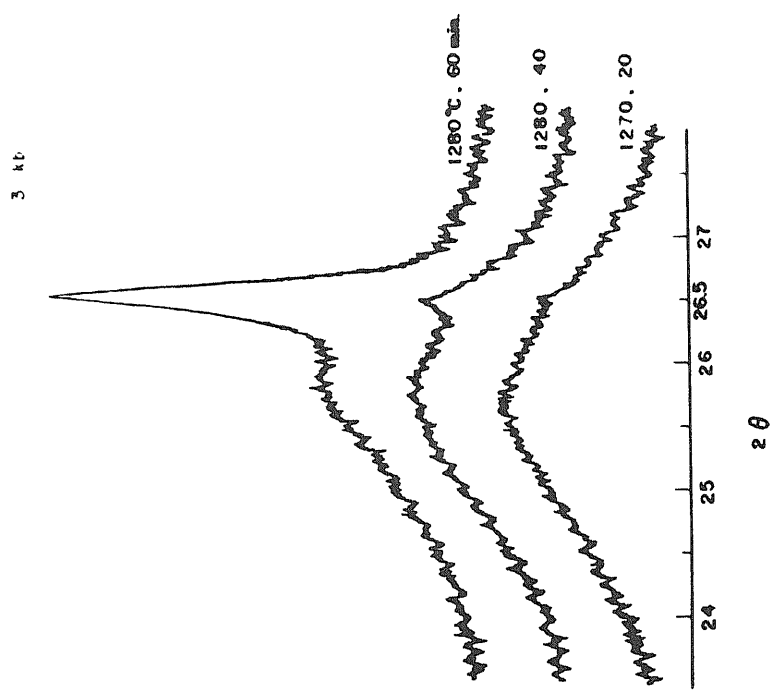


Fig.22 Change of profile of (002) diffraction line with residence time at constant temperature of 1280 °C

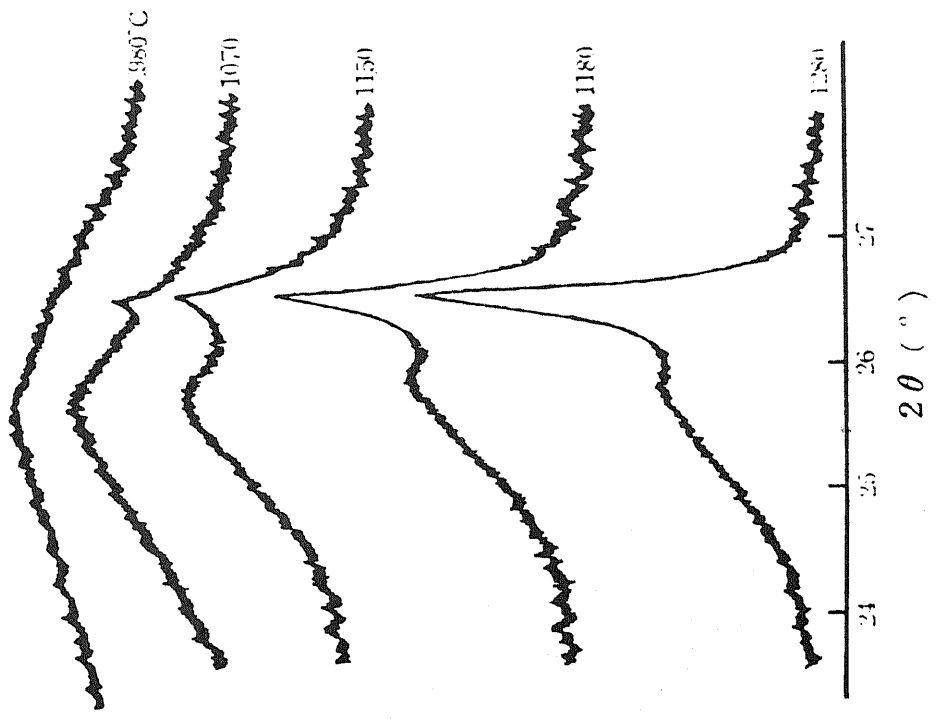


Fig.21 Change of profile of (002) diffraction line with HTT

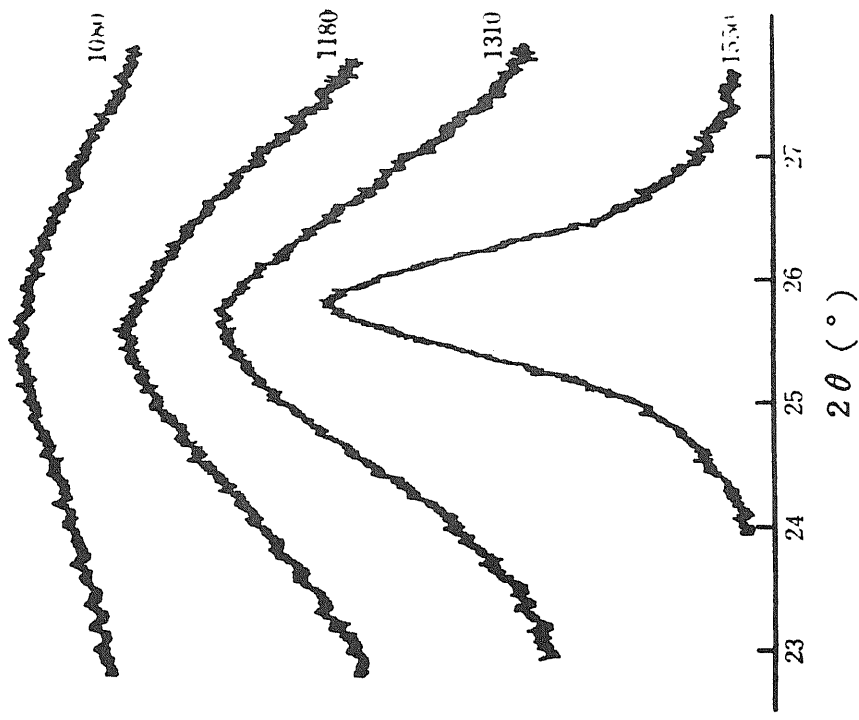


Fig.24 Change of profile of (002) diffraction line with HTT under flow of nitrogen

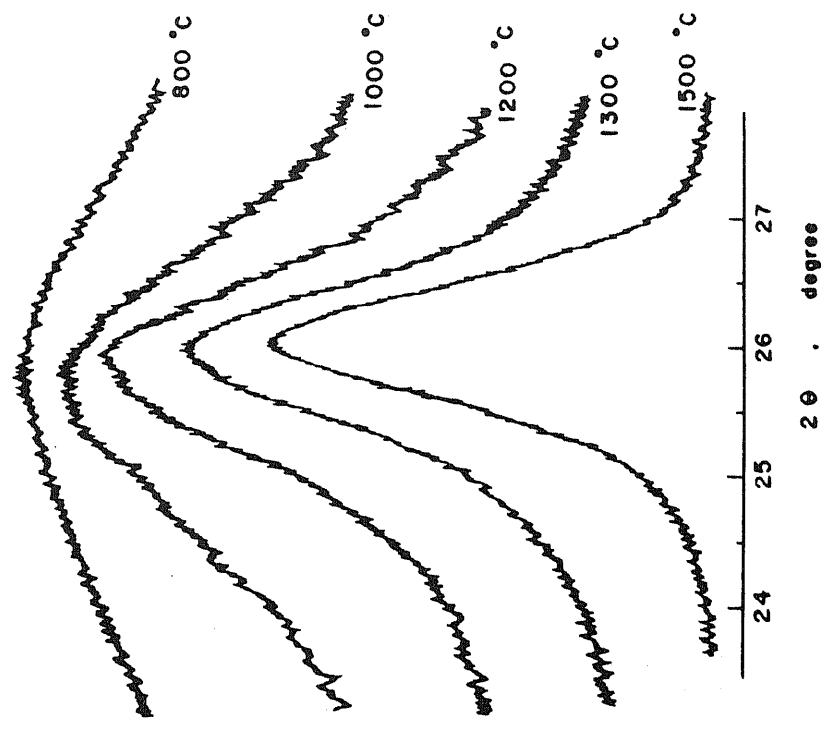


Fig.23 Change of profile of (002) diffraction line with HTT without any coexisting minerals



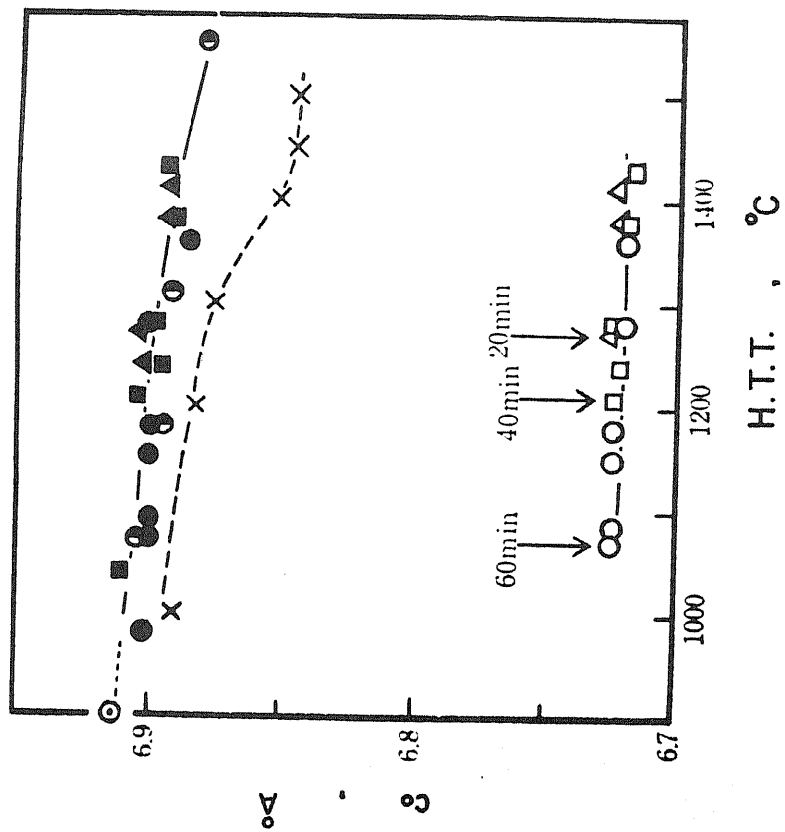


Fig.25 Variation of co-spacing with HTT

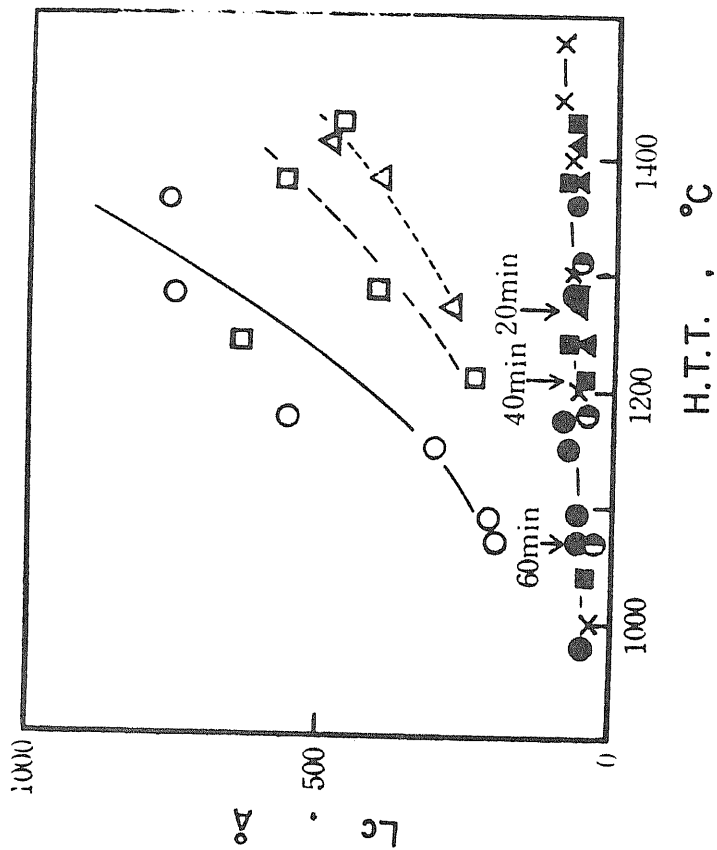


Fig.26 Variation of crystallite size  $L_c$  with HTT

- ▲ : 20 min } in the presence of calcium carbonate under 3.2 kbar
- : 40 min }
- : 60 min }
- : 60 min in the presence of  $\text{CaCO}_3$  under flow of nitrogen
- X : 60 min without any minerals under 3.2 kbar

$c_o$ -spacing of the component  $A_M$  in the carbon specimen heat-treated with calcium carbonate under pressure decreased gradually from the value of about  $6.91\text{\AA}$  of the original carbon sample with the increase in HTT and reached about  $6.89\text{\AA}$  at  $1360^\circ\text{C}$ . The crystallite size  $L_c$  of the component  $A_M$  increased slightly to about  $80\text{\AA}$  with the increase in HTT. The component  $G_M$  was observed on the profile of (002) diffraction line obtained for the carbon specimens heat-treated above  $1070^\circ\text{C}$  for 60min, above  $1210^\circ\text{C}$  for 40min and above  $1270^\circ\text{C}$  for 20min. The  $c_o$ -spacing of the component  $G_M$  was almost constant at around  $6.72\text{\AA}$  and the crystallite size  $L_c$  increased rapidly with the increase in HTT. The value of  $c_o$ -spacing of the component  $G_M$  was also estimated as about  $6.72\text{\AA}$  from the profile of (004) diffraction line.

Figure 27 shows the changes of the content of the component  $G_M$  with HTT. The content of the component  $G_M$  was found to increase with the increase in HTT. By comparing with the result for limestone (Fig. 18), one can see that the increasing rate of the content of component  $G_M$  in the presence of limestone is much higher than that in the presence of calcium carbonate. In both cases of limestone and calcium carbonate, the higher HTT was, the shorter the time for the occurrence of the component  $G_M$ .

The thickness of recrystallized part of the disk of calcium carbonate increased with the increase in HTT and residence time. The good relation between this thickness and the content of the component  $G_M$  in the central part of the carbon specimen was found as shown in Fig. 28. This relation seemed to be held regardless of HTT and residence time. The relation between the content of the component  $G_M$  and the thickness of the recrystallized layer of the calcium carbonate disk is in good accord with that of limestone presented by the dotted line in the same figure.

### (c) Electron Microscopic Observations.

Electron microscopic observations were done on the carbon specimens heat-treated under pressure in the presence of calcium carbonate and those without any minerals. The particles

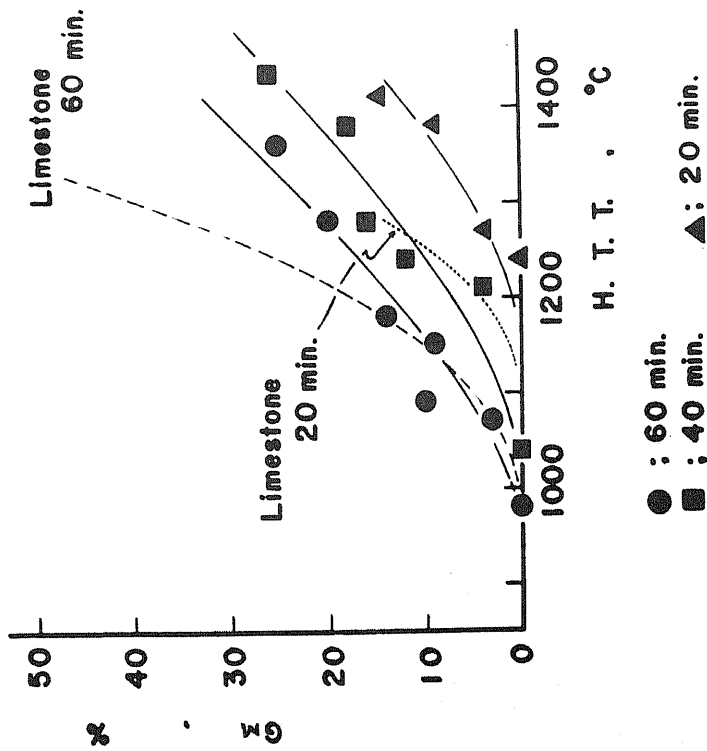


Fig.27 Change of content of component GM with H.T.T

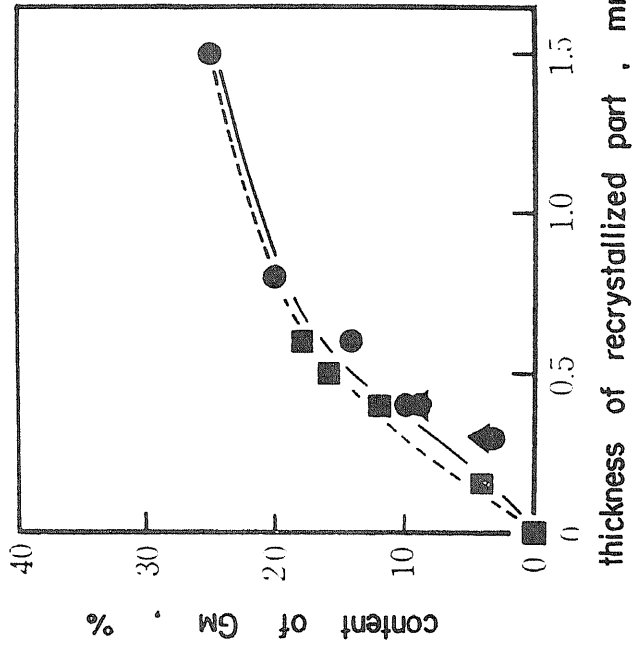


Fig.28 Relation between thickness of recrystallized part of disk of calcium carbonate and content of component GM

having the diffraction pattern of six-fold symmetry of graphite single crystal were found in the carbon specimens which showed the existence of the component  $G_M$  on the profile of (002) X-ray diffraction line. Therefore, these particles seemed to be responsible to the graphitic component  $G_M$  on X-ray diffraction profile. The number of those particles tended to grow in concert with the increase in the content of the component  $G_M$  which was estimated from the profiles of (002) diffraction line. Other particles showed the rings of (10) and (11) reflections. These particles seemed to be the turbostratic component  $A_M$ . There also existed some particles which showed the diffraction pattern of six-fold symmetry of graphite single crystal overlapping on the reflection rings (Fig. 29). However, these particles were proved to consist of two kinds of particles, that is the particles of graphitic and turbostratic structures, by dark field microscopy. For example, the bright-field micrographs and selected area diffraction patterns taken on the carbon specimen heat-treated at  $1070^{\circ}\text{C}$  for 60min with calcium carbonate under 3.2kbar are shown for each kinds of particles in Figs. 30 a) and b).

In the carbon specimen heat-treated up to  $1500^{\circ}\text{C}$  under 3.2kbar without any minerals, no particles showed the diffraction pattern of six-fold symmetry.

From both of electron microscopic observation and the profile of (002) X-ray diffraction line, it can be concluded that the component  $G_M$  has the graphitic structure and the component  $A_M$  has the turbostratic structure.

Conclusively, the graphitization of carbon under 3.2kbar is evidently accelerated by calcium carbonate. The temperature at which the graphitic component  $G_M$  began to appear was almost the same as that in the case of limestone. Therefore, the chief species in limestone having the accelerating effect on graphitization of carbon seems to be calcium carbonate itself. Phenomenally, the development of the graphitic component seems to be closely related to the recrystallization of the coexisting calcium carbonate on the basis of the good relation between the content of the graphitic component  $G_M$  and the thickness of the recrystallized layer of calcium carbonate disk.

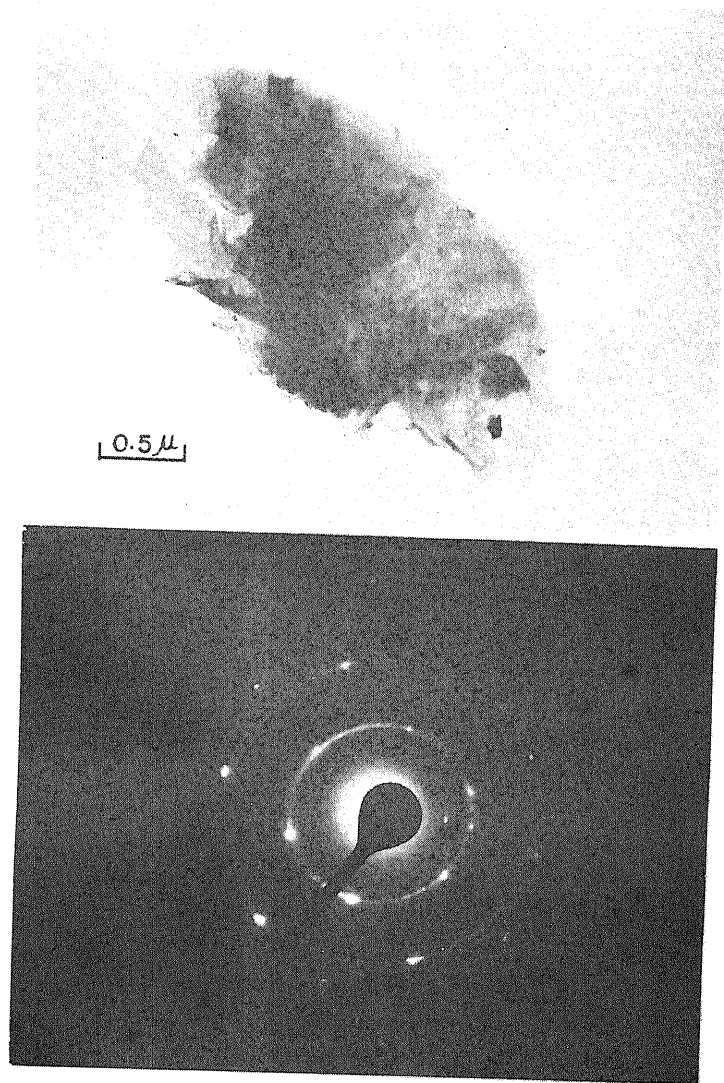
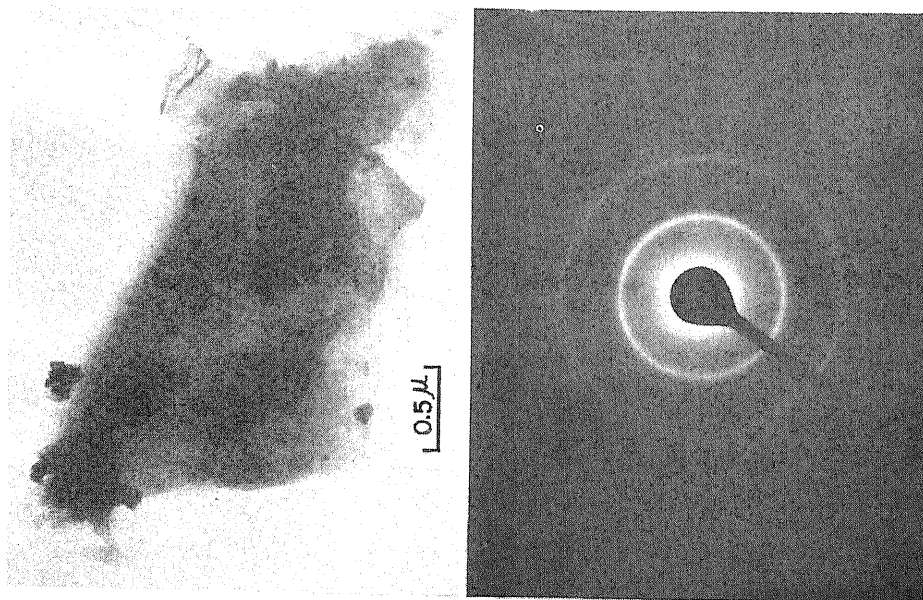
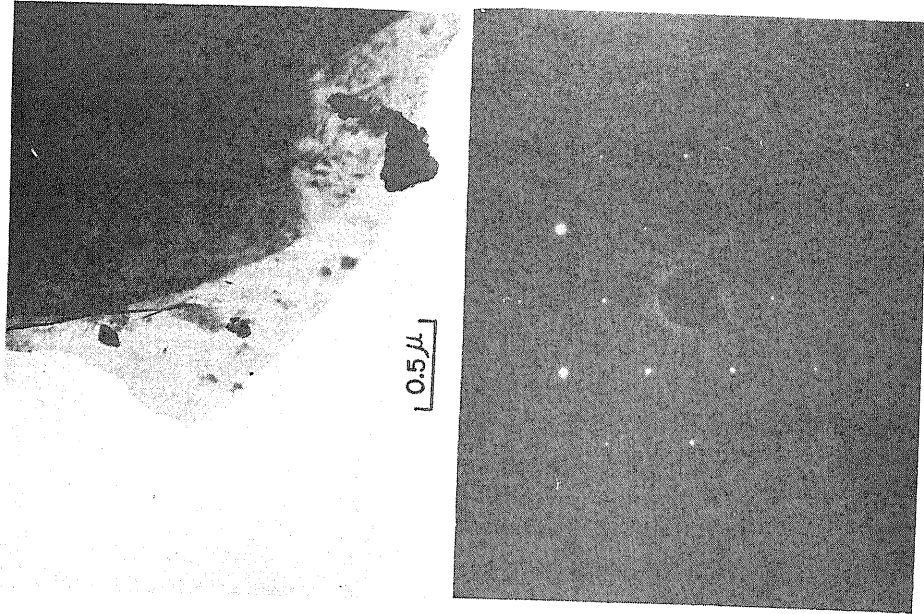


**Fig.29 Particle showing diffraction pattern of six-fold symmetry of graphite single crystal overlapping on reflection ring**



(a) particle having turbostratic structure



(b) particle having graphitic structure

Fig.30 Bright-field micrographs and selected area diffraction patterns taken on carbon specimen heat-treated at 1070 °C for 60 min with calcium carbonate under 3.2 kbar

### c. Accelerating Effect of Calcium Hydroxide.

#### (1) Introduction.

It was found in the works described in above sections that the graphitization of carbon is accelerated by the heat treatments under pressure in the presence of limestone and calcium carbonate. The beginning of graphitization, that is, the appearance of the component having the graphitic structure, was found to be closely related to the recrystallization of coexisting minerals (see Fig. 28).

According to Wyllie and Tuttle, the melting point of calcium carbonate is greatly depressed by the addition of a small amount of water. For example, the melting point of calcium carbonate,  $1310^{\circ}\text{C}$  at 1kbar, is depressed to  $1130^{\circ}\text{C}$  by the addition of only 8wt% of water. In the preliminary experiment, the carbon sample was heat-treated under pressure in the presence of calcium carbonate disks, which absorbed about 8wt% of water. The graphitization of carbon was found to start at about  $1000^{\circ}\text{C}$ , about  $100^{\circ}\text{C}$  lower than that in the case of dry calcium carbonate. However, it was difficult to draw any conclusion, because the exact control of the amount of water in calcium carbonate disks was technically difficult with the arrangement of pressure cell used and because it was not known whether water vapor affects the graphitization of carbon or not.

In the present work, the heat treatments of carbon were performed under pressure in the presence of calcium hydroxide, whose melting point is known to be  $840^{\circ}\text{C}$  at 3kbar, in order to confirm the relation between the graphitization of carbon and recrystallization or melting of coexisting minerals.

#### (2) Experimental and Results.

The carbon sample used was the coke PV-7 (see section 2.a.). The disks of calcium hydroxide, 8.0mm in diameter and 3.5mm thick, were prepared by compressing calcium hydroxide powder (chemical reagent grade) under 3.5kbar. The bulk density of the disks was about  $2.2\text{g}/\text{cm}^3$  (ca. 15% porosity). The disks and powder of calcium hydroxide were kept in an evacuated desiccator to avoid the absorption of carbon dioxide during the

storage. The heat treatment were performed at temperatures between  $600^{\circ}\text{C}$  and  $850^{\circ}\text{C}$  for residence times of 20 - 240min under 3.2kbar. The arrangement of pressure cell and the procedure for the heat treatments were exactly the same as described previously. The heat treatments above  $850^{\circ}\text{C}$  were failed because the melt of the coexisting calcium hydroxide reacted with the graphite heater and invaded into the graphite heater.

The profiles of (002) diffraction line for the central part of the heat-treated specimens were measured by using Ni-filtered  $\text{CuK}\alpha$  radiation (see section 2.f.). The same part of the specimen was dispersed in trichloroethylene by ultrasonic vibration, supported on an evaporated carbon film, and then observed with transmission electron microscope.

The carbon specimens heat-treated above  $600^{\circ}\text{C}$  were obtained as caked tablets. In the cakes, calcium hydroxide was detected by X-ray diffraction method. The disks of calcium hydroxide recrystallized when the carbon specimen was heat-treated above  $600^{\circ}\text{C}$ , and were found to melt above  $800^{\circ}\text{C}$  at the part in contact with carbon specimen. Above  $800^{\circ}\text{C}$ , a small amount of calcium oxide was detected by X-ray diffraction method not only in the disks of calcium hydroxide but in the carbon specimen.

Figure 31 shows the change of observed profile of (002) diffraction line by heat treatment. Above  $800^{\circ}\text{C}$ , a sharp peak corresponding to the graphitic component  $G_M$  was observed overlapping on a broad band. The composite profiles were separated graphically into two component profiles for the graphitic component  $G_M$  having almost constant  $c_o$ -spacing of  $6.72\text{\AA}$ , and the component  $A_M$  of  $6.90\text{\AA}$  which was not so different from the original value of  $6.91\text{\AA}$ . The measured content of the component  $G_M$  is given for each profile in Fig. 31. The content of the component  $G_M$  increased slightly with the increase of residence time. However, it was evident that the increase of HTT seemed to be more effective than that of residence time, if the result at  $850^{\circ}\text{C}$  for 20min was compared with that at  $800^{\circ}\text{C}$  for 60min.



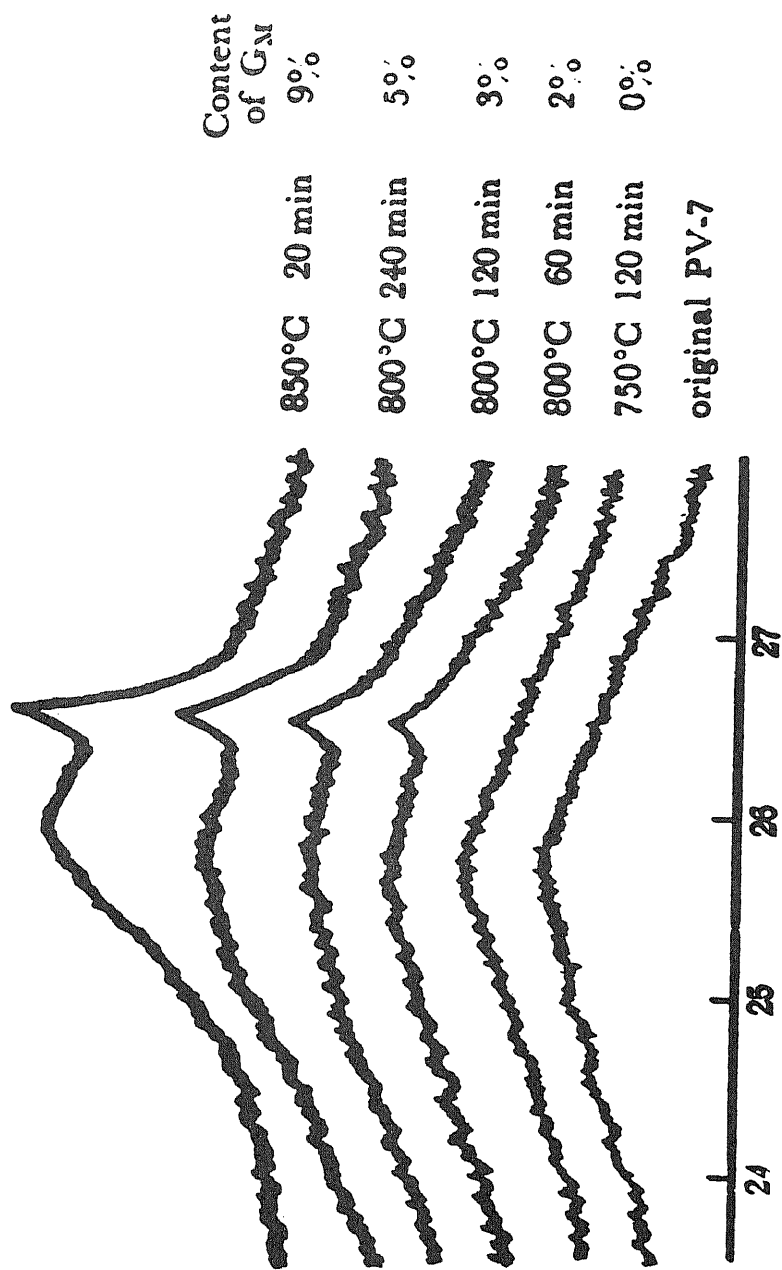


Fig.31 Change of observed profile of (002) diffraction line with heat treatment

By electron microscopic observation, the particles having the diffraction pattern of six-fold symmetry of graphite single crystal were found besides the particles having the turbostratic structure even in the specimen heat-treated at 600°C for 60min, for which any indication of the presence of the graphitic component  $G_M$  was not found on the profile of (002) line. Bright-field micrographs and selected area diffraction patterns of graphitic and turbostratic particles in the carbon specimen heat-treated at 600°C are shown in Figs. 32 and 33, respectively.

#### d. Discussion and Summary.

The graphitization of carbon under pressure was evidently accelerated in the presence of limestone. Under 3.2kbar in the presence of limestone, the graphitic component  $G_M$  began to appear just above 1050°C and consequently the composite profile of (002) line was observed. This temperature was found to be much lower than that in the case of the heat treatment of the same carbon sample under the same pressure without limestone. As mentioned before, the graphitic component  $G_M$  appeared in the carbon specimen heat-treated at 1070°C for 60min under 3.2kbar with calcium carbonate, while no graphitic component  $G_M$  could be found in the carbon specimens heat-treated up to 1500°C under 3.2kbar without any minerals and under a flow of nitrogen with calcium carbonate. The temperature at which the formation of the graphitic component began was almost the same in the case of limestone and of calcium carbonate. Conclusively, calcium carbonate itself, which is the chief ingredient of limestone, accelerates the graphitization of carbon under pressure; (1) The increase of content of the graphitic component with heat treatment temperature was less steep in the case of calcium carbonate than in the case of limestone, (2) The  $c_o$ -spacing of the component  $A_M$  in the case of limestone decreased rapidly with heat treatment temperature and reached about 6.80Å at 1300°C, while the  $c_o$ -spacing in the case of calcium carbonate decreased only to 6.89Å even with the same heat treatment, (3) The heat treatment temperature, at which a trace of decomposition was found in the disk, was 1250°C in the case of

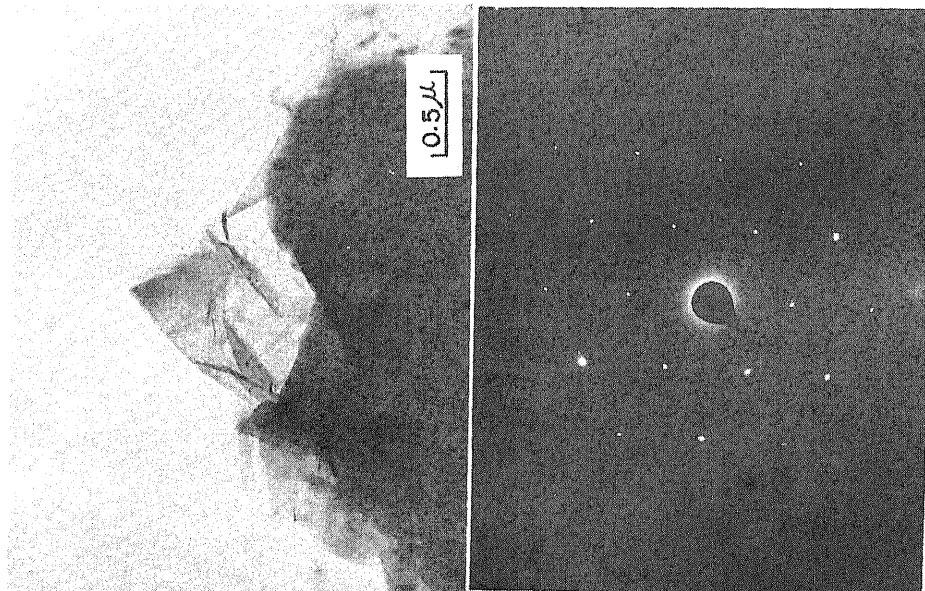


Fig.32 Bright-field micrograph and selected area diffraction pattern of graphitic particle in carbon specimen heat-treated at 600 °C for 60 min under 3.2 kbar

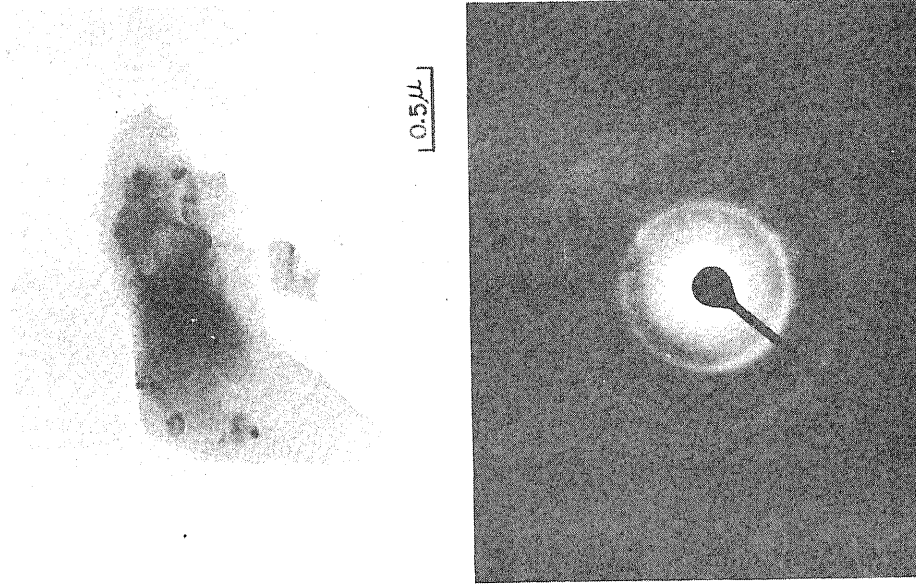


Fig.33 Bright-field micrograph and selected area diffraction pattern of turbostratic particle in carbon specimen heat-treated at 600 °C for 60 min under 3.2 kbar

limestone, but  $1350^{\circ}\text{C}$  in the case of calcium carbonate. (4) In addition, the thickness of the recrystallized layer in the disk of limestone was larger than that of calcium carbonate at the same heat treatment temperature.

These differences in accelerating effect on graphitization between limestone and calcium carbonate seem to result from higher purity and lower density of the disks of calcium carbonate than limestone. Silica, alumina and iron oxide, which were reported as impurities in Fusulina limestone used, are known as the catalysts for graphitization of carbon. Since these minerals are also known to react with calcium oxide at higher temperatures to form low melting compounds, the recrystallization of limestone must be accelerated. On the other hand, lower density of the disks causes the decrease in the thermal conductivity. Thus the gradients of pressure and temperature in the graphite heater may be different in these two cases, that is the gradients of pressure and temperature in the case of calcium carbonate seemed to be more steeper than those in the case of limestone. However, it is suggestive that the same relation between the thickness of the recrystallized layer of the disk and the content of the component  $G_M$  holds both in the cases of limestone and calcium carbonate.

The accelerating effect of coexisting calcium hydroxide on graphitization of carbon is more remarkable than those of limestone and calcium carbonate. Even at a heat treatment temperature as low as  $600^{\circ}\text{C}$ , the particles having the graphitic structure were found with electromicroscope. The temperature of the beginning of formation of the graphitic component  $G_M$  on the (002) profile is much lower than those found in the heat treatments of the same coke in the presence of limestone and calcium carbonate, as well as without any minerals.

The experimental results obtained from X-ray diffraction and electromicroscopy on the heat-treated carbon sample, described in details in previous sections, suggested that the component  $A_M$  and the component  $G_M$  coexisted individually with fairly large-sized crystallite in the same heat-treated carbon specimen and the turbostratic component  $A_M$  had transformed directly to the graphitic component without going through any

intermediate state between turbostratic and graphitic structures. This heterogeneous process of graphitization looks like to be similar to that observed on the same carbon heat-treated under pressure without any coexisting mineral . However, there is a definite difference in the graphitization process between the heat treatments of carbon only and of carbon with calcium compounds under pressure. In the case of the heat treatments of carbon under pressure without any minerals, the graphitic component could be observed on the X-ray diffraction profiles only after the  $c_0$ -spacing of the turbostratic component decreased to about  $6.84\text{\AA}$ . In the case of the heat treatments of carbon under pressure with calcium compounds, however, the transformation of the turbostratic component to the graphitic component began to occur even when the  $c_0$ -spacing of the turbostratic component  $A_M$  was measured to be around  $6.90\text{\AA}$  which was not so different from the original value. These facts seem to suggest that the mechanism of these two processes may be different from each other. This deduction is considered to be certified reasonable by the additional fact that the graphitic component began to appear at much lower temperature in the heat treatments of carbon with coexisting minerals, for instance, at  $600^\circ\text{C}$  in the presence of calcium hydroxide, than that without any coexisting minerals.

The fact that a small amount of free calcium oxide was found in the heat-treated specimens suggests a chemical theory of acceleration of graphitization. Reactive calcium oxide formed by the decomposition of calcium compounds, such as calcium carbonate and calcium hydroxide, is well known to react with amorphous carbon at relatively low temperature to form an intermediate compound which decomposes inversely to form stable graphite and calcium oxide.

#### 4. Effect of Reactivity of Coexisting Calcium Oxide on the Graphitization of Carbon under Pressure.

In this chapter, the experimental result of the heat treatments of carbon under pressure in the presence of three kinds of calcium oxide, which have different reactivity from one another, and the result of the measurement of the distribution of calcium element in the carbon specimens heat-treated in the presence of calcium compounds were presented. These results are discussed in relation to the mechanism of accelerating effect of calcium compounds on graphitization under pressure.

##### a. Accelerating Effect of Calcium Oxide.

###### (1) Introduction.

It was found in the previous works that the graphitization of carbon was accelerated by the coexistence of calcium carbonate and hydroxide during the heat treatment under the pressure of 3kbar. The graphitic component began to appear in carbon specimen at about 1050°C in the presence of calcium carbonate or limestone and at about 600°C in the presence of calcium hydroxide. The (002) diffraction line of these specimens had a composite profile, that is, graphitic component co-existed side by side with turbostratic component. The turbostratic component transformed directly to the graphitic component without going through intermediate state. Though this heterogeneous process of graphitization seems to be similar to that observed on the same carbon heat-treated under pressure without any coexisting mineral, the mechanism of accelerating effects of these two processes were considered to be different from each other. As one of the possible mechanism of accelerating effect, the intermediate formation of unstable carbide was suggested to occur by a chemical reaction of carbon with co-existing compounds.

In the present work, calcium oxide calcined at different temperatures were used as the coexisting mineral in the heat treatment of carbon under pressure of 3.2kbar. The effect of reactivity of calcium oxide on the acceleration of graphitization

was examined.

(2) Experimental.

The carbon sample used was the coke PV-7 (see section 2.a.). Three kinds of calcium oxide were prepared in the form of disk of 8.0mm in diameter and 3.5mm in thickness by calcination of disk of calcium carbonate at 920, 1050 and 1470°C for 60min, respectively. It was checked by X-ray diffraction method whether calcium carbonate had decomposed completely or not. The disks of calcium oxide thus prepared were covered with calcium oxide powder and kept in an evacuated desiccator. Any indication of calcium hydroxide and carbonate could not be detected in X-ray diffraction pattern in the disks of calcium oxide remained in the evacuated desiccator after all the experiments were finished. The crystallite size and bulk density of three kinds of calcium oxide thus prepared (designated as CaO-9, CaO-10 and CaO-15) are shown in the following Table 1.

Table 1. Properties of Calcium Oxide used.

Sample	Calcination °C	min	Crystallite Size Å	Bulk Density g/cm <sup>3</sup>	Porosity %
CaO-9	920	60	720	2.78	18
CaO-10	1050	60	950	2.88	15
CaO-15	1470	60	>1000	2.95	13

Calcium oxide calcined at a lower temperature is known to be more reactive <sup>(67)~(69)</sup>.

The heat treatment of the carbon sample in the presence of calcium oxide was carried out at various temperatures between 900 and 1500°C for 60min under the quasi-hydrostatic pressure of 3.2kbar in a simple piston-cylinder type vessel. The cell arrangement and the procedure for the experiments were exactly the same as described before (see section 2.e.).

The profile of (002) diffraction line was measured from the central part of the heat-treated carbon specimen by using Ni-filtered CuK $\alpha$  radiation and a recording goniometer. The composite profile observed was separated graphically into two

component profiles corresponding to the graphitic component  $G_M$  and turbostratic component  $A_M$ , and then the  $c_0$ -spacing, crystallite size  $L_c$  and the content of the graphitic component  $G_M$  were measured.

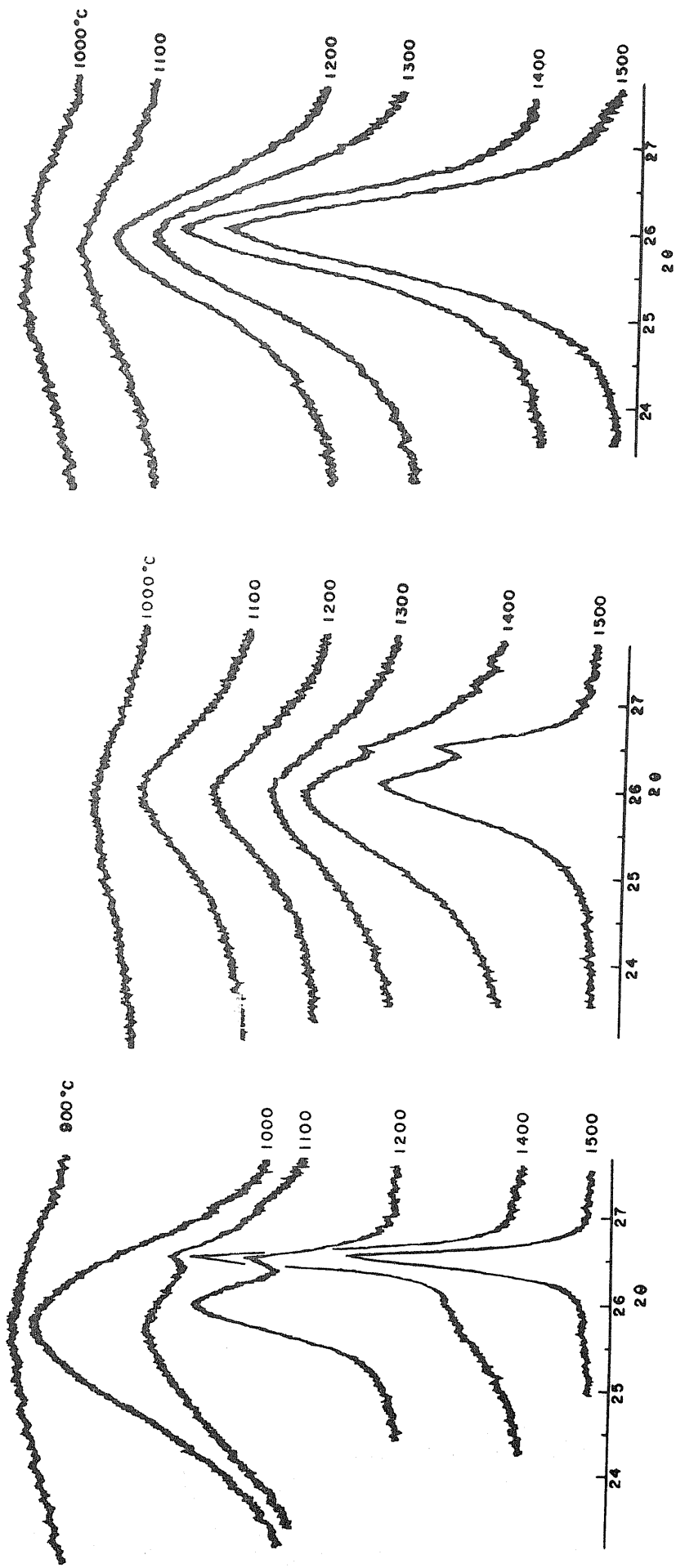
### (3) Results.

Carbon specimens heat-treated above  $1000^\circ\text{C}$  were obtained as a caked tablets. In these caked specimens, calcium oxide was always detected by X-ray diffraction method and its amount increased with the increase of heat treatment temperature (HTT). In the specimens heat-treated above  $1300^\circ\text{C}$  in the presence of CaO-9 and those heat-treated above  $1400^\circ\text{C}$  in the presence of CaO-10, calcium carbide was detected in the part where carbon and calcium oxide contacted with each other. Recrystallization of calcium oxide was not observed in the present experiment.

The changes of profile of (002) line with HTT are shown in Figs. 34 a), b) and c). It can be seen from these figures that there is a certain difference in the accelerating effect of the three kinds of calcium oxide on graphitization of carbon. In the presence of CaO-9, the graphitization of the carbon began at about  $1100^\circ\text{C}$  and the profile for the graphitic component  $G_M$  developed rapidly with the increase of HTT. The graphitization of the same carbon was found to begin at about the same HTT in the presence of limestone and calcium carbonate as shown in the last chapter. In the presence of CaO-10, the graphitic component  $G_M$  was detectable on (002) profile above  $1400^\circ\text{C}$ . In the presence of CaO-15, however, the graphitic component  $G_M$ , even hump at the corresponding diffraction angle, could not be detected up to  $1500^\circ\text{C}$ . From profile of (004) line, the same results were deduced.

The variations of content of the graphitic component  $G_M$  in the presence of calcium oxides are shown in Fig. 35 as a function of HTT. In the presence of the most reactive calcium oxide CaO-9, the graphitic component  $G_M$  increased very rapidly. It turned out almost 100% at HTT of  $1500^\circ\text{C}$ . In the presence of less reactive CaO-10, however, only a small amount of the graphitic component  $G_M$  was found above  $1400^\circ\text{C}$  and in the presence of CaO-15 no graphitic component  $G_M$  was observed





(a) in the presence of CaO-9

(b) in the presence of CaO-10

(c) in the presence of CaO-15

Fig.34 Change of profile of (002) diffraction line with HTT

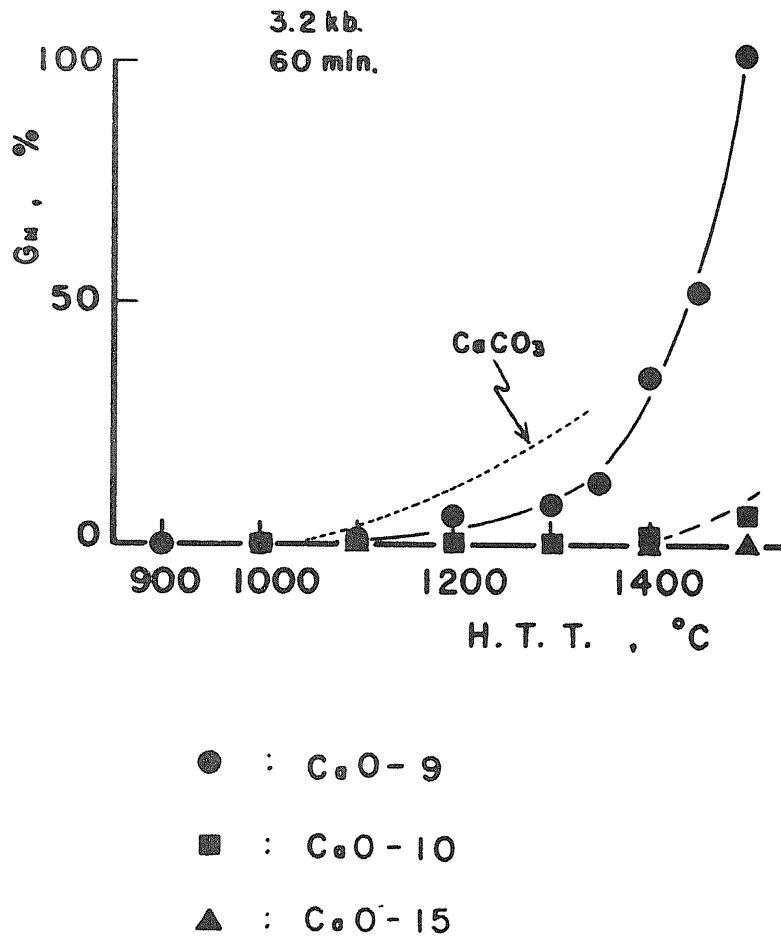


Fig.35 Variation of content of graphitic component GM with HTT

up to 1500°C.

The changes of  $c_0$ -spacing and crystallite size  $L_c$  with HTT are given in Figs. 36 a) and b) together with the results in the presence of calcium carbonate and without any coexisting mineral. The  $c_0$ -spacing of the graphitic component  $G_M$  was almost constant at 6.72Å in all cases. The crystallite size  $L_c$  of the component  $G_M$  increased with the increase of HTT, and become larger than 1000Å at 1500°C in the case of CaO-9. The  $c_0$ -spacing of the turbostratic component  $A_M$  decreased gradually and its crystallite size  $L_c$  increased only slightly with the increase of HTT.

In the specimens heat-treated above 1100°C in the presence of CaO-9 and those heat-treated above 1400°C in the presence of CaO-10, well-crystallized flaky particles, having the same six-fold diffraction pattern as graphite single crystal, were found under an electron microscope, besides the particles having continuous diffraction rings. Bright-field micrographs and selected area diffraction patterns of graphitic and turbostratic particles in the carbon specimen heat-treated at 1100°C with CaO-9 are shown in Figs. 37 and 38, respectively.

#### b. Distribution of Calcium and Graphitic component in Heat-Treated Specimens.

##### (1) Introduction.

It was found that the graphitization of carbon was remarkably accelerated by the heat treatment under pressure in the presence of coexisting calcium compounds. The mechanism of the accelerating effect on the graphitization was suggested to be a chemical one. If so, there must be certain relation between the content of calcium and that of the graphitic component  $G_M$  in the carbon specimen heat-treated under pressure.

In the present work, the distribution of calcium element in carbon specimens heat-treated in the presence of calcium compounds under pressure was measured by using an electron microprobe analyser, and compared with the distribution of the graphitic component  $G_M$  which was determined from the X-ray diffraction method.

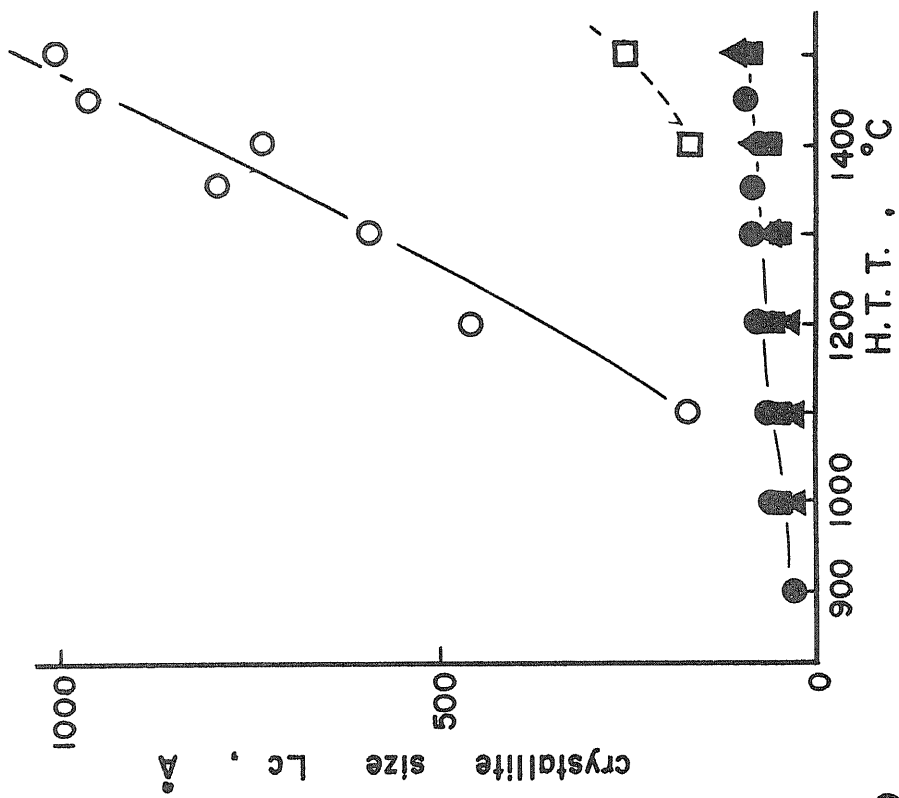


Fig.36 b) Change of crystallite size Lc with HTT

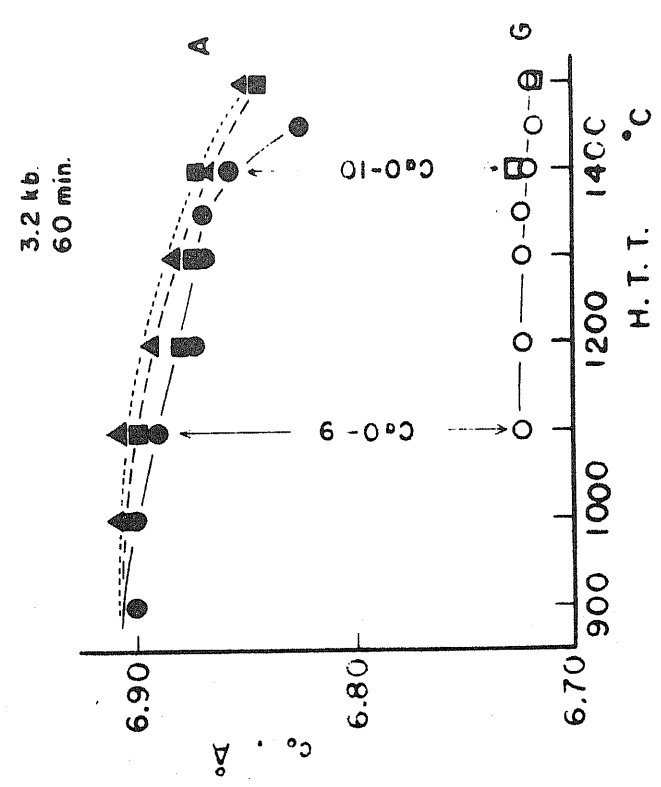


Fig.36 a) Change of co-spacing with HTT

- : CaO-9
- : CaO-10
- ▲ : CaO-15

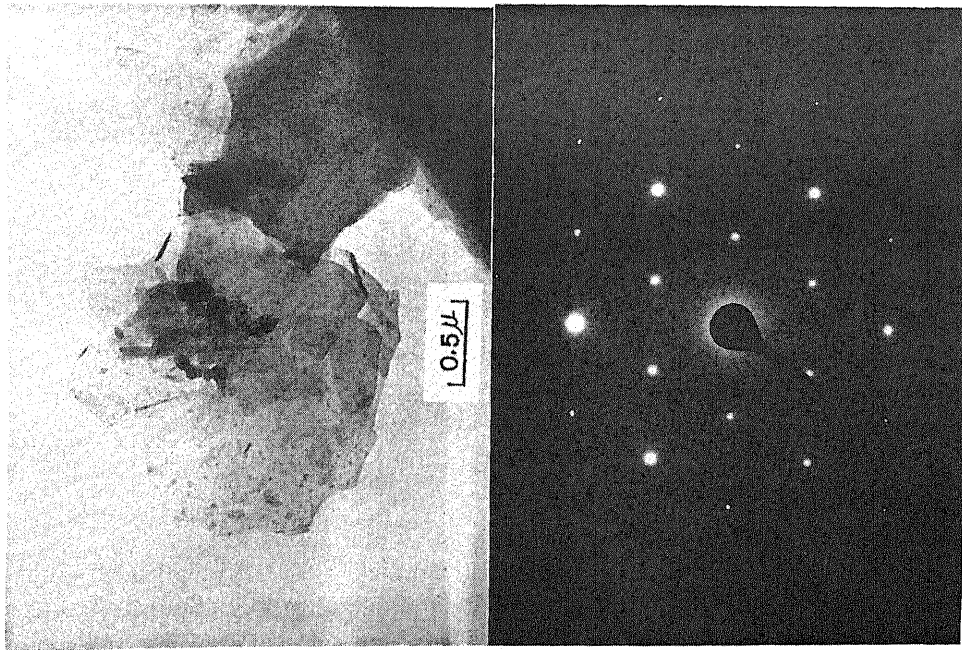


Fig.37 Bright-field micrograph and selected area diffraction pattern of graphitic particle in carbon specimen heat-treated with CaO-9 at 1100 °C under 3.2 kbar

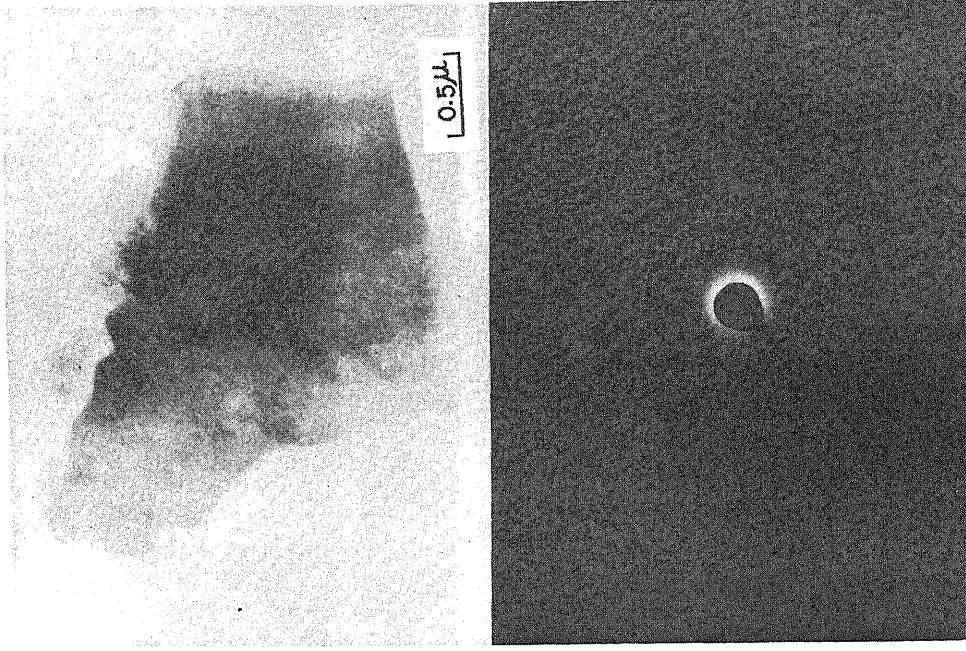


Fig.38 Bright-field micrograph and selected area diffraction pattern of turbostratic particle in carbon specimen heat-treated with CaO-9 at 1100 C under 3.2 kbar

## (2) Experimental and Results.

The specimens used were the caked ones heat-treated under 3.2kbar for 60min at 1090° and 1360°C in the presence of calcium carbonate, and at 1100°, 1400° and 1500°C in the presence of calcium oxide CaO-9. The details of the heat treatments are described in the previous section. The size of the caked specimens was about 7.6mm in diameter and 2.5mm in thickness.

The specimen was cut into halves across their diameter. One half was used for the electron microprobe analysis and the other for the X-ray diffraction analysis.

The half for the electron microprobe analysis was mounted in resin, and the surface of the cross section was polished on an abrasive paper and finished to a very flat surface by using a felt with very fine corundum powder dispersed in ethanol. The use of ethanol was essential so as to avoid reactions between calcium compounds in the carbon specimen and water. Two kinds of width of electron beam, 10 $\mu$  and 100 $\mu$ , were used in the present work. Electron beam was scanned along the thickness (h-direction) and also along the radial direction (r-direction) on the polished section of the caked specimen as shown in Fig. 39.

The sample for the X-ray diffraction analysis was taken from the different parts of the other half of the caked specimen as shown in Fig. 40.

In Figs. 41 a) and b), the profiles of (002) diffraction line are shown for different parts of the specimen heat-treated under 3.2kbar at 1280°C in the presence of calcium carbonate and at 1300°C in the presence of CaO-9, respectively. The content of the graphitic component  $G_M$  was measured from these profiles (see section 2.f.(2)).

The distributions of calcium obtained with the electron beam width of 100 $\mu$  are shown in Figs. 42 and 43. In these figures, the distribution of the component  $G_M$  is shown in figures. The content of the component  $G_M$  could be determined as an average over a range of distance showed with the arrows, because certain mass of the carbon was needed for X-ray diffraction. In the presence of calcium carbonate, the content of the graphitic component  $G_M$  was found to be larger in the

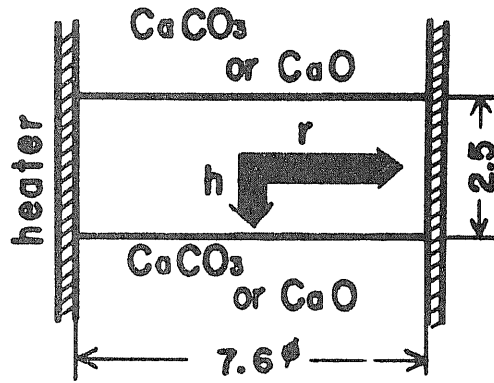


Fig.39 Direction of scanning of electron beam on polished section of caked carbon specimen

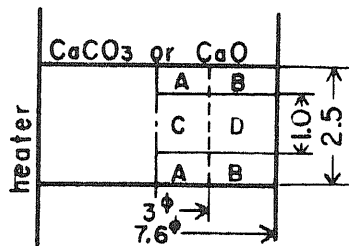
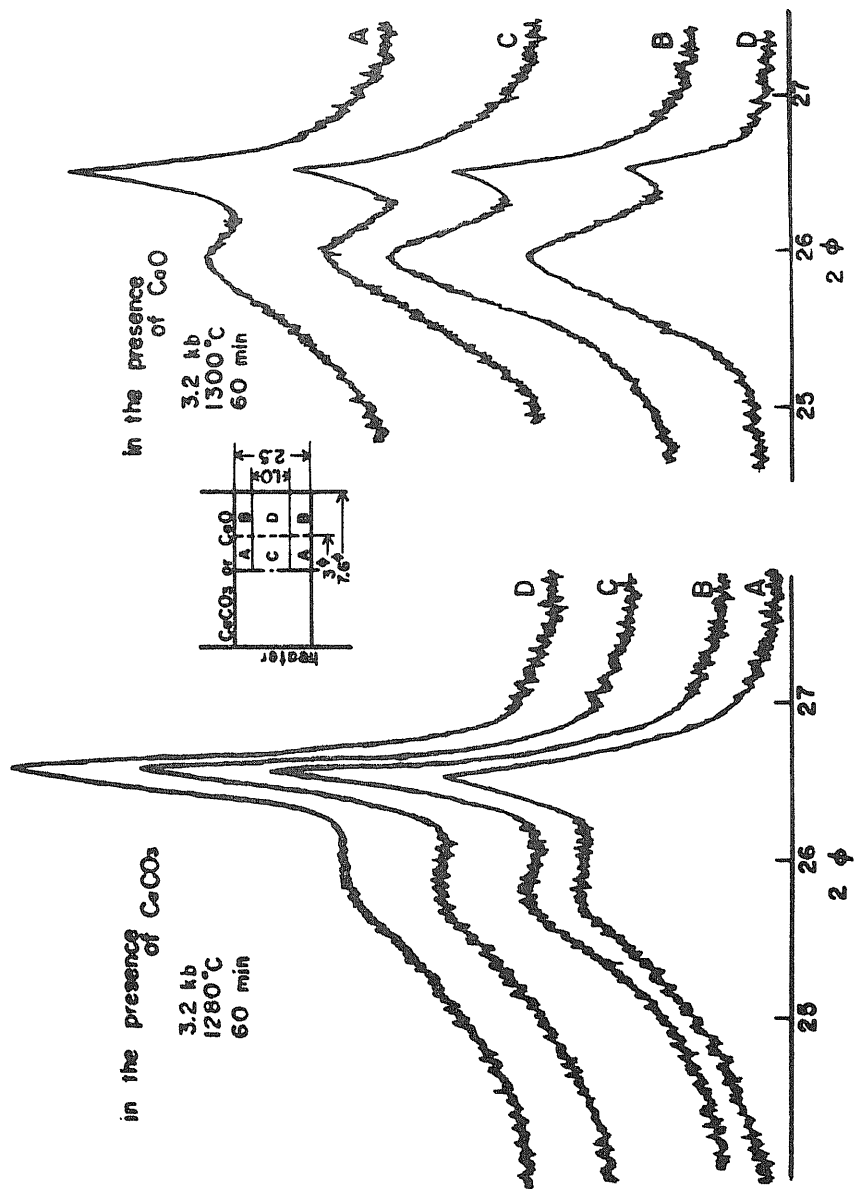


Fig.40 Schema of part from which sample for X-ray diffraction analysis was taken



(a) heat-treated under 3.2 kbar at 1280°C in the presence of  $\text{CaCO}_3$  (b) heat-treated under 3.2 kbar at 1300°C in the presence of CaO-9

Fig.41 Profiles of (002) diffraction line for different parts of carbon specimen



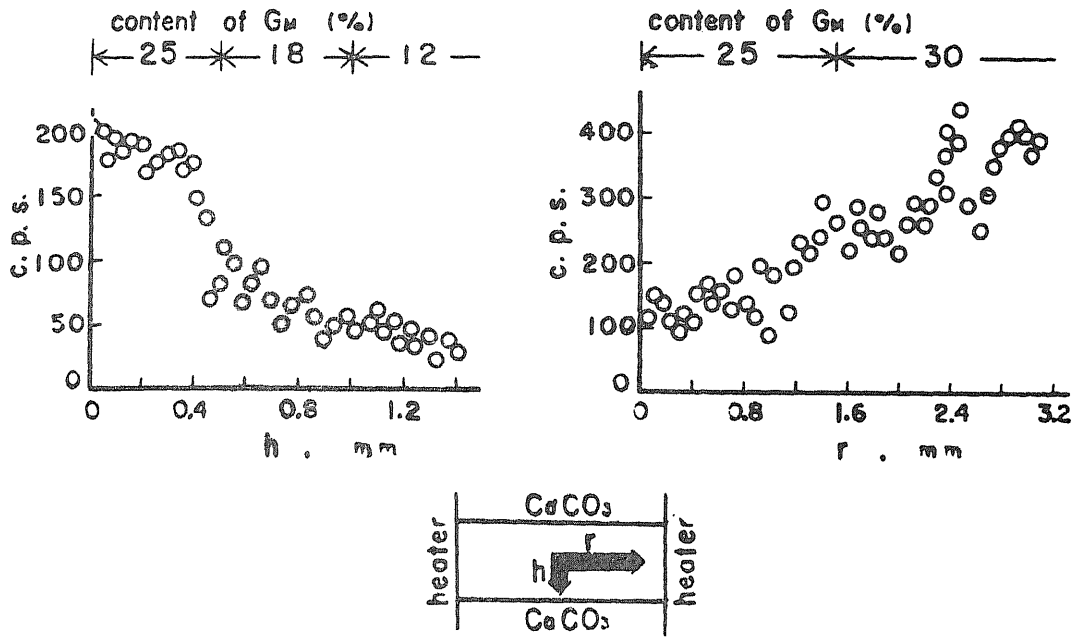


Fig.42 Distribution of calcium obtained with electron beam width of  $100\mu$  on carbon specimen heat-treated at  $1360^\circ C$  under 3.2kbar in the presence of  $CaCO_3$

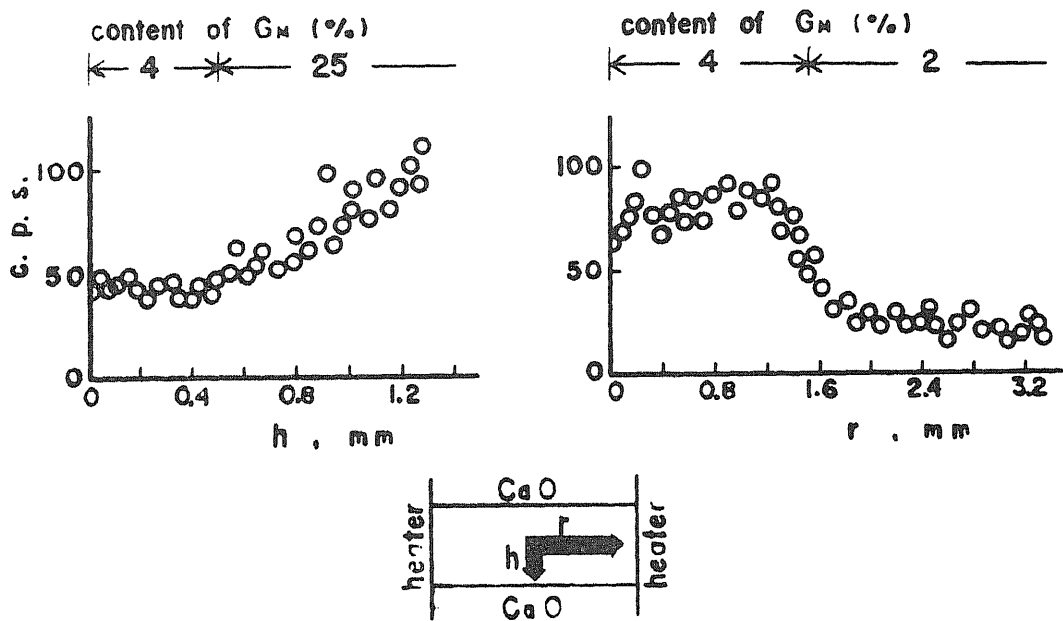


Fig.43 Distribution of calcium obtained with electron beam width of 100 on carbon specimen heat-treated at  $1100^\circ C$  under 3.2kbar in the presence of  $CaO-9$

central part of the specimen than in the peripheral part which was close to carbonate layer. This distribution of the graphitic component seemed to correspond with a temperature gradient in the specimen described in the section 2.d. and also coincide with the distribution of calcium. In the presence of calcium oxide, on the other hand, the reverse distribution of the graphitic component  $G_M$  was observed as shown in Fig. 43, that is the content of the graphitic component was smaller in the central part than in the peripheral part. However both distributions of the component  $G_M$  and of calcium coincided with each other. The reason why the distribution of calcium in the heat-treated carbon specimen was different in these two cases are not clear yet. However in both cases the part having a larger content of the graphitic component  $G_M$  has a larger concentration of calcium. The same relation was observed for all specimens examined in this work. With the use of the electron beam width of  $10\mu$ , the similar relations were also obtained. Figures 44 and 45 show the results on the specimens heat-treated under 3.2kbar in the presence of calcium carbonate and calcium oxide, respectively.

X-ray fluorescence photographs for carbon and calcium in the central area ( $400\mu \times 400\mu$ ) of the specimen heat-treated at  $1360^\circ\text{C}$  under 3.2kbar in the presence of calcium carbonate are shown in Figs. 46 a) and b). The concentration variation of calcium scanned from A to B (in Fig. 46 b)) across a carbon grain is shown in Fig. 46 c). From these results one can see that calcium was accumulated mainly in boundaries of carbon grains. The concentration of calcium in the carbon grain decreased very steeply within the distance of about  $10\mu$  from the boundary and only a minute amount of calcium was detected in the inner part of grain. The same result was obtained for the specimen heat-treated at  $1100^\circ\text{C}$  under 3.2kbar in the presence of calcium oxide, as shown in Figs. 47 a), b) and c).

### c. Heat Treatments of Calcium Carbide under Pressure.

#### (1) Introduction.

From the fact that calcium carbide was formed in the carbon specimen heat-treated above about  $1300^\circ\text{C}$  under 3.2kbar

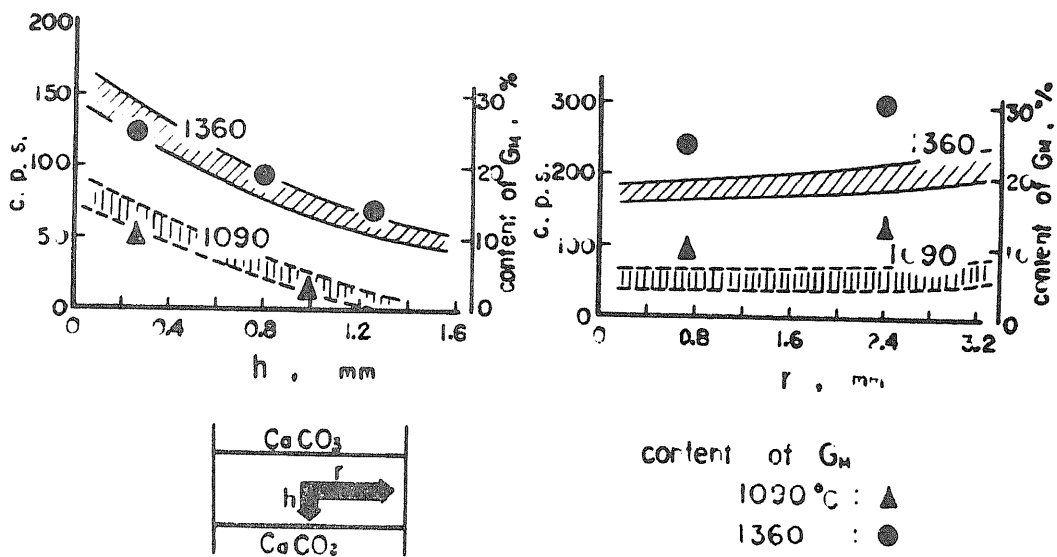


Fig.44 Distribution of calcium obtained with electron beam width of  $10\mu$  on carbon specimens heat-treated at  $1090^\circ\text{C}$  and  $1360^\circ\text{C}$  under 3.2kbar in the presence of  $\text{CaCO}_3$

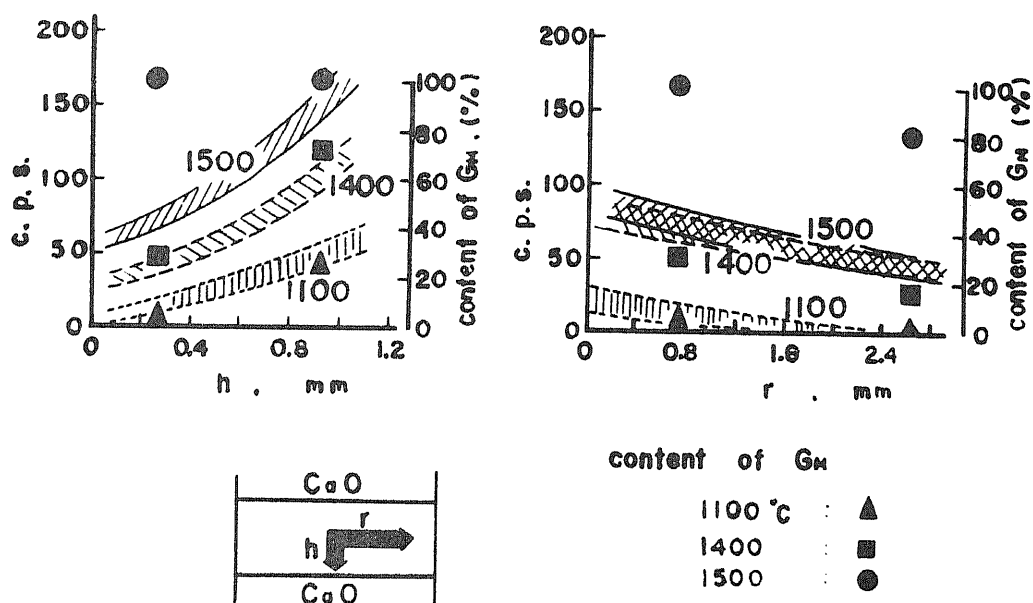


Fig.45 Distribution of calcium obtained with electron beam width of  $10\mu$  on carbon specimens heat-treated at  $1100$ ,  $1400$  and  $1500^\circ\text{C}$  under 3.2kbar in the presence of  $\text{CaO-9}$

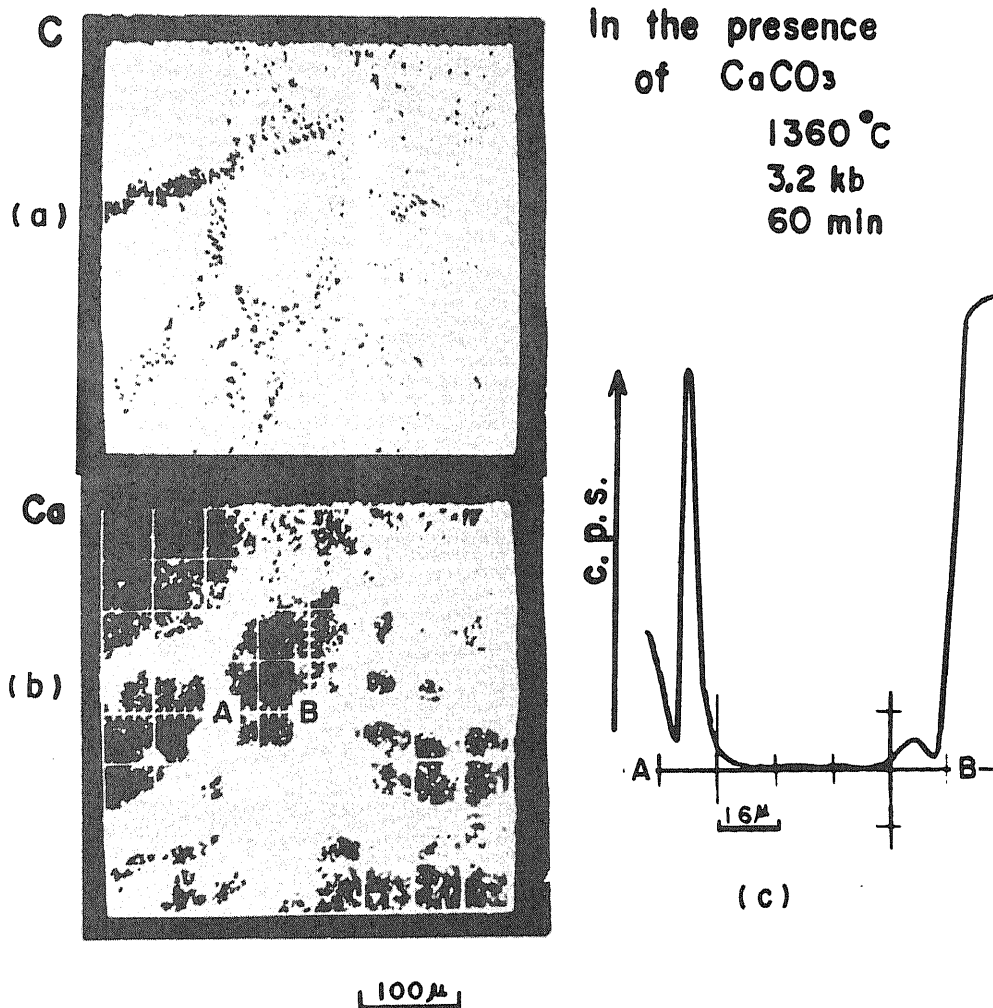


Fig.46 X-ray fluorescence photographs for carbon and calcium in the central area of carbon specimen heat-treated at 1360 °C under 3.2kbar in the presence of  $\text{CaCO}_3$

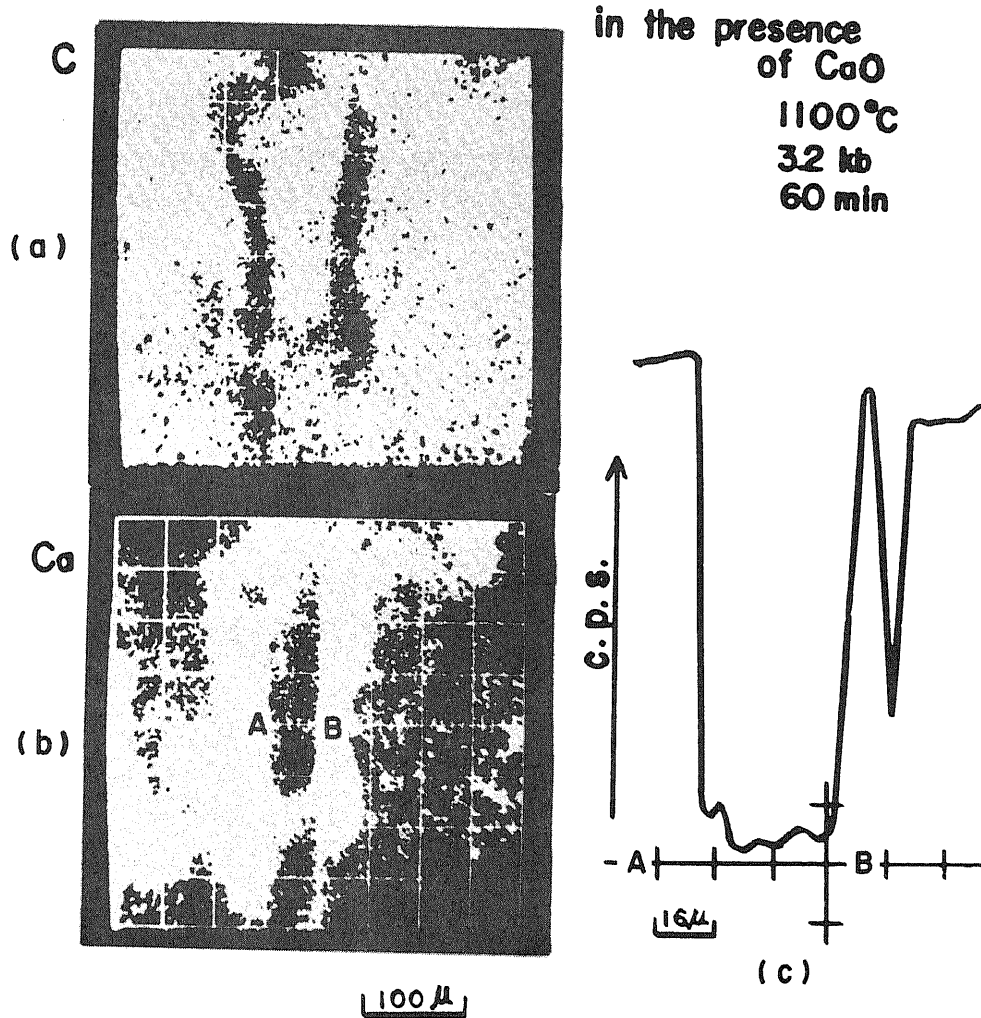


Fig.47 X-ray fluorescence photographs for carbon and calcium in the central area of carbon specimen heat-treated at 1100°C under 3.2kbar in the presence of CaO-9

in the presence of calcium oxide, it was necessary to examine the possibility of the formation of graphitic component through decomposition of calcium carbide under pressure in order to deduce the possible mechanism of the formation of the graphitic component  $G_M$ . In this section, the heat treatments of calcium carbide were carried out under 3.2kbar and the formation of the graphitic component was discussed.

## (2) Experimental and Results.

Calcium carbide used was powder of the grain size of 0.1 - 0.7mm, which was obtained by pulverizing calcium carbide mass (ca. 95% purity), and kept in an evacuated desiccator during storage and handled carefully.

Heat treatments of calcium carbide were performed under 3.2kbar at various temperatures between 900 and 1500°C with the cell arrangement shown in Fig. 48. In this cell arrangement, calcined pyrophyllite sleeve was used around the graphite heater so as to avoid the reaction of calcium carbide with water vapor caused from the decomposition of pyrophyllite during heat treatment.

The content of the graphitic component formed by heat treatment under 3.2kbar was measured according to the following chemical method. (1) The specimen taken from the central part of the heat-treated calcium carbide specimen was weighed (A in mg). (2) It was put into diluted hydrochloric acid. After dissolving calcium compound completely, the solution was filtered with a glass filter. (3) After drying the residue completely, it was weighed (B in mg). This residue was known by X-ray diffraction method to consist of the graphitic component and the turbostratic component. The turbostratic component seemed to result from free carbon contained in the original calcium carbide as an impurity. (4) The original calcium carbide was treated by the same method as mentioned above and the proportion of free carbon was estimated (C in wt%). Thus the content of the graphitic component formed was estimated by using the following equation;

the content of  
the graphitic component G (in wt%)  $= \frac{B}{A} \times 100 - C$

assuming that the amount of free carbon (C) did not change after heat treatment.

The heat-treated specimens were also observed under an electron microscope according to the procedure described before.

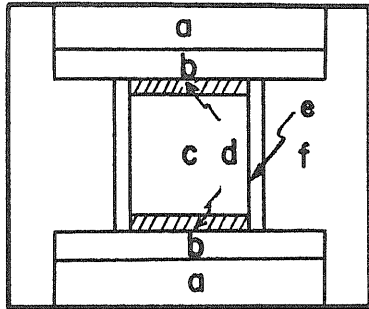
Figure 49 shows the dependence on HTT of the content of the graphitic component formed by the decomposition of calcium carbide under 3.2kbar. The graphitic component was formed in the calcium carbide specimen heat-treated at 1200°C. However, below 1200°C no graphitic component could be detected by X-ray diffraction method. It can be known from this fact that calcium carbide can be decomposed above 1200°C to form the graphitic component and calcium metal.

It should be noted that the determined content of the component  $G_M$  is a sum of the graphitic component formed by the decomposition of calcium carbide and of that formed possibly by the catalytic graphitization of amorphous carbon, which was included in calcium carbide as impurity, by metallic calcium.

Figure 50 shows the bright-field micrograph and selected area diffraction pattern of the graphitic component formed by the decomposition of calcium carbide at 1200°C.

#### d. Discussion.

In the present work, many important facts were found that were essential to elucidate the mechanism of the accelerating effect of the coexisting minerals on graphitization under pressure. From the results of the heat treatments of carbon under 3.2kbar in the presence of three kinds of calcium oxides, it was found that more reactive calcium oxide had more remarkable accelerating effect on graphitization. In the presence of the most reactive calcium oxide calcined at 920°C, the graphitization of carbon began at about the same heat treatment temperature of 1100°C as in the presence of limestone and calcium carbonate and the content of the graphitic component  $G_M$  attained to almost 100% at 1500°C for 60min. While in the presence of the least reactive calcium oxide calcined at 1470°C,



- a : steel disk (18x3)
- b : graphite plate (18x2)
- c : calcium carbide powder
- d : graphite plate (8x1)
- e : graphite heater  
(10-8x10)
- f : pyrophyllite holder

Fig.48 Arrangement of pressure cell for heat treatment of calcium carbide under 3.2 kbar

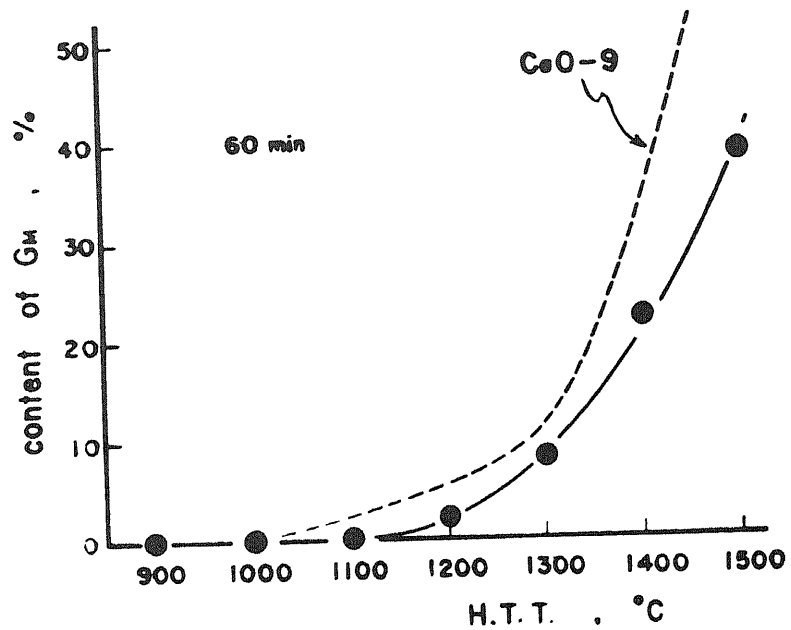


Fig.49 Dependence on HTT of content of graphitic component formed by decomposition of calcium carbide under 3.2kbar



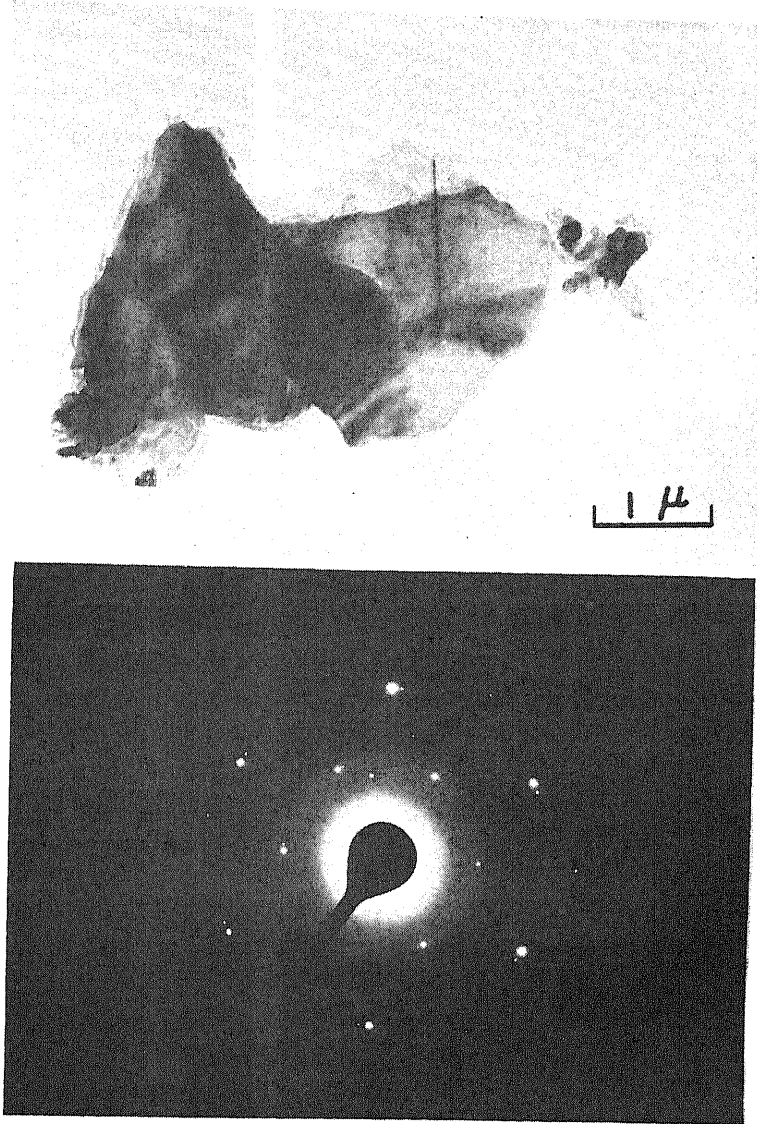
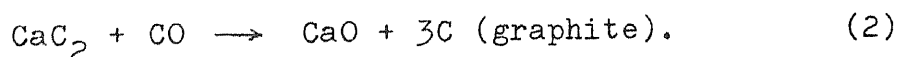
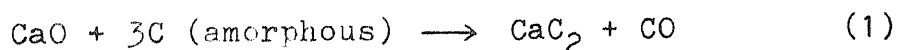


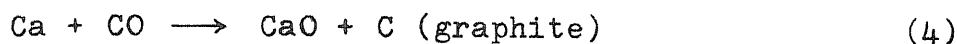
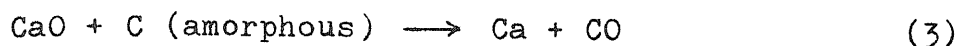
Fig.50 Bright-field micrograph and selected area diffraction pattern of graphitic component formed by decomposition of calcium carbide at 1200°C

the graphitic component, even hump on the profile of (002) diffraction line at the corresponding diffraction angle, could not be detected in specimens heat-treated at 1500°C. It was also found that a part having a larger content of calcium had a larger content of the graphitic component. Calcium carbide was found to decompose above 1200°C under 3.2kbar to form the graphitic component and calcium metal. In addition to these experimental facts, it was supposed that recrystallization or melting of the coexisting minerals might not concern directly with the mechanism of the accelerating effect on graphitization under pressure, because any recrystallization of coexisting calcium oxide could not be observed.

It is suggested from these facts that the formation of the graphitic component in the presence of calcium compounds under pressure proceeds by the following mechanisms. One of possible mechanisms is the intermediate formation and subsequent decomposition of calcium carbide. This mechanism may be explained clearly by using the following formulae,



This mechanism may be effective at temperatures above 1200°C because the formation of the graphitic component  $G_M$  from the decomposition of calcium carbide itself was found above 1200°C under 3.2kbar. Calcium oxide distributed in the carbon specimen must be the decomposition product of calcium carbide according to Eq. (2). The content of the graphitic component should vary with the content of calcium oxide in the carbon specimen and this was in good accordance with the experimental results as shown in the last section 4.b. However, the fact that calcium carbide was not detected below 1200°C in the specimen and the difficulty of the decomposition of calcium carbide under such condition (see Fig. 36) make it impossible to explain the formation of the graphitic component at temperatures below 1200°C by this mechanism. Below 1200°C, the formation of the graphitic component may proceed through the following reactions:



This mechanism must be supported only by the further extensive experiments. However, the formation of the graphitic component by this mechanism is also possible at temperatures higher than 1200°C, though it is not main one. The driving force of the graphite formation through the intermediate formation of calcium carbide or calcium metal is the difference in the free energy between amorphous carbon and graphite, according to two mechanisms mentioned above.

The more reactive calcium oxide reacts with carbon easier or at lower temperature. When calcium carbonate (limestone) or calcium hydroxide was used as the coexisting mineral, nascent oxide formed during the heat treatment may have reacted actively with carbon to form calcium metal.

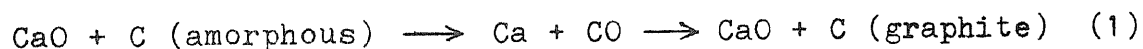
Therefore, the apparent close relation of recrystallization or melting of coexisting calcium carbonate (limestone) and hydroxide with the acceleration of graphitization seems to be mainly due to the increasing rate of reaction of the coexisting minerals with carbon in the neighborhood of temperatures where recrystallization or melting of minerals occurs.

## 5. Accelerating Effect of Some Metal Oxides on Graphitization of Carbon under Pressure.

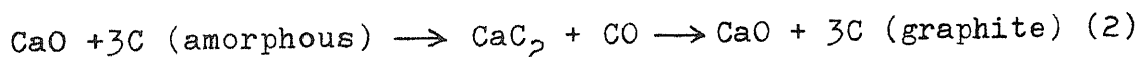
In this chapter, the heat treatments of carbon under pressure were performed in the presence of sodium carbonate, alumina, silica and magnesia in order to verify the mechanism suggested in the last chapter. The possible mechanism was discussed under taking into consideration of the obtained results.

### a. Introduction.

In the previous works, it was found that the accelerating effect of coexisting minerals on graphitization of carbon under pressure was greatly accelerated in the presence of calcium compounds. Two possible mechanisms for the accelerating effect of calcium compounds were proposed on the basis of the experimental results. The formation of the graphitic component was suggested to proceed by the reactions;



below 1200°C and the reactions;



and also by the reactions (1) above 1200°C.

In order to verify these two mechanism for the formation of the graphitic component, the heat treatments of the coke were carried out under 3.2kbar in the presence of sodium carbonate, alumina, silica and magnesia.

### b. Experimental and Results.

(1) Heat Treatments of Carbon under 3.2kbar in the Presence of Sodium Carbonate.

The carbon sample used was the coke PV-7. Disks of sodium carbonate, 8.0mm in diameter and 3.5mm thick, were made by compressing sodium carbonate powder (chemical reagent

grade) under about 4.0kbar. The porosity of the disks was about 87%. The heat treatments were performed at temperatures between 400 and 750°C for the residence time of 60 - 240min under 3.2kbar in a simple piston-cylinder type vessel. As the sodium carbonate decomposes completely and melts at about 820°C, the heat treatment above 800°C was difficult to carry out. The procedure for the heat treatments was exactly the same as used in the previous works. The arrangement B of the pressure cell (Fig. 4) was used, in which the calcined pyrophyllite sleeve is used to avoid the reaction of sodium carbonate with water vapor, which came from the decomposition of pyrophyllite.

The profile of (002) diffraction line of the central part of the heat-treated specimen was measured by using Ni-filtered  $\text{CuK}\alpha$  radiation. The same part of the specimen was observed with transmission electron microscope.

The carbon specimens heat-treated above 500°C for 60min were obtained as caked tablets in which sodium carbonate was found as much as seen with the naked eye. Any graphitic component could not be found on (002) diffraction profile even for the specimen heat-treated at 750°C for 240min, probably due to a small amount of the graphitic component formed. However, by electron microscopic observations, the particles, having the diffraction pattern of six-fold symmetry of graphite single crystal, were found besides the particles, having the turbostratic structure, even in the specimen heat-treated at 500°C for 60min. The number of the graphitic particle seemed to increase with the increases in HTT and in residence time. A bright-field micrograph and a selected area diffraction pattern of such a particle in the carbon specimen heat-treated at 500°C for 60min are shown in Figs. 51 a) and b), respectively.

## (2) Heat Treatments of Carbon under Pressure in the Presence of Alumina and Silica.

The carbon sample used was the coke PV-7. The disks of alumina, 8.0mm in diameter and 3.5mm thick, were prepared by compressing  $\alpha$ -alumina powder which had been obtained by the calcination of alumina powder (chemical reagent grade) at 1200°C for 60min. The porosity of the disks used was about

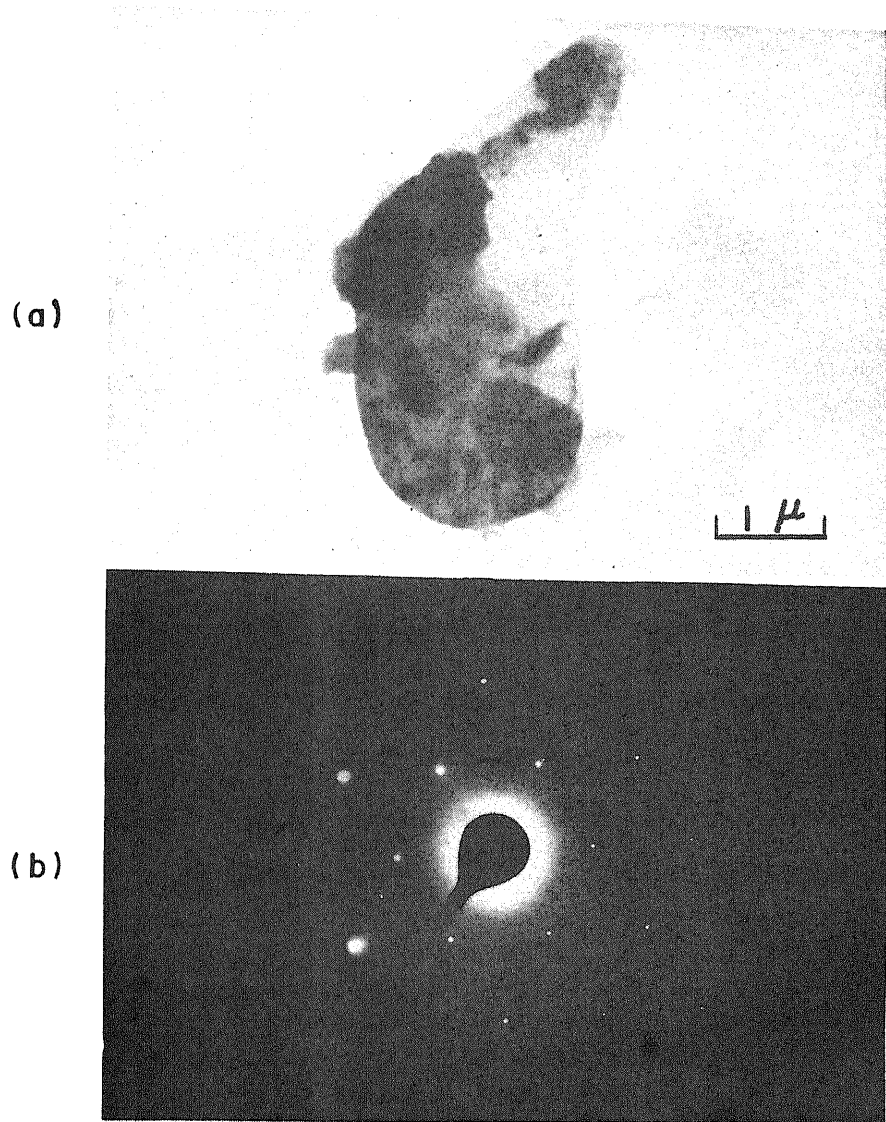


Fig.51 Bright-field micrograph and selected area diffraction pattern of graphitic particle in carbon specimen heat-treated at 500 C for 60min under 3.2kbar in the presence of sodium carbonate

- (a) Bright-field micrograph
- (b) Selected area diffraction pattern

85%. The disks of silica were made by compressing silica powder of which grain size was limited to 250 - 325mesh after calcining silica gel (WAKO Silica-Gel B-0) at 1000°C for 60min. The porosity of the disks of silica was about 83%.

The heat treatments of carbon were performed at various temperatures between 900 and 1500°C for 60min under 3.2kbar. The arrangement A of pressure cell (Fig. 4) was used in the present experiments. The procedure for the heat treatments was the same as described before.

In the presence of alumina, the carbon specimens heat-treated above 1200°C were obtained as caked tablets in which a small amount of aluminum oxide was detected by X-ray diffraction method and, for the carbon specimen heat-treated at 1500°C for 60min, aluminum carbide was detected by X-ray diffraction method in the part of contact with the alumina disk.

In the case of the presence of silica, the carbon specimens heat-treated above 1300°C were obtained as caked tablets. By X-ray diffraction method, a small amount of silicon dioxide was detected in all the caked specimens and even after the heat treatment at 1500°C no silicon carbide was detected.

The changes of the content of the graphitic component  $G_M$  with HTT were shown in Fig. 52. The graphitic component  $G_M$  began to appear in the carbon specimens heat-treated at 1200°C and 1300°C in the presence of alumina and silica, respectively. At 1500°C, the content of the graphitic component  $G_M$  turned out to about 30% in the presence of alumina, but only about 10% in the presence of silica.

A bright-field micrograph and a corresponding selected area electron diffraction on the specimen heat-treated at 1200°C with alumina are shown in Fig. 53.

### (3) Heat Treatments of Carbon in the Presence of Magnesia.

Basic magnesium carbonate, obtained by the reaction between magnesium chloride and sodium carbonate, was dried up and then calcined at 600°C for 60min. The magnesia powder thus prepared was compressed in the form of disk, 8.0mm in

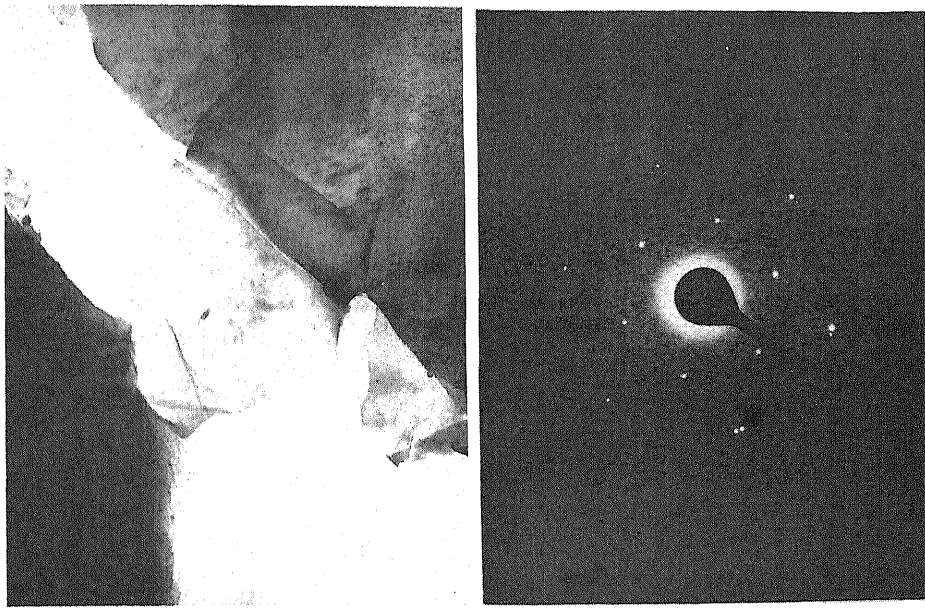


Fig.53 Bright-field micrograph and selected area diffraction pattern on carbon specimen heat-treated at 1200°C with alumina

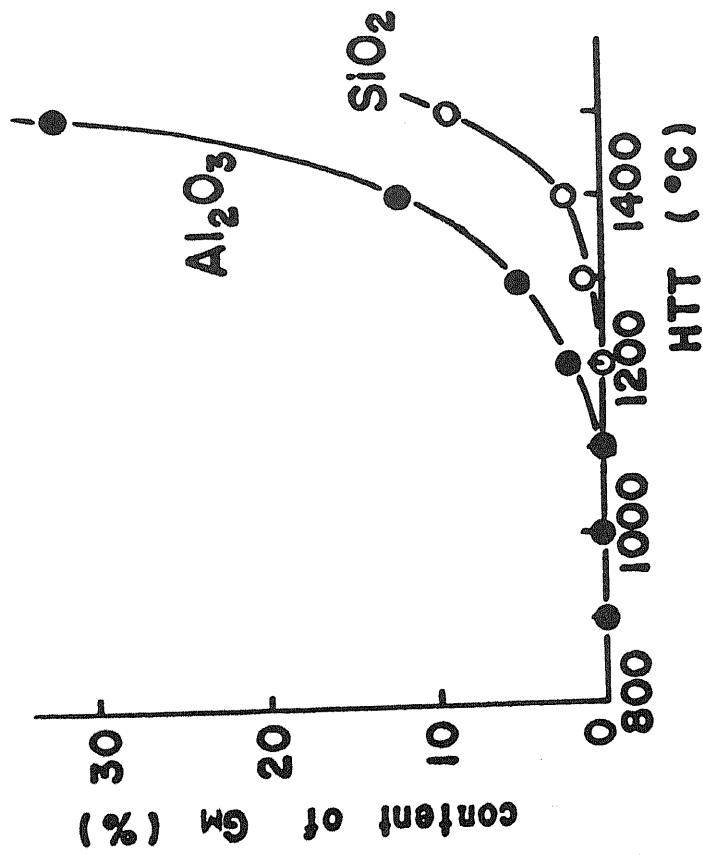


Fig.52 Change of content of graphitic component GM with HTT in the presence of alumina and silica



diameter and 3.5mm thick, and then heat-treated at 750°C for 60min. These disks were kept in an evacuated desiccator. Such a disk was checked by X-ray diffraction method to be completely decomposed to magnesia. The porosity of the disk was about 90%.

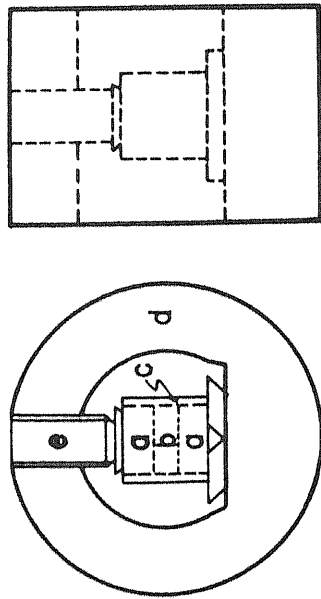
Two series of heat treatments of carbon were carried out in the presence of the disks of magnesia; the heat treatment under 3.2kbar and that under a flow of nitrogen at ordinary pressure.

The heat treatments of carbon under 3.2kbar were performed at various temperatures between 900 and 1500°C for residence times of 60 - 360min using the cell arrangement A (shown in Fig. 4). The heat treatments of carbon under a flow of nitrogen were done at temperatures between 1400 and 2400°C for 60min. In this case, the carbon sample which was placed between two sets of magnesia disk and a graphite plate was put in a glassy carbon tube. The arrangement used was shown in Fig. 54. In a graphite plate, which was used as a cover of the glassy carbon tube, a few narrow orifices were made so as to let gaseous products go out. Whole of this assembly was heat-treated under a flow of nitrogen at ordinary pressure in a graphite resistance furnace. The heat treatments above 2500°C were difficult to carry out, because magnesia reacted with the glassy carbon tube to make a hole.

The profile of (002) diffraction line of the central part of the heat-treated carbon specimen was measured. The same part of the specimen was also observed with an electron microscope.

In both cases of the heat treatments, no amount of magnesium carbide could be detected by X-ray diffraction method, and all carbon specimens could not be obtained as caked tablet.

In the case of heat treatments under a flow of nitrogen, the weight loss of the carbon specimen because appreciable above 1400°C and remarkable above 1900°C, as shown in Fig.55. This fact may suggest that the reaction of magnesia with the carbon sample began to occur at around 1400°C. However, any deposit of carbon could not be detected in the glassy carbon tube up to 2400°C.



- a : magnesia tablet
- b : carbon sample PV-7
- c : glassy carbon tube
- d : graphite holder
- e : graphite screw

Fig.54 Arrangement used for heat treatment of carbon under flow of nitrogen in the presence of magnesia

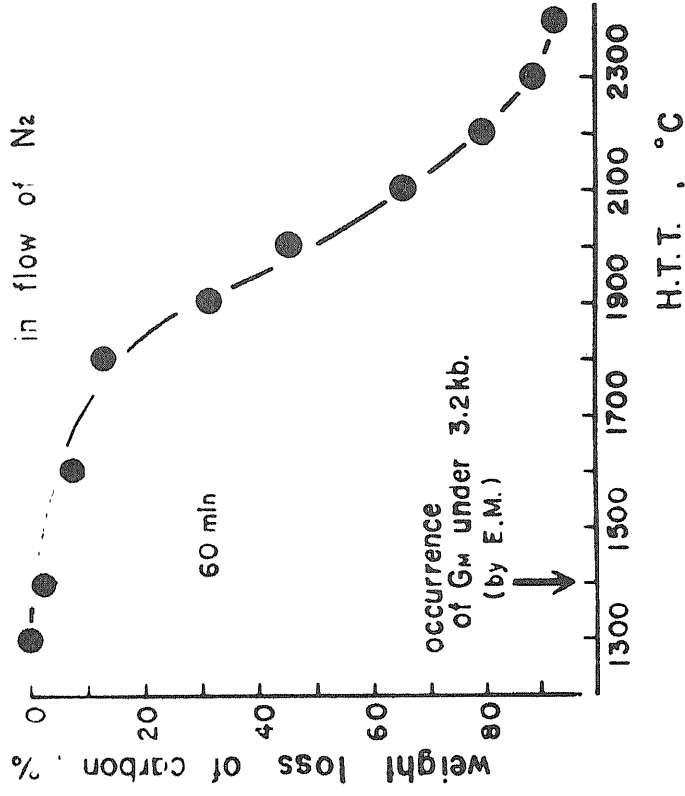


Fig.55 Weight loss of carbon specimen by heat treatment under flow of nitrogen in the presence of magnesia

In the case of heat treatments under 3.2kbar, no graphitic component  $G_M$  could be found on the profile of (002) diffraction line for the carbon specimen heat-treated at 1500°C for 60min, as well as that heat-treated at 1400°C for 360min. The changes of  $c_0$ -spacing and crystallite size  $L_c$  with HTT are shown in Figs. 56 a) and b).

However by the electron microscopic observations, small number of the particles having the diffraction pattern of six-fold symmetry of graphite single crystal were found in the specimen heat-treated under 3.2kbar at 1400°C for 60min. The number of such particle was found to grow with heat treatment. While in the case of the heat treatments under a flow of nitrogen, such particle could not be detected in all carbon specimens heat-treated up to 2400°C. Figure 57 shows a bright-field micrograph and a corresponding selected area diffraction pattern of such a particle in the carbon specimen heat-treated under 3.2kbar at 1400°C for 60min.

### c. Discussion and Summary.

In relation to the supposed mechanisms for the accelerating effect of coexisting calcium compounds on graphitization of carbon under pressure, the heat treatments were performed in the presence of sodium carbonate, alumina, silica and magnesia.

In the heat treatment of carbon under pressure in the presence of reactive sodium carbonate, the particles having the diffraction pattern of six-fold symmetry of graphite single crystal were found even at the temperature as low as 500°C. Sodium carbonate is known to react with carbon to form unstable carbide, which is completely dissociated at a temperature as low as 600°C. This fact seemed to support that the minerals which react with carbon at a lower temperature to form unstable carbide should accelerate the graphitization of carbon at a lower temperature. Though sodium carbonate was used as a coexisting mineral because of the difficulty of handling sodium oxide of high reactivity, carbon dioxide resulted from the decomposition of carbonate seemed not to have an appreciable

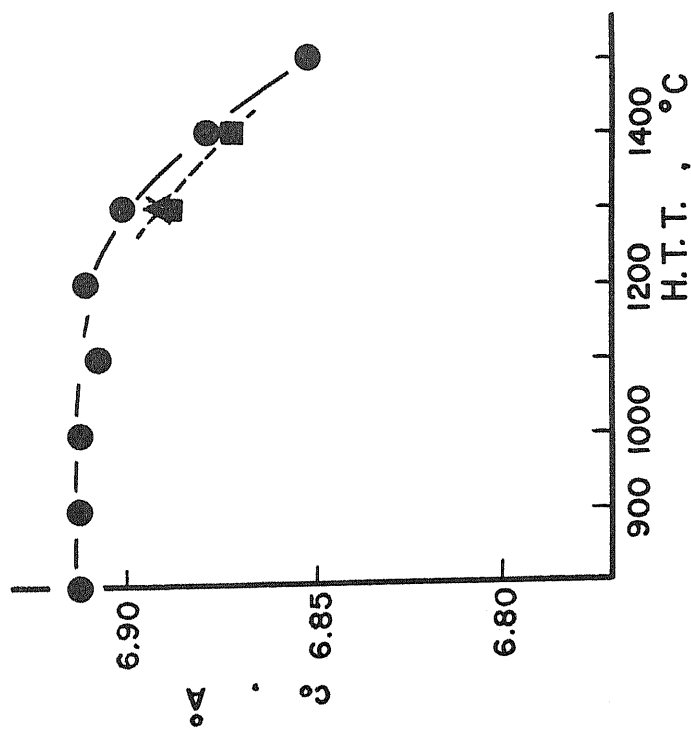


Fig-56 a) Change of  $c_0$ -spacing with heat treatment

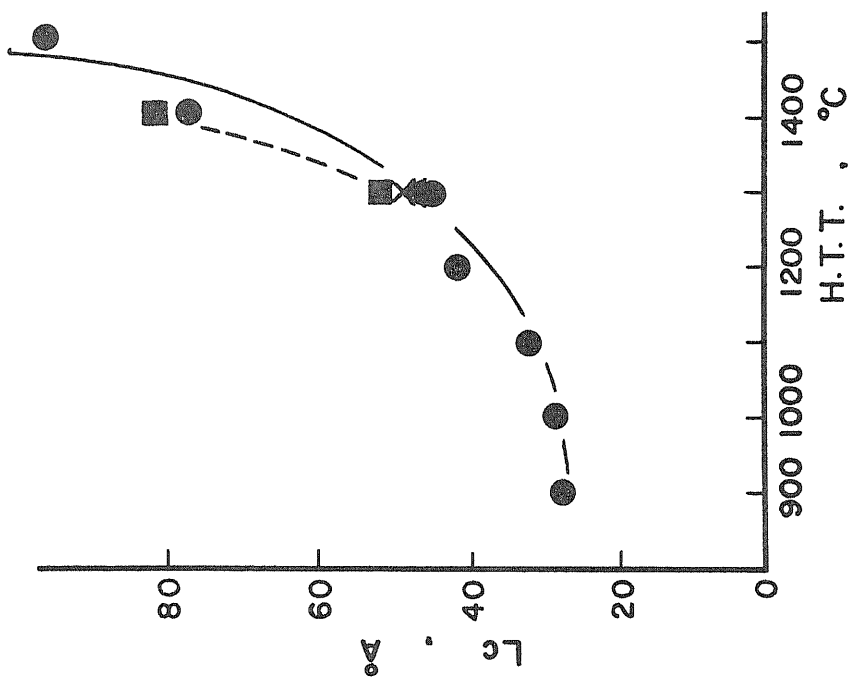


Fig.56 b) Change of crystallite size  $L_c$  with heat treatment

- : 60 min
- ▲ : 120
- X : 240
- : 360

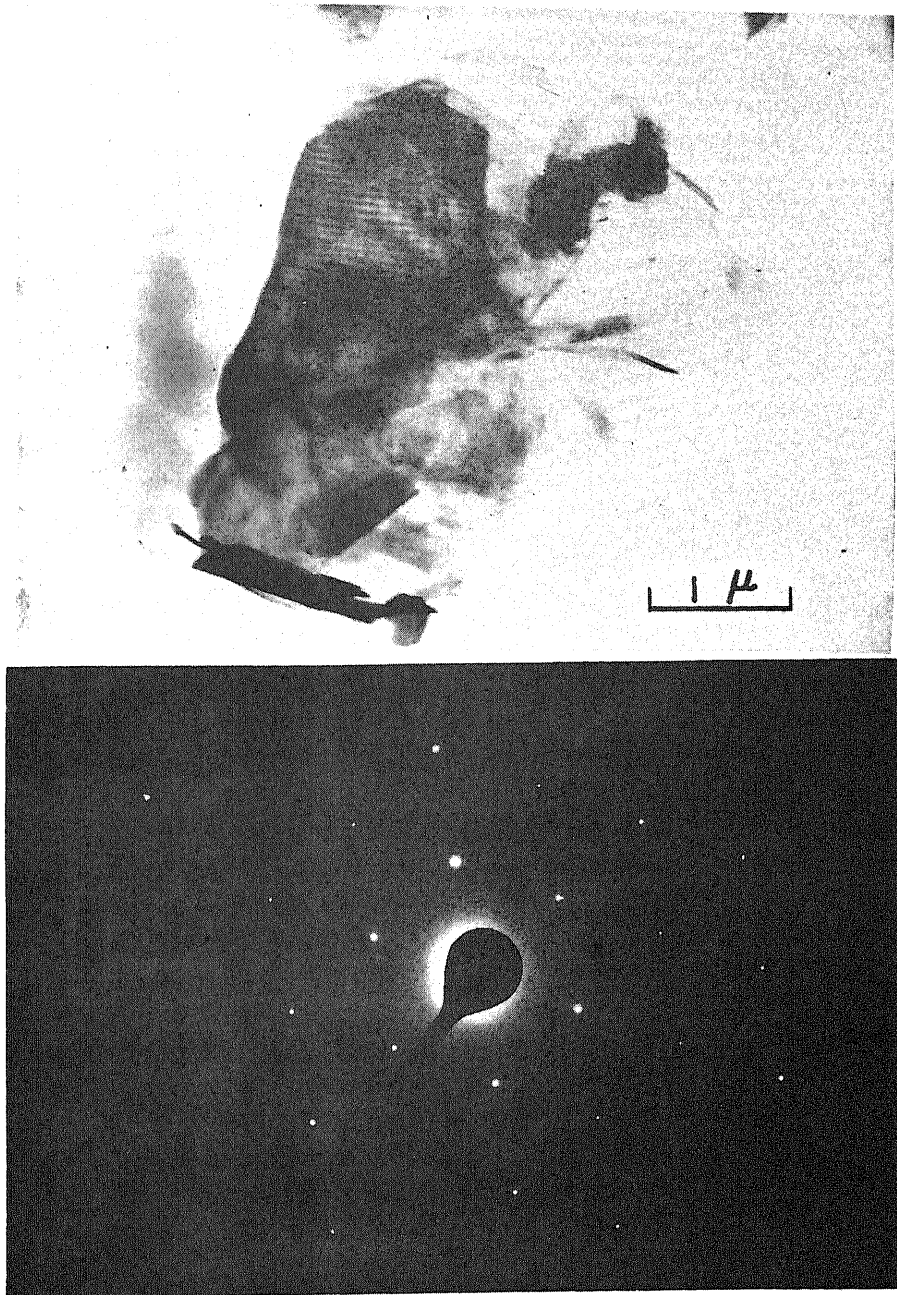
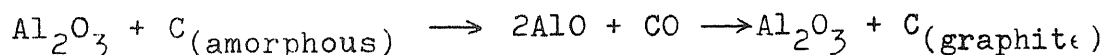


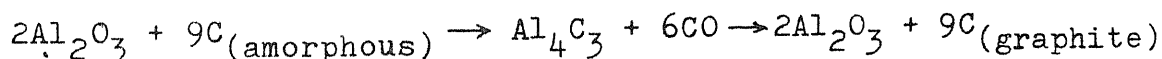
Fig.57 Bright-field micrograph and selected area diffraction pattern of graphitic particle in carbon specimen heat-treated at 1400 C for 60 min under 3.2kbar in the presence of magnesia

effect on graphitization of carbon under pressure. The graphitic component was reported before to appear at almost the same temperature both in the presence of calcium carbonate and calcium oxide calcined at 920°C (CaO-9).

It is known that alumina begins to react with carbon at relatively low temperature of around 1300°C. The reaction products between alumina and carbon were reported to be unstable gaseous product Al<sub>2</sub>O, stable oxycarbides Al<sub>4</sub>O<sub>4</sub>C, Al<sub>2</sub>OC and stable carbide Al<sub>4</sub>C<sub>3</sub><sup>71)~73)</sup>. Aluminum carbide Al<sub>4</sub>C<sub>3</sub><sup>72)~74)</sup> is thermally stable up to about 1600°C. In the case of heat treatments of carbon in the presence of alumina, the graphitic component G<sub>M</sub> began to appear above 1200°C and at 1500°C traces of Al<sub>4</sub>C<sub>3</sub> were detected at the contact part of the carbon specimen with alumina disk. This experimental result shows no discrepancy with the reported facts mentioned above. Below 1400°C, therefore, the graphitic component is considered to be caused by the reactions;

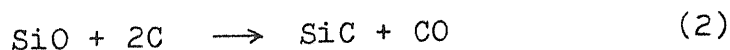
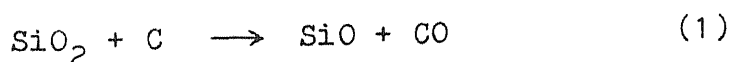


and at 1500°C, in addition to the above reactions, the following reactions seems to be a main cause of the formation of graphitic component.



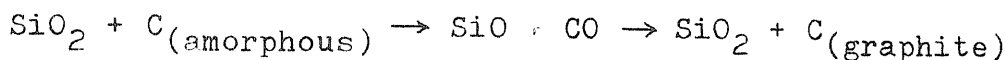
Although aluminum oxide is known to have many modifications, one of modifications, α-alumina, was used in the present work because it is the most stable and well-known about its structure.

Silicon carbide is assumed to be formed in two steps as follows;

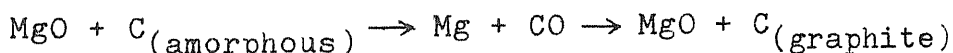


A thermodynamical estimation and the experimental results

which have been reported have shown that silicon carbide is formed above 1400°C and decomposed above 2000°C. In the present experiment, the formation of silicon carbide could not be observed, while the graphitic component was found in the carbon specimen above 1300°C and its content turned out to about 10% at 1500°C. These experimental facts seem to suggest that the possible mechanism of the accelerating effect of silica on graphitization of carbon under pressure may be explained as the following reactions without the formation of silicon carbide.



This mechanism for the formation of the graphitic component without any carbide might be supported by the experimental results on the heat treatment of carbon in the presence of magnesia. The reaction between magnesia and carbon is the basis of the Hansgirg process for the carbothermic production of magnesium. Two kinds of magnesium carbides  $\text{MgC}_2$  and  $\text{Mg}_2\text{C}_3$  are known and both of them are thermodynamically unstable over the whole temperature range of 900 - 1500°C<sup>77)~78)</sup>. In the present experiment, however, any magnesium carbides were not detected up to 1500°C, but the graphitic component was evidently found under electron microscope. Therefore, a similar mechanism as in the case of silica might be considered,



It has been reported that this reaction begins to occur around 1300°C<sup>71)</sup>. The experimental result of Fig. 55, that is, the weight loss of the carbon sample became observable above 1300°C in the presence of magnesia under a flow of nitrogen, might be attributed to the effluence of magnesium vapor and carbon monoxide (see above Equation) and so it is reasonable that the graphitic component was not formed in the heat treatments under a flow of nitrogen because of the effluence of the resulting gaseous products. In the closed system, such as under pressure, however, magnesium vapor and carbon monoxide

might not skip out from the system and react with each other to form magnesia and the graphitic component. This reaction may be favorable in the high pressure system because the gas pressure of the system would be reduced.

The present experimental result that the graphitic component  $G_M$  was not found in the carbon specimen heat-treated under a flow of nitrogen, but was found in the carbon specimen heat-treated under pressure, is considered to support the above mentioned mechanism.

Conclusively, the present results on sodium carbonate seemed to support one of the mechanism of the formation of the graphitic component, that is the formation and successive decomposition of intermediate carbides. but the results on magnesia and silica seemed to support another mechanism, that is the formation of the graphitic component without going through the decomposition of carbide. The results on co-existing alumina may be explained from both mechanisms.

The accelerating effect of these oxide, such as sodium oxide, alumina, silica and magnesia is expected to give certain informations on the occurrence of natural graphite in the sandstone beds.



## 6. Accelerating Effect of Water Vapor on Graphitization of Carbon under Pressure in the Presence of Coexisting Minerals.

### a. Introduction.

In the previous works, the graphitization of carbon was found to be accelerated in the presence of calcium compounds, such as oxide, carbonate and hydroxide, and phenomenally related to the recrystallization or melting of the compounds. Two possible mechanisms were proposed for the accelerating effect of these compounds. Calcium fluoride has the melting point (about 1370°C) close to that of calcium carbonate and it has been known that natural graphite occurs often in the bed of fluorite in the nature. In the present work, the heat treatments of carbon were performed under 3.2kbar in the presence of calcium fluoride. However, calcium fluoride has been known to react with water vapor to form reactive calcium oxide above 1200°C<sup>79,80)</sup> and also it is known that pyrophyllite ( $\text{Al}_2\text{Si}_4\text{O}_{10}(\text{OH})_2$ ) used as the pressure transmitter is decomposed above 450°C under 3kbar to release water vapor. In the present work, therefore, the effect of water vapor come from pyrophyllite was observed particularly.

Since magnesium fluoride is also known to react with water vapor above 1200°C, the same heat treatments of carbon were performed under 3.2kbar in the presence of magnesium fluoride.

Heat treatments under 3.2kbar were performed in the presence of calcium carbonate contained 8wt% water and the results obtained were compared with those in the presence of dry calcium carbonate.

Similar heat treatments were also carried out under 3.2kbar in the presence of calcium oxide using two different kinds of cell arrangement used in the case of calcium fluoride.

### b. Experimental and Results.

#### (1) Heat Treatments of Carbon in the Presence of Calcium Fluoride.

The carbon sample used was the same coke PV-7. The disks

of calcium fluoride, 8.0mm in diameter and 3.5mm thick, were made by compressing calcium fluoride powder (chemical reagent grade) under 3.5kbar. The porosity of the disks was about 82%.

Three kinds of heat treatment were carried out in the presence of calcium fluoride, that is, the first under 3.2kbar using the cell arrangement A in Fig. 58 a), the second under 3.2kbar using the cell arrangement B in Fig. 58 b), and the third under the flow of nitrogen at one atmospheric pressure using the arrangement in Fig. 58 c). The graphite heater was surrounded by raw pyrophyllite. In the arrangement B, however, it was surrounded by pyrophyllite sleeve (14.2mm in outer and 10mm in inner diameter) calcined at 970°C for 60min. Therefore, the water vapor come from the decomposition of raw pyrophyllite was not expected to go into the graphite heater and to react with calcium fluoride in the arrangement B. In the arrangement C, the positional relation between carbon specimen and calcium fluoride was reserved to be the same as those under pressure.

The heat treatments under 3.2kbar were performed at various temperatures between 900 and 1500°C for 60min by means of the same procedure as described before. The heat treatments under the flow of nitrogen at ordinary pressure were carried out at various temperatures between 1000°C and 2000°C for 60min. The details of the procedure of the heat treatment will be described in the next chapter.

The profile of (002) diffraction line of the central part of the heat-treated carbon specimen was taken by using Ni-filtered  $\text{CuK}\alpha$  radiation. The same part of the specimen was observed with an electron microscope.

In the heat treatments of carbon under 3.2kbar with the arrangement A, the carbon specimen was obtained as caked tablets above 1000°C. In the caked tablets heat-treated at various temperatures between 1000 and 1250°C, any amount of calcium fluoride could not be detected by X-ray diffraction method, while in the caked tablets heat-treated above 1300°C, a small amount of calcium fluoride could be detected. A trace of the melt was observed in the disks of calcium fluoride

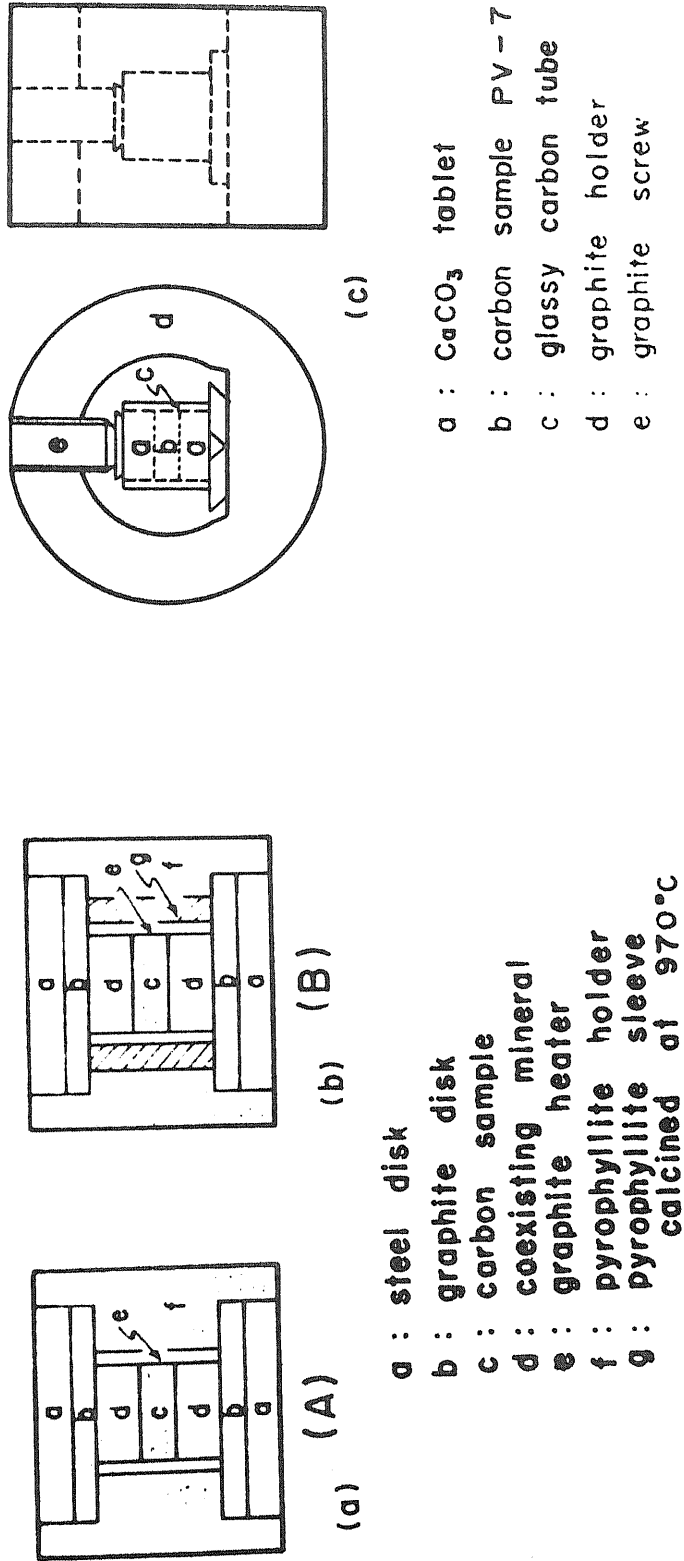
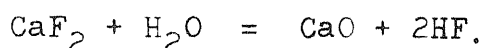


Fig.58 Arrangements of pressure cell for three kinds of heat treatment

could be detected. A trace of the melt was observed in the disks of calcium fluoride at the part in contact with the carbon specimens heat-treated above 1300°C as shown in Fig. 59. The melted parts of the disks were examined with the solution of the phenol-phthalein indicator, which was free from carbon dioxide. The presence of calcium oxide was detected in the disks of calcium fluoride in contact with the carbon specimen heat-treated above 1300°C. This calcium oxide is supposed to be attributed to the following reaction,



In the heat treatments of carbon under 3.2kbar with the arrangement B, the carbon specimen was obtained as caked tablets above 1100°C and the disks of calcium fluoride in contact with the carbon specimens heat-treated above 1300°C was recognized to melt. However in the disks of calcium fluoride, calcium oxide could not be detected.

In the heat treatments of carbon under the flow of nitrogen, any reaction between the coexisting calcium fluoride and the carbon sample could not be observed, but the melting of calcium fluoride was observed above 1300°C.

Figure 60 shows the change of the profile of (002) diffraction line with HTT in the heat-treatments of carbon under 3.2kbar with the arrangement A. The profiles of (002) diffraction line were found to be composite above 1300°C and at 1500°C the single profile of the graphitic component was observed.

In this case, the particles having the graphitic structure were found with electron microscope in the carbon specimen heat-treated above 1300°C, as shown in Fig. 61.

In both heat treatments of carbon under 3.2kbar with the arrangement B and under the flow of nitrogen, no graphitic component could be detected by the X-ray diffraction method and even by the electron microscopic observations. All particles in the carbon specimens heat-treated at 1500°C under 3.2kbar with the arrangement B showed the continuous (hk) diffraction rings, as shown in Fig. 62.



Fig.59 Photograph of disk of calcium fluoride in contact with carbon specimen heat-treated at 1300°C for 60 min under 3.2 kbar

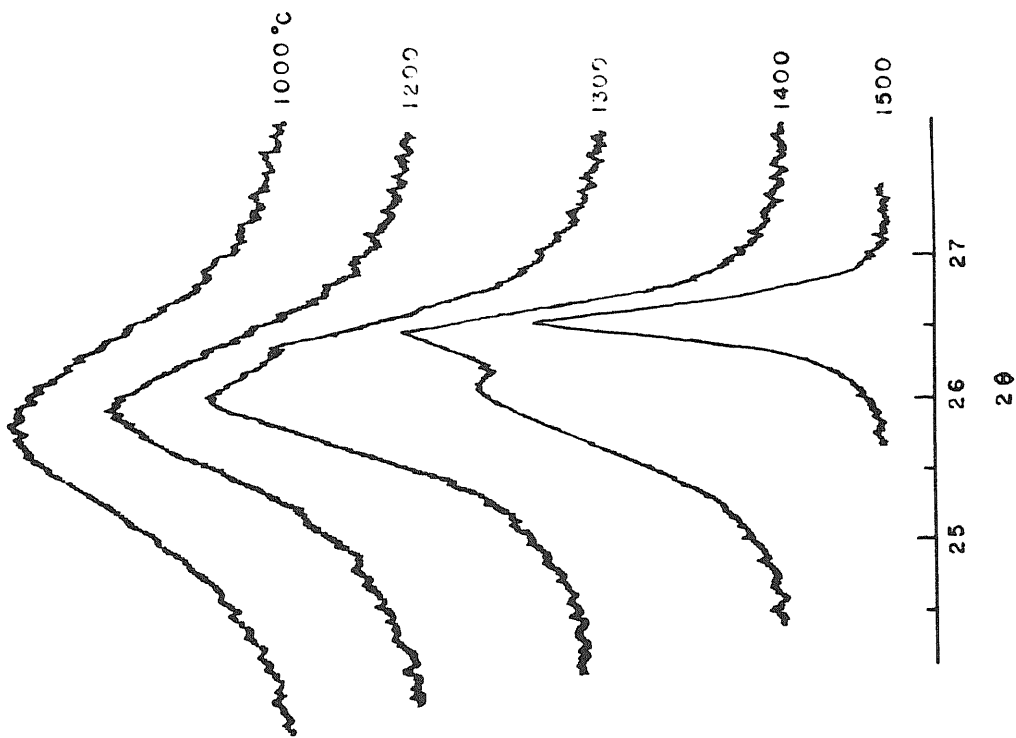


Fig.60 Change of profile of (002) diffraction line with HTT in heat treatment of carbon under 3.2 kbar for 60 min with cell arrangement A

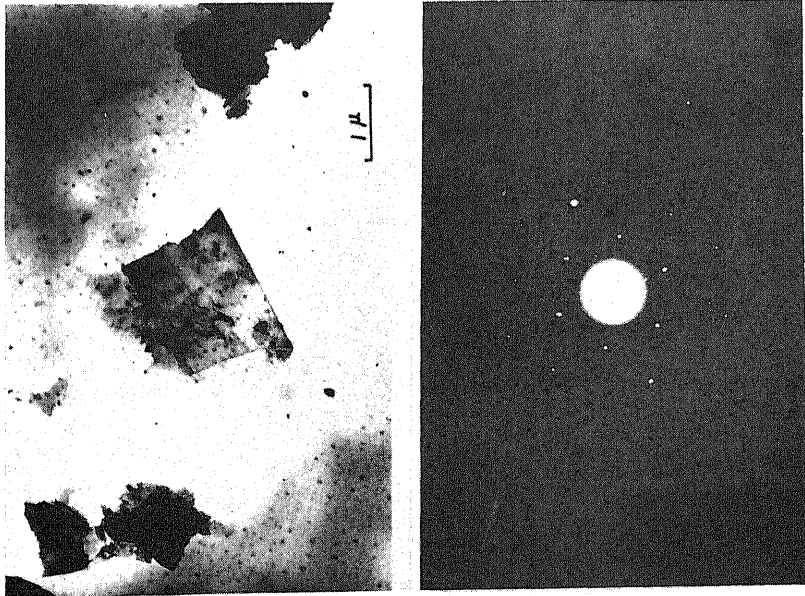


Fig.61 Bright-field micrograph and selected area electron diffraction pattern of graphitic particle in carbon specimen heat-treated at 1300°C for 60min under 3.2kbar with cell arrangement A in the presence of calcium fluoride

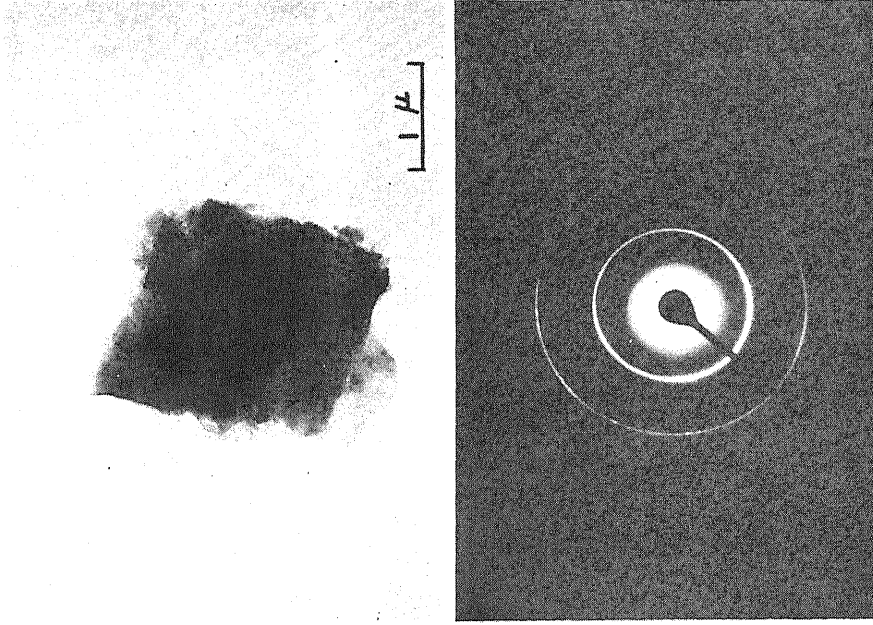


Fig.62 Bright-field micrograph and selected area electron diffraction pattern of particle in carbon specimen heat-treated at 1500°C for 60min under 3.2kbar with cell arrangement B in the presence of calcium fluoride

The changes of the  $c_0$ -spacing for the carbon specimens with HTT are shown in Fig. 63. The  $c_0$ -spacing of the turbostratic component  $A_M$  was found to change with HTT in the same way in both heat treatments with the cell arrangement A and with the cell arrangement B. The  $c_0$ -spacing of the graphitic component  $G_M$  was almost constant value of about  $6.72\text{\AA}$ .

Figure 64 shows the changes of the content of the graphitic component  $G_M$  with HTT together with that of the heat treatment of the same carbon under 3.2kbar in the presence of the most reactive calcium oxide calcined at  $920^\circ\text{C}$  (CaO-9). The changes of the content of the graphitic component  $G_M$  in the presence of CaO-9 and calcium fluoride with the cell arrangement A were very similar with each other.

## (2) Heat Treatments of Carbon under Pressure in the Presence of Magnesium Fluoride.

The carbon sample used was the same coke PV-7. The disks of magnesium fluoride, 8.0mm in diameter and 3.5mm thick, were prepared by compressing magnesium fluoride powder (chemical reagent grade) under 3.5kbar. The porosity of the disks was about 85%.

The heat treatment of carbon was carried out at various temperatures between 900 and  $1500^\circ\text{C}$  for 60min under 3.2kbar by the same procedure as used previously. The arrangement A in Fig. 58 a) was used.

The disk of magnesium fluoride at the part in contact with the carbon specimen heat-treated at  $1200^\circ\text{C}$  was observed to melt and above  $1300^\circ\text{C}$  the melted zone became thicker. The carbon specimens heat-treated above  $1200^\circ\text{C}$  were obtained as caked tablets. The graphitic component  $G_M$  could not be observed on the profile of (002) diffraction line of the carbon specimen heat-treated even at  $1500^\circ\text{C}$ .

By the electron microscopic observations, however, the particles having the graphitic structure, though its number was very small could be found besides the particles having the turbostratic structure. In the carbon specimen heat-treated at  $1500^\circ\text{C}$ , the number of the graphitic particle seemed to increase. This result is in good agreement with the

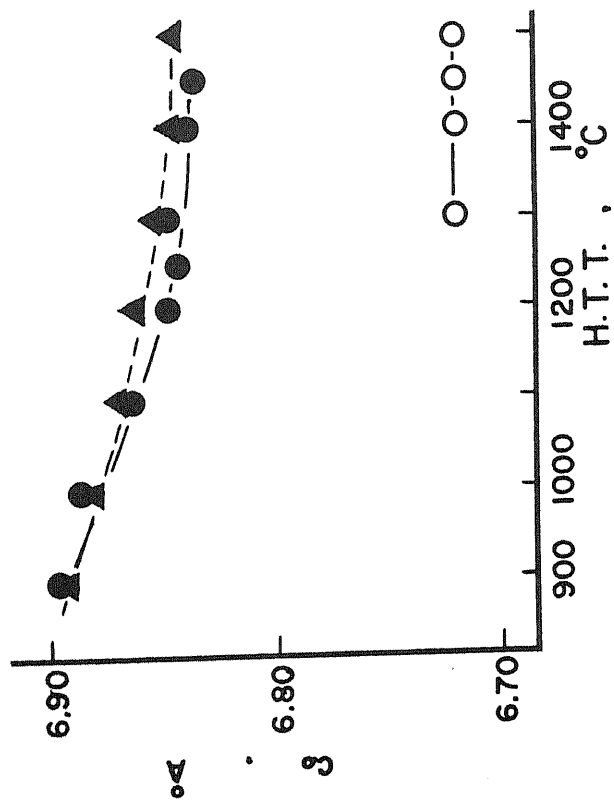


Fig.63 Changes of co-spacing with HTT

- : heat treatment with cell arrangement A
- ▲ : heat treatment with cell arrangement B
- : heat treatment in the presence of CaO with cell arrangement A

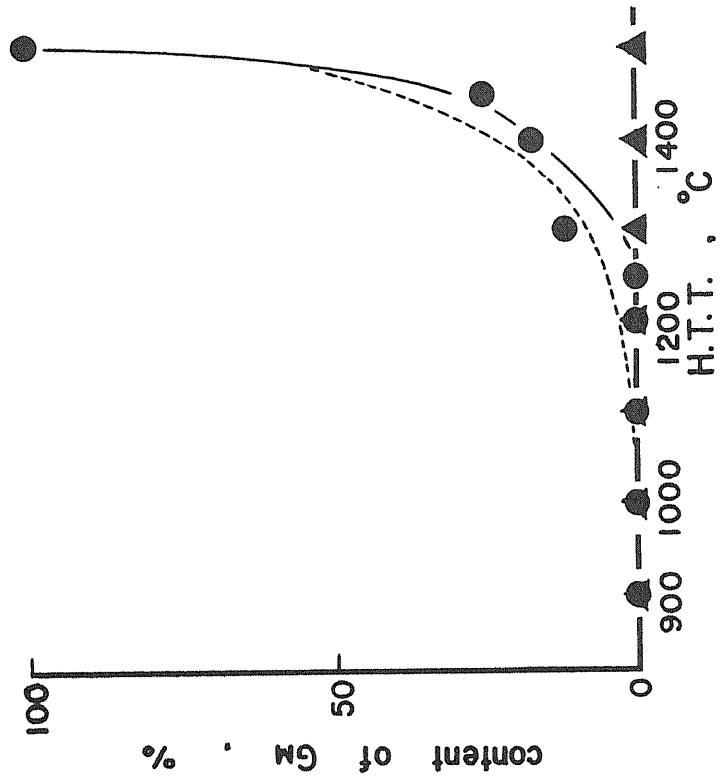


Fig.64 Changes of content of graphitic component GM with HTT



results in the case of the presence of magnesium oxide. Figure 65 shows a bright-field micrograph and a selected area diffraction pattern of the particle having the graphitic structure in the carbon specimen heat-treated at  $1400^{\circ}\text{C}$  for 60min under 3.2kbar in the presence of magnesium fluoride.

### (3) Heat Treatments of Carbon under Pressure in the Presence of Calcium Carbonate absorbed Water.

The carbon sample used was the coke PV-7. The disks of calcium carbonate were prepared by the same way as described in the section 3.c. About 8wt% of water was absorbed in these disks of calcium carbonate in equilibrium with water vapor at room temperature.

The heat treatment was carried out at various temperatures between  $900$  and  $1200^{\circ}\text{C}$  for 60min under 3.2kbar using the arrangement A in Fig. 58, which is the exactly the same as in the case of the presence of dry calcium carbonate.

The disks of calcium carbonate absorbed water were recognized to melt and dissociate into calcium oxide at the part in contact with the carbon specimen heat-treated above  $1200^{\circ}\text{C}$ . Above  $1300^{\circ}\text{C}$ , further heat treatments were difficult because the melt attacked the graphite heater to form calcium carbide.

The graphitic component  $G_M$  began to appear in the carbon specimen heat-treated at  $1000^{\circ}\text{C}$ . Figure 66 shows the change of the content of the graphitic component  $G_M$  with HTT together with that in the presence of "dry" calcium carbonate. The graphitization of carbon was found to start in the presence of "wet" calcium carbonate, about  $100^{\circ}\text{C}$  lower than that in the case of "dry" calcium carbonate. In Fig. 66, there was also presented the result of the heat treatments of the same carbon under 3.2kbar in the presence of calcium oxide calcined at  $920^{\circ}\text{C}$  (CaO-9) using the cell arrangement as shown in Fig.58 b). In the presence of calcium oxide, no appreciable effect of water vapor on graphitization was found.

### c. Discussion.

In the heat treatment of carbon under pressure in the presence of calcium fluoride using the arrangement A, the disks

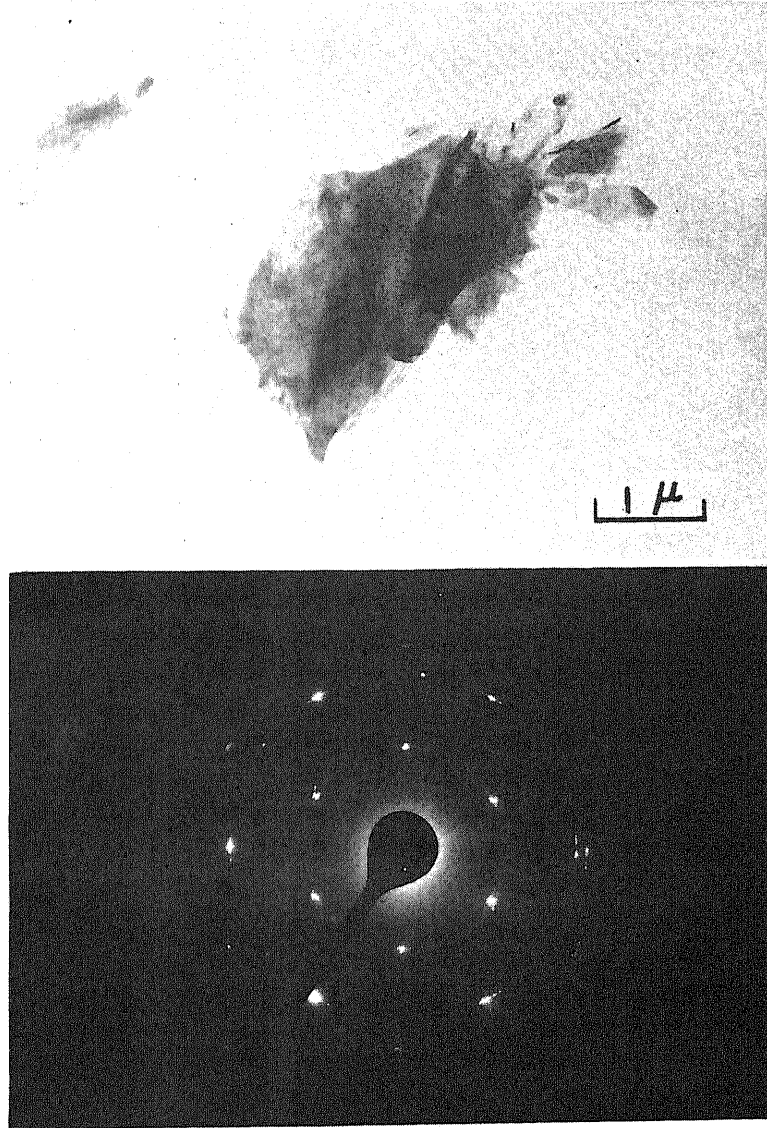
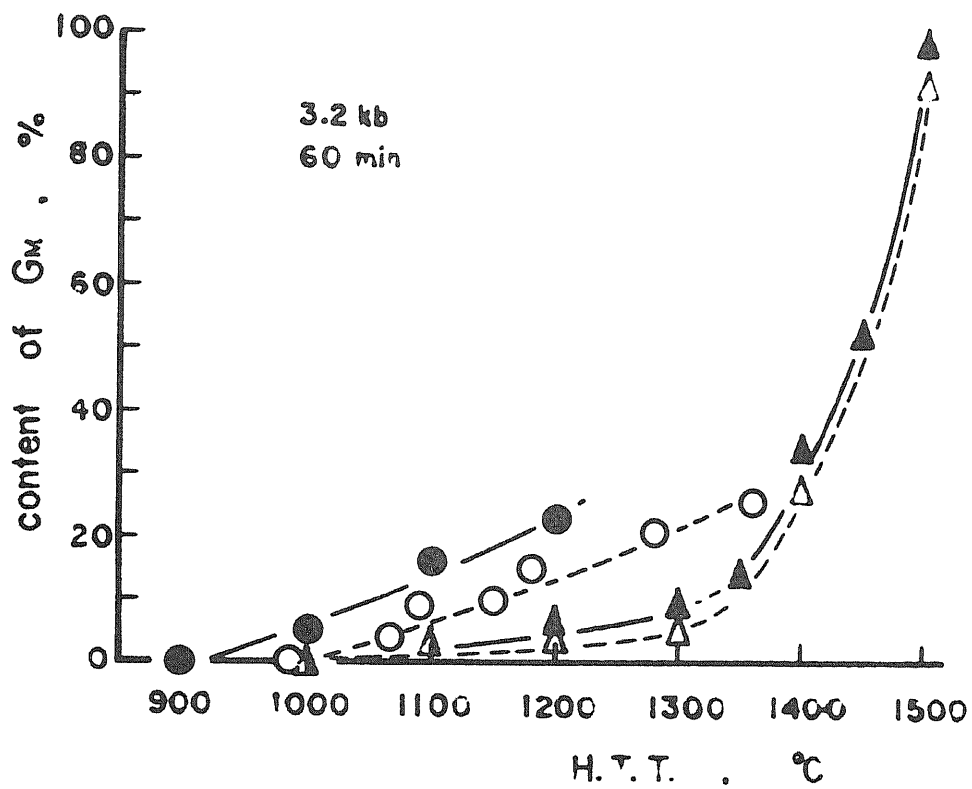


Fig.65 Bright-field micrograph and selected area diffraction pattern of graphitic particle in carbon specimen heat-treated at 1400°C for 60min under 3.2kbar in the presence of magnesium fluoride with cell arrangement A



- |   |   | Cell |
|---|---|------|
| { | ● : CaCO <sub>3</sub> + 8wt% H <sub>2</sub> O | (A)  |
|   | ○ : CaCO <sub>3</sub>                         | (A)  |
| { | ▲ : CaC-9                                     | (A)  |
|   | △ : CaO-9                                     | (B)  |

Fig.66 Change of content of graphitic component GM with HTT

of calcium fluoride was recognized to melt and partly transform to calcium oxide at the part in contact with the carbon specimen heat-treated above 1300°C. On the other hand, no chemical reaction between calcium fluoride and the carbon sample could be found in the specimens heat-treated up to 2000°C under the flow of nitrogen without any water vapor.

The graphitization of carbon began to start at 1300°C in the case of the use of cell arrangement A, while no graphitic component could be observed in both cases of the use of cell arrangement B and under the flow of nitrogen. Furthermore, the change of the content of the graphitic component  $G_M$  with HTT well resembled with that in the case of most reactive calcium oxide calcined at 920°C. These experimental facts might be explained as follows; water vapor caused by decomposition of pyrophyllite during heat treatment, reacted with coexisting calcium fluoride according to the following equation, that is



The reaction between calcium fluoride and water became remarkable at a temperature near the melting point of calcium fluoride and nascent calcium oxide was formed. This reaction is reasonable to occur at the part in contact with the carbon specimen in the present work because of the temperature gradient in the disk of calcium fluoride. The resultant reactive calcium oxide accelerated the graphitization of carbon according to the mechanisms mentioned in chapter 4.

In the nature, water vapor is known to be one of the important basic compound. Therefore, the present result may suggest a mechanism for the formation of natural graphite associating with fluoride.

The result on magnesium fluoride seemed to be explained from the similar mechanism, that is the reaction of magnesium fluoride with water vapor and the subsequent formation of reactive magnesium oxide. Because accelerating effect of magnesium oxide on graphitization of carbon is not so remarkable as calcium oxide, as discussed in chapter 5, however,

the amount of the graphitic component was very small.

Figure 67 shows the isobaric equilibrium diagram for the join  $\text{CaCO}_3\text{-H}_2\text{O}$  at 1000bar . From this diagram, the addition of water to calcium carbonate is suggested to decrease greatly the dissociation temperature of calcium carbonate.

The present results on the effect of coexisting calcium carbonate containing water on graphitization of carbon (Fig.66) seemed to be explained by the presence of water, in other words, by the formation of reactive calcium oxide at low temperature. Unfortunately, however, the exact content of water in the reaction system could not be known and so the dissociation temperature could not be estimated in the present work.

This result is also to consistent with that obtained in the case of the presence of calcium oxide, that is, the lower the calcination temperature of calcium oxide was, the easier the formation of the graphitic component.

On the other hand, no remarkable effect of water vapor on graphitization of carbon was recognized in the presence of calcium oxide itself. This fact seems to be attributed to the following reason. Since the coexisting calcium oxide was suffered the calcination at the temperature of about  $900^\circ\text{C}$  beforehand and the heating rate if it was very fast, it cannot react with water vapor to form calcium hydroxide so that the oxide remain almost the same reactivity as the original one.

The effect of water vapor on graphitization of carbon seemed to suggest one possibility that the formation of natural graphite under moderate conditions in the bed of limestone of water vapor. This seems to be one of the reasons why metasomatism or mineralization with magma or pneumatolysis theory has been considered as the mechanism for the genesis of natural graphite.

In order to have the additional and quantitative informations for the effect of water vapor in the presence of calcium compounds, further detailed experiments would be required to carry out with cold-seal type pressure vessel so as to examine the relation between the content of the graphitic component  $G_M$  formed and the proportion of added water..

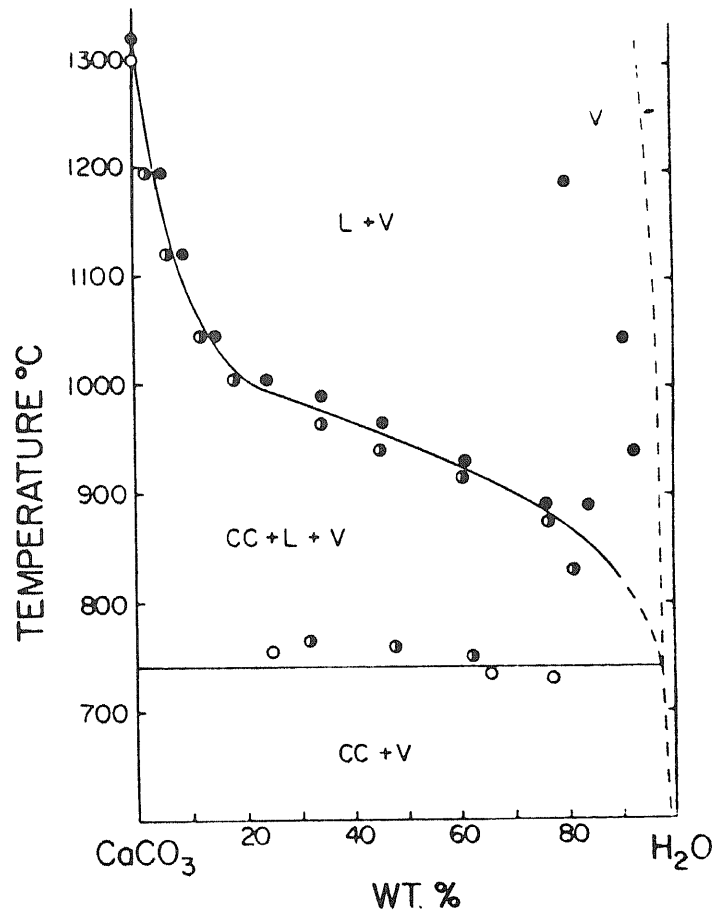
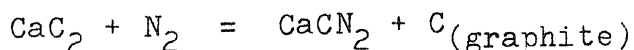


Fig.67 Isobaric equilibrium diagram for join  $\text{CaCO}_3$  -  $\text{H}_2\text{O}$  at 100 bar

## 7. Effect of Nitrogen Gas on Graphitization of Carbon in the Presence of Calcium Carbonate.

### a. Introduction.

It was suggested in the previous chapters that the graphitization of carbon under pressure in the presence of coexisting minerals would proceed by the reaction of the coexisting mineral with the carbon sample. One of the possible mechanisms for the formation of the graphitic component at a higher temperature was proposed to be the chemical process going through the intermediate formation of carbide and successive decomposition to form the graphitic component. If the mechanism suggested was the reasonable one, the graphitization of carbon in the presence of the coexisting minerals would be also affected by nitrogen gas as a chief component of air, according to the following reaction of the formation of calcium cyanamide;



Therefore in the present work, heat treatments of the carbon were carried out under both flows of nitrogen and argon at ordinary pressure in the presence of calcium carbonate so as to examine the effect of the atmosphere on graphitization of carbon. Another heat treatments were also performed under both flows of nitrogen and argon using calcium carbide in order to elucidate the mechanism for the effect of nitrogen on graphitization in the presence of coexisting calcium carbonate.

### b. Experimental.

#### (1) Heat Treatment of Carbon in the Presence of Calcium Carbonate.

The carbon sample used was the coke PV-7. The disks of calcium carbonate (8.0mm in diameter and 2.5mm thick) were made by the same method as mentioned in the section 3.b.

The heat treatments under the flows of nitrogen and argon

(industrial grade) were proceeded as follows. The cell arrangement for heat treatment is shown in Fig. 68. The carbon sample (b) was set in the sandwich type form between the two disks of calcium carbonate (a) in glassy carbon tube (c) with graphite lids (f) (8mm in inner diameter). In order to introduce gas into the inside of the glassy carbon tube, a few narrow ditches were dug in the graphite lid. This assembly was set in a graphite holder (d) and compressed slightly by using a graphite screw (e) so as to make the carbon specimen touch with the disks of calcium carbonate. Then, whole of this graphite holder (d) was inserted into the graphite resistance furnace which had been already heated up to a given heat treatment temperature under the flow of nitrogen or argon.

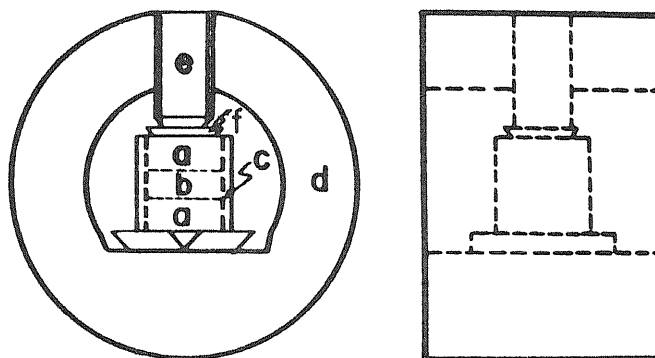
The carbon sample was heat-treated for the residence time of 60min after its temperature reached to the designated temperature (about 10min was needed in the present case). The temperature of heat treatment was measured with a corrected optical pyrometer watching the glassy carbon tube.

## (2) Heat Treatment of Calcium Carbide.

Calcium carbide used was prepared by pulverizing to the grain size of 0.5 - 1mm just before used from a mass (ca. 95% purity) which had been covered with fine calcium carbide powder and kept in an evacuated desiccator.

The heat treatments of calcium carbide were performed by the same procedure as mentioned above except that the disks of calcium carbonate and the carbon sample were replaced with calcium carbide powder. In this case, it was difficult to determine the content of the graphitic component formed only by means of X-ray diffraction method. Therefore, the chemical analysis as shown in Fig. 69 were used for the measurement of content of the graphitic component formed. The amount of calcium ion in the specimen was also checked by the chemical analysis. The amount of free carbon, which was contained in the original calcium carbide as impurity, was estimated (C in wt%) by the same chemical analysis. Then, the content of the graphitic component was estimated according to the following equation,





- a :  $\text{CaCO}_3$  tablet
- b : carbon sample PV-7
- c : glassy carbon tube
- d : graphite holder
- e : graphite screw
- f : graphite lid

Fig.68 Cell arrangement for heat treatment under flow of nitrogen or argon

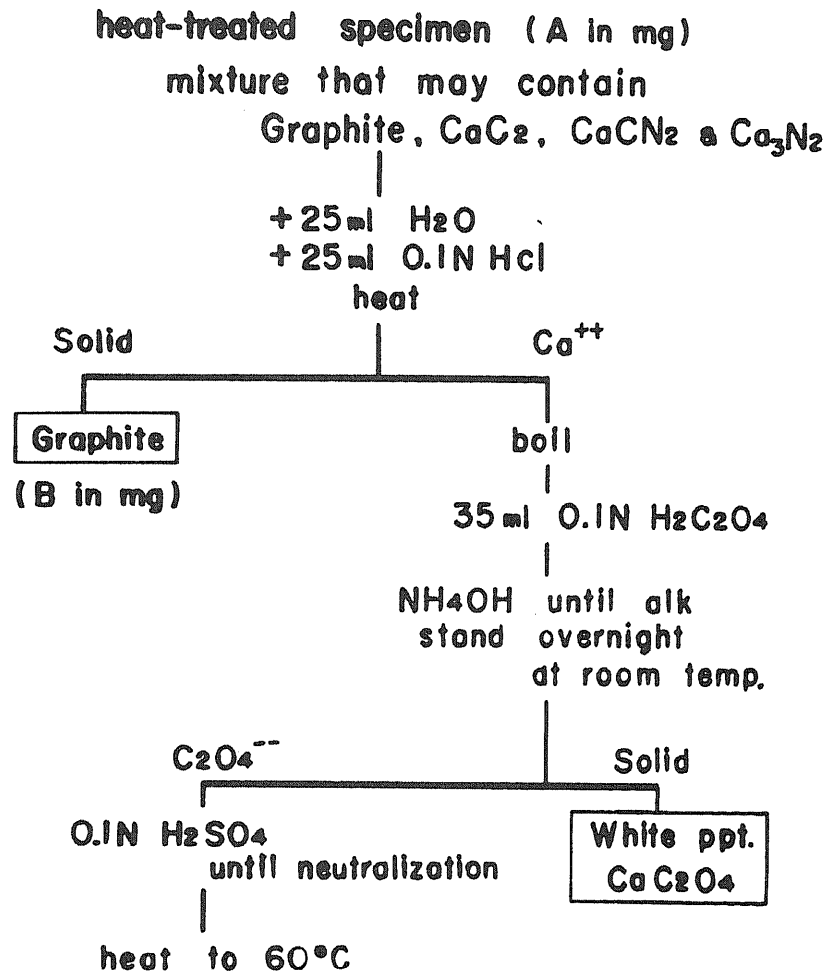


Fig.69 Chemical analysis for measurement of content of graphitic component

the content of  
the graphitic component formed (in wt%)  $= \frac{B}{A} \times 100 - C,$

by assuming that the turbostratic component  $A_M$  was resulted from the free carbon in the original carbide and its amount was not changed by the heat treatment.

The heat-treated specimens were also observed under a transmission electron microscope.

### c. Results.

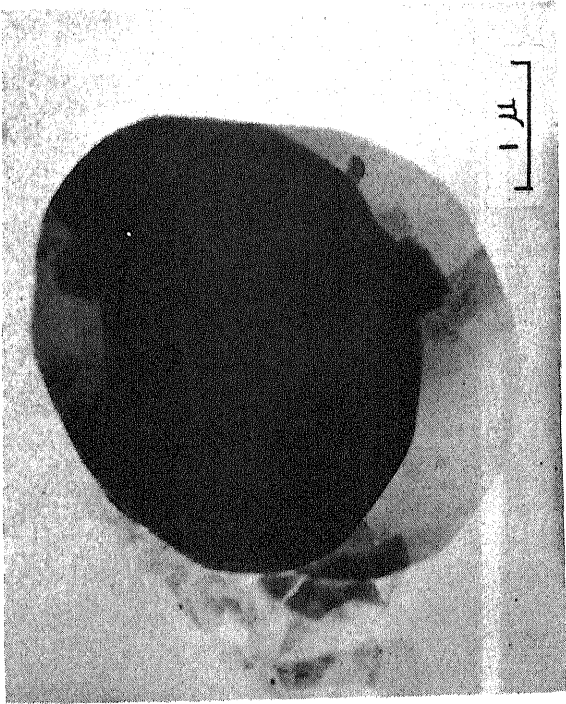
#### (1) Heat Treatments of Carbon in the Presence of Calcium Carbonate under the Flows of Nitrogen and Argon.

In the heat treatment under the flow of nitrogen, the graphitic component began to appear in the carbon specimen at 1730°C. By electron microscopic observations, the graphitic particles having the diffraction pattern of six-fold symmetry of graphite single crystal were found in the carbon sample heat-treated above 1730°C. The graphitic particles had well-crystallized flaky appearance and some of them had the singular discoidal appearance as shown in Fig. 70.

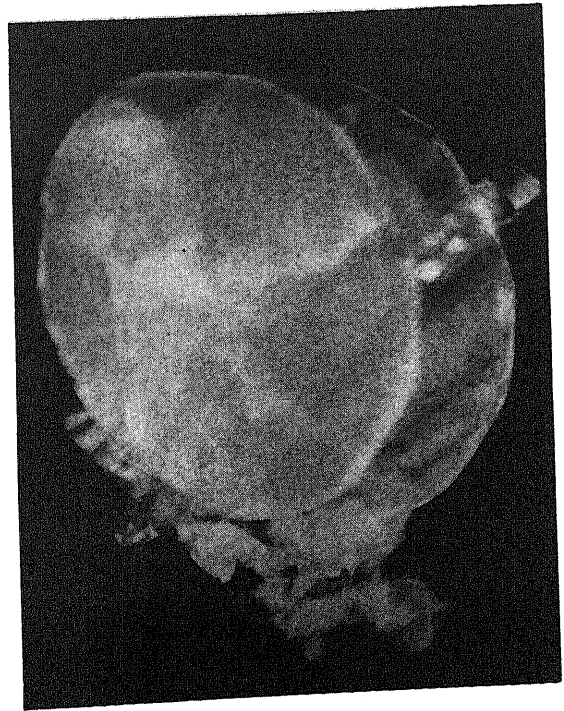
In the heat treatment under the flow of argon, the graphitic component began to appear barely in the carbon specimen at 1930°C. In this case, any discoidal particle could not be found under electron microscope.

Figures 71 a) and b) show the bright-field micrograph and the corresponding selected area electron diffraction pattern of the graphitic particle in the carbon specimen heat-treated at 1850°C under the flow of nitrogen and at 1930°C under the flow of argon.

The changes of the content of the graphitic component with HTT were shown in Fig. 72 for both cases. In the heat treatments under the flow of nitrogen, the content of the graphitic component turned out to about 75% at 2020°C, while under the flow of argon it reached only to about 20% even at 2070°C. The accelerating effect of nitrogen on graphitization of carbon in the presence of calcium carbonate was known to be as remarkable as expected.



**Bright - field micrograph**



**Dark - field micrograph**

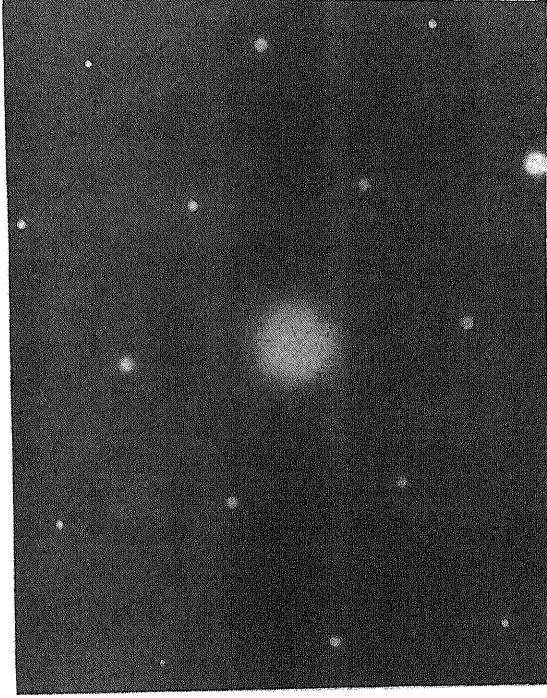
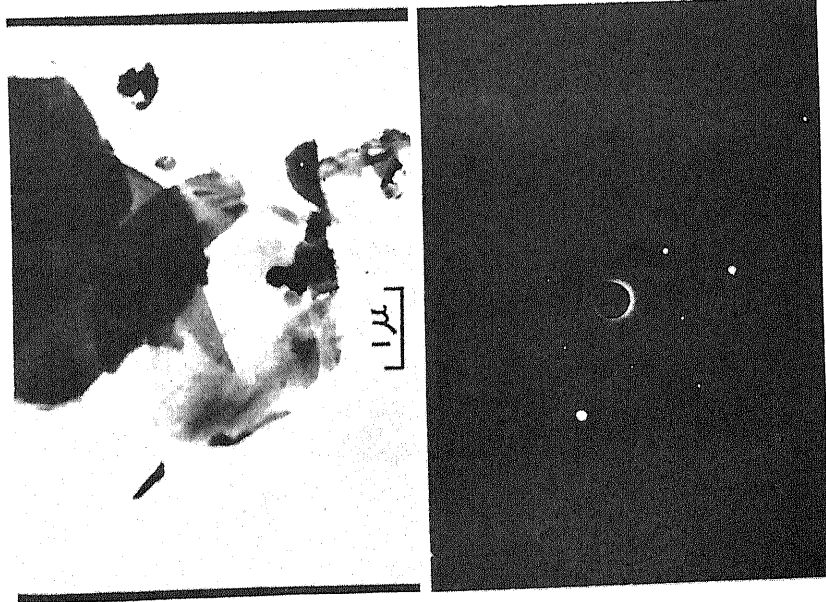
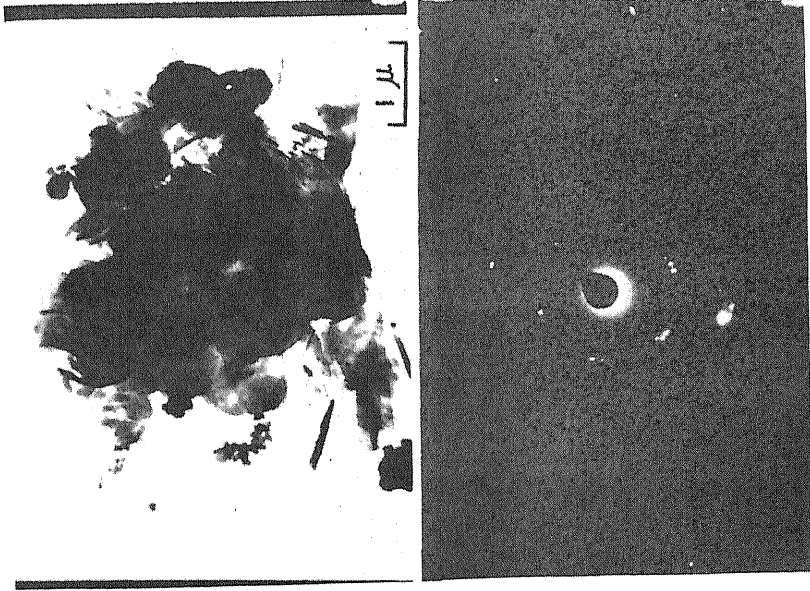


**Fig.70 Electron micrograph and selected area diffraction pattern of particle having singular discoidal appearance in carbon specimen heat-treated at 1730 c for 60min under flow of nitrogen in the presence of calcium carbonate**

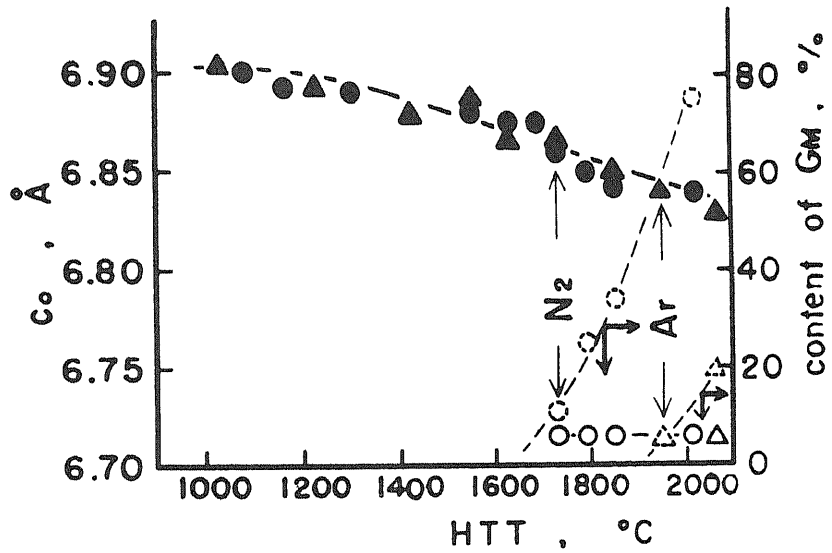


(a) at 1850 °C under flow of nitrogen



(b) at 1930 C under flow of argon

Fig.71 Bright-field micrographs and selected area diffraction patterns of graphitic particle in carbon specimen heat-treated



● : in the flow of N<sub>2</sub>  
 ▲ : in the flow of Ar

Fig.72 Change of content of graphitic component GM with HTT

## (2) Heat Treatments of Calcium Carbide under the Flow of Nitrogen and Argon.

In the heat treatments of calcium carbide under the flows of nitrogen and argon, the content of the graphitic component was found to change with HTT as shown in Fig. 73. In both cases, the graphitic component could be observed at 1000°C. Over the whole temperature range employed, however, the content of the graphitic component formed under the flow of nitrogen was much larger than that under the flow of argon. With response to the increase of content of the graphitic component, the amount of calcium compound remained in the specimen decreased.

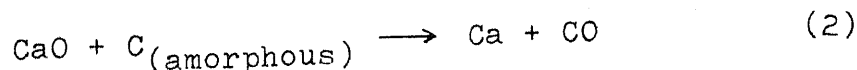
The bright-field micrographs and the corresponding selected area electron diffraction patterns of the particles are shown in Fig. 74.

In the heat treatment under the flow of nitrogen, calcium cyanamide  $\text{CaCN}_2$  was identified by X-ray diffraction method above 1220°C and above 1730°C calcium nitride  $\text{Ca}_3\text{N}_4$  was also detected as well as calcium cyanamide.

### d. Discussion.

From the comparison between the experimental results under the flow of nitrogen and of argon, it was found that the formation of the graphitic component was much easier, in other words, occurred at lower temperature and much faster, under the flow of nitrogen than of argon. In the flow of nitrogen without any coexisting minerals, such a formation of the graphitic component has never been observed on the same coke PV-7. Therefore, nitrogen was concluded to have certain accelerating effect on graphitization of carbon in the presence of calcium carbonate.

The formation of the graphitic component in the coexistence of calcium carbonate and nitrogen seemed to be formulated as follows;



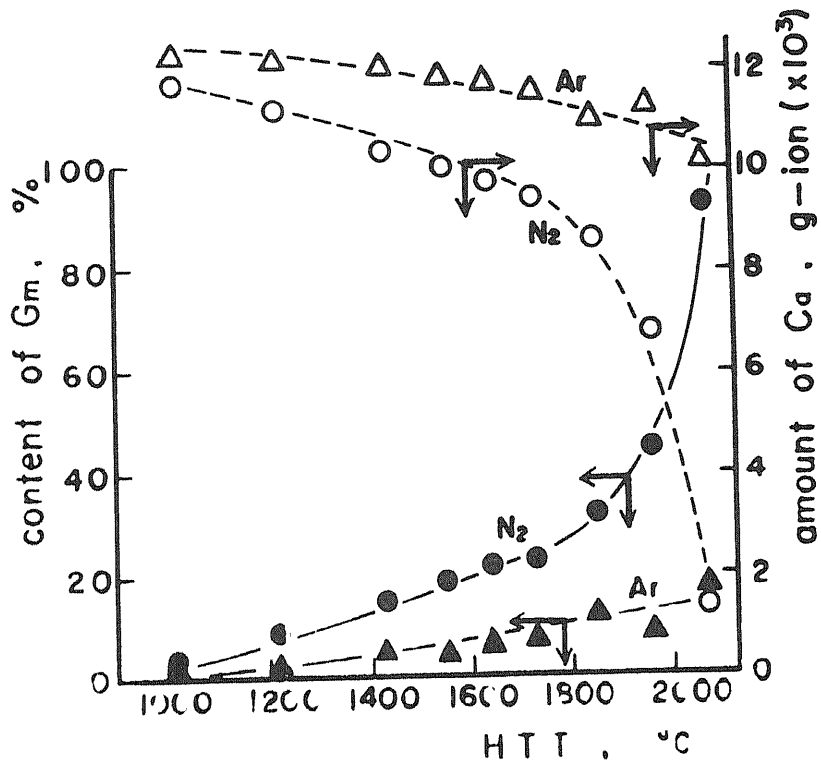
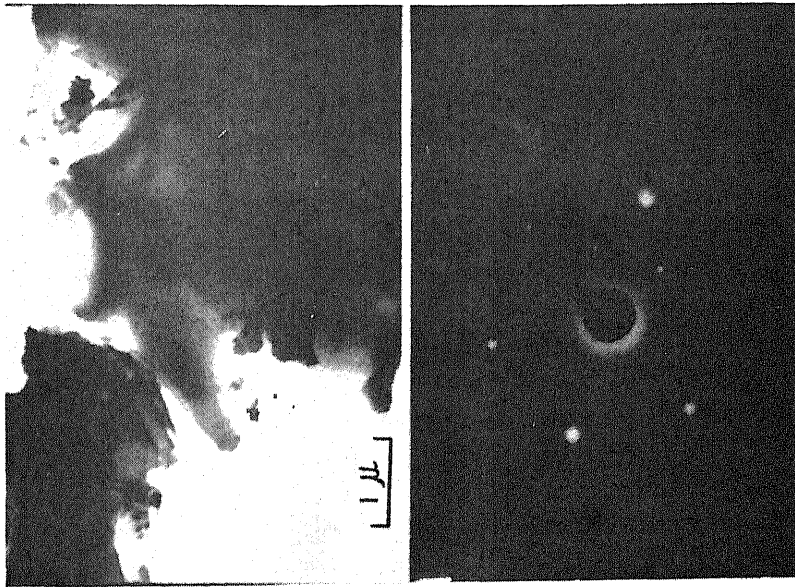


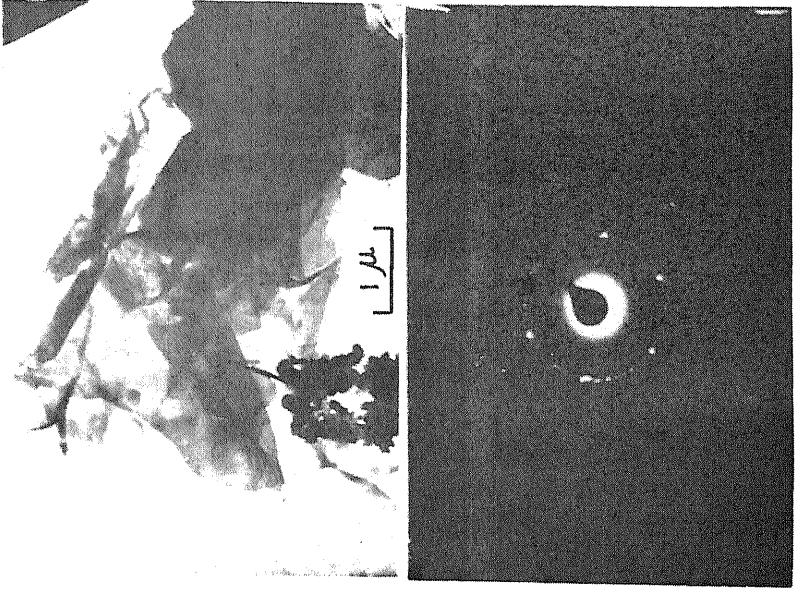
Fig.73 Change of content of graphitic component produced from calcium carbide with HTT

- : heat treatment under flow of nitrogen
- ▲ : heat treatment under flow of argon



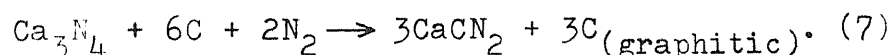
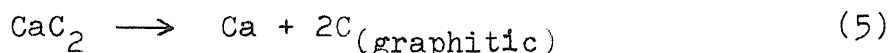
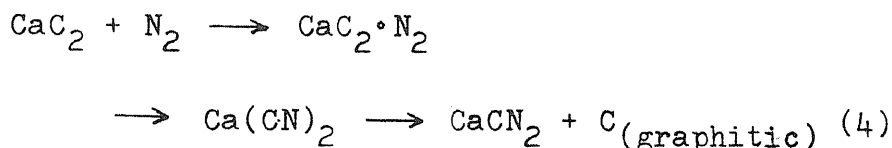
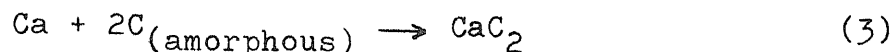


(a) under flow of nitrogen



(b) under flow of argon

**Fig.74 Bright-field micrographs and selected area electron diffraction patterns of graphitic particles produced from calcium carbide heat-treated at 1850 °C**



The formation of the graphitic component is possible by the formation of calcium cyanamide (Eq. 4), the decomposition of calcium carbide (Eq. 5) and/or the reaction among calcium nitride, carbon and nitrogen (Eq. 7). Under the flow of argon, evidently, the possible reaction for the formation of the graphitic component is only the decomposition of calcium carbide, except a small effect of nitrogen as impurity in argon gas might come about because used argon gas was not the extra pure grade but the industrial grade.

Under the flow of argon, the graphitic component was found to form from the calcium carbide above 1000°C though its amount was as small as about 10% even at 1900°C, but it appeared at about 1900°C in the presence of calcium carbonate. In latter, the formation of calcium carbide from calcium carbonate and carbon (Eqs. 1, 2 and 3) was necessary at first and it occurred above 1700°C. Moreover the higher temperature was required for the decomposition of calcium carbide (Eq. 5).

Under the flow of nitrogen, all three possible reactions (Eqs. 4, 5 and 7) must be considered. From calcium carbide, the graphitic component was obtained above 1000°C and calcium cyanamide was identified by X-ray diffraction method above 1220°C. In this case, therefore, the main reaction to form the graphitic component is the formation of calcium cyanamide (Eq. 4). At the temperature higher than 1700°C, other two reactions (Eqs. 5 and 7) seemed to occur with the accompany

of Eq. 4, because calcium nitride was detected in the specimen above 1730°C. In the heat treatment of carbon in the presence of calcium carbonate under the flow of nitrogen, the graphitic component was observed above 1730°C, because high temperature was needed to form calcium carbide at first.

Since such an accelerating effect of nitrogen on graphitization of carbon requires the formation of calcium carbide, the possible mechanism suggested for the effect of calcium compounds on graphitization under pressure is unlikely to become unavailable below 1300°C, because no calcium carbide could be detected below 1300°C. Even above 1300°C, from the facts that no calcium cyanamide could be identified but calcium carbide and the amount of nitrogen gas is supposed to be very small in the pressure cell, it is also seemed not to be recognized that the reaction of calcium carbide with nitrogen (Eq.4) might take place above 1300°C to form the graphitic component.

From the present result, it is possible to suggest that the catalytic graphitization of carbon seems to be affected by the atmosphere in the heating system so that the experimental results thus far reported on the accelerating effect of catalysts on graphitization of carbon should be reexamined.

## 8. Mechanism of Accelerating Effect of Coexisting Minerals on Graphitization of Carbon under Pressure.

### a. Possible Processes of Graphitization of Carbon under Pressure in the Presence of Coexisting Minerals.

The graphitization of carbon was found to be remarkably accelerated by the heat treatment under pressure in the presence of coexisting minerals, such as natural limestone, calcium carbonate, calcium hydroxide, calcium oxide, sodium carbonate, alumina, silica and magnesia.

From the follow-up of the change of the composite profile of (002) diffraction line with HTT, it was found that the turbostratic component  $A_M$  transformed directly to the graphitic component  $G_M$  without going through intermediate state. The similar change of the composite profile has been reported on the carbon heat-treated under pressure without any coexisting minerals. In the graphitization of carbon in the presence of coexisting minerals, however, the mechanism of graphitization seemed to be different from the graphitization without any coexisting minerals.

Since the temperature, at which the graphitic component appeared, depended strongly upon the coexisting mineral and was much lower than that in the heat treatment of the same coke under the same pressure without coexisting mineral, chemical reactions between carbon sample and coexisting mineral had to be taken into considerations in the present study (in the heat treatment of carbon under 3.2kbar in the presence of coexisting minerals). In the presence of sodium carbonate and calcium hydroxide, the graphitization occurred even at the temperature as low as 500°C and 600°C, respectively, which was much lower than that in the heat treatment of the same carbon sample under the same pressure of 3.2kbar as well as under normal pressure. In the case of the presence of calcium carbonate, the temperature at which the graphitic component began to appear was almost the same as that in the case of limestone. Because the main species in limestone is calcium carbonate, this result shows that calcium carbonate

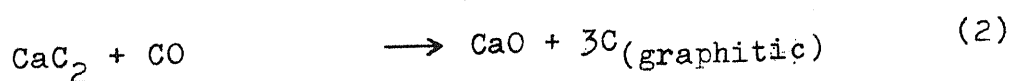
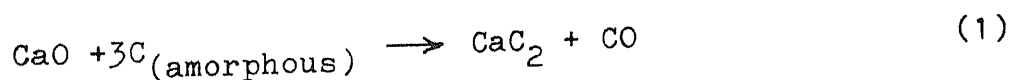
itself accelerates the graphitization of carbon.

It was also found that the accelerating effect of calcium oxide on the graphitization of carbon depended strongly upon its reactivity. In the presence of the most reactive calcium oxide used in the present study, the graphitization of carbon took place at about 1100°C which was almost the same temperature as those in the cases of limestone and calcium carbonate. While in the presence of the least reactive calcium oxide, any graphitic component could not be detected up to 1500°C.

A certain relation between content of the graphitic component and thickness of the recrystallized zone of the coexisting minerals were observed in the heat treatment of carbon in the presence of calcium carbonate, limestone and calcium hydroxide. This relation made the author imagine that the graphitization of carbon might be related to the physical phenomena, such as recrystallization or melting, of the coexisting minerals. In the case of calcium oxides, however, any recrystallization could not be observed.

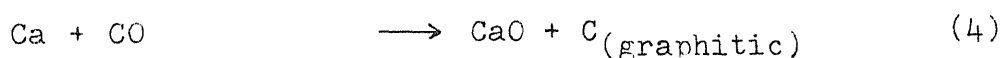
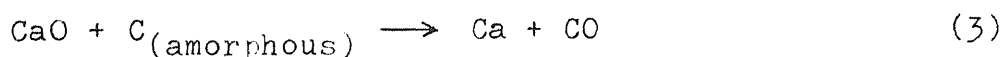
On the other hand, a small amount of free calcium oxide was identified in all cases of calcium compounds not only in the coexisting minerals but also in the carbon specimen. In addition, calcium carbide was observed in the carbon specimens heat-treated above 1300°C under 3.2kbar in the presence of calcium compounds and calcium carbide itself was found to decompose above 1200°C to form the graphitic component experimentally.

These experimental results in the presence of calcium compounds suggest that the intermediate formation and subsequent decomposition of calcium carbide seems to lead to the formation of the graphitic component. Above 1300°C, the formation of the graphitic component seems to be expressed by the following formulae;



On the other hand, there were the experimental facts that no

calcium carbide was identified in the carbon specimen heat-treated up to 1300°C under 3.2kbar in the presence of calcium compounds and that the decomposition of calcium carbide was difficult to be found after the heat treatment under 3.2kbar up to 1200°C. Therefore, it is impossible to interpret the formation of the graphitic component below 1300°C by the same mechanism as that above 1300°C. Below 1300°C, the formation of the graphitic component may proceed through the following reactions:



The formation of the graphitic component by this mechanism is also possible for the high temperature process but it may not be the major one.

It has been known by the earlier investigations<sup>84)~88)</sup> about calcium carbide that the reaction (3) begins at lower temperature than that of the reaction (1). However, it is difficult to define the exact temperatures of the beginning of these reactions because the temperature has been known to vary over a wide range with experimental conditions. The temperatures reported for the beginning of the reactions (3) and (1) spread from about 700°C to 1200°C and from 1300°C to 1900°C, respectively. The reverse reactions (4) and (2) of the reactions (3) and (1) are also well recognized to take place because both of metallic calcium and carbide are the very powerful reducing agents. It has been also known that the more reactive calcium oxide reacts with carbon easier or at lower temperature<sup>88)</sup>.

Calcium oxide distributed in the carbon specimen heat-treated must be the reaction products according to the reaction (4) or (2). If so, the content of the graphitic component should vary with the content of calcium oxide. This was verified by X-ray diffraction method and electron microprobe analysis.

The free energy of the formation of the graphitic

component through either the reaction (3) to (4) or the reaction (1) to (2) is given by the following equation;

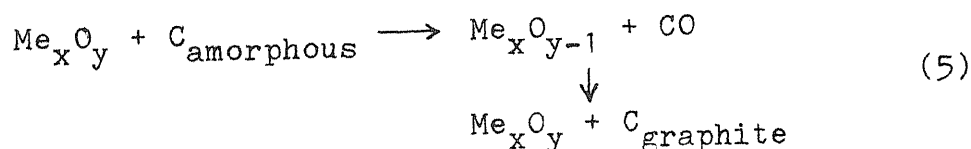
$$\begin{aligned}\Delta G &= (\Delta G_{\text{graphite}} + \Delta G_{\text{CaO}}) - (\Delta G_{\text{CaO}} + \Delta G_{\text{amorphous}}) \\ &= (\Delta G_{\text{graphite}} - \Delta G_{\text{amorphous}})\end{aligned}$$

Thus, the driving force of the graphite formation through the intermediate formation of metallic calcium or calcium carbide is considered to be the difference in the free energy between amorphous carbon and ordered graphite. Figure 75 shows the free energy diagram of amorphous carbon and graphite, presented by Fitzer and Kegel<sup>(42)</sup> for the pressure of 100atm. As known from this free energy diagram, one can recognize that the value of  $(\Delta G_{\text{graphite}} - \Delta G_{\text{amorphous}})$  is negative so that the reactions (3) to (4) and (1) to (2) surely proceed to form the graphitic component.

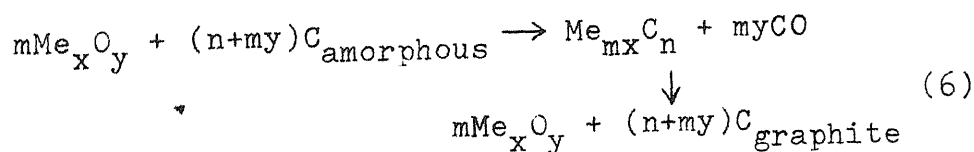
The results concerning with heat treatments of the same carbon under pressure in the presence of alumina, silica and magnesia also support these mechanisms. Especially in the case of magnesia which was known to react with carbon above 1300°C but not to form any carbide over the whole experimental temperature range, it was proved that the graphitic component could be formed through a similar reaction to Eq. (3) and (4).

In general, therefore, the following mechanisms can be proposed to the accelerating effect of coexisting oxides on graphitization of carbon under pressure;

at lower temperature by the reaction



and at higher temperature mainly by the reaction



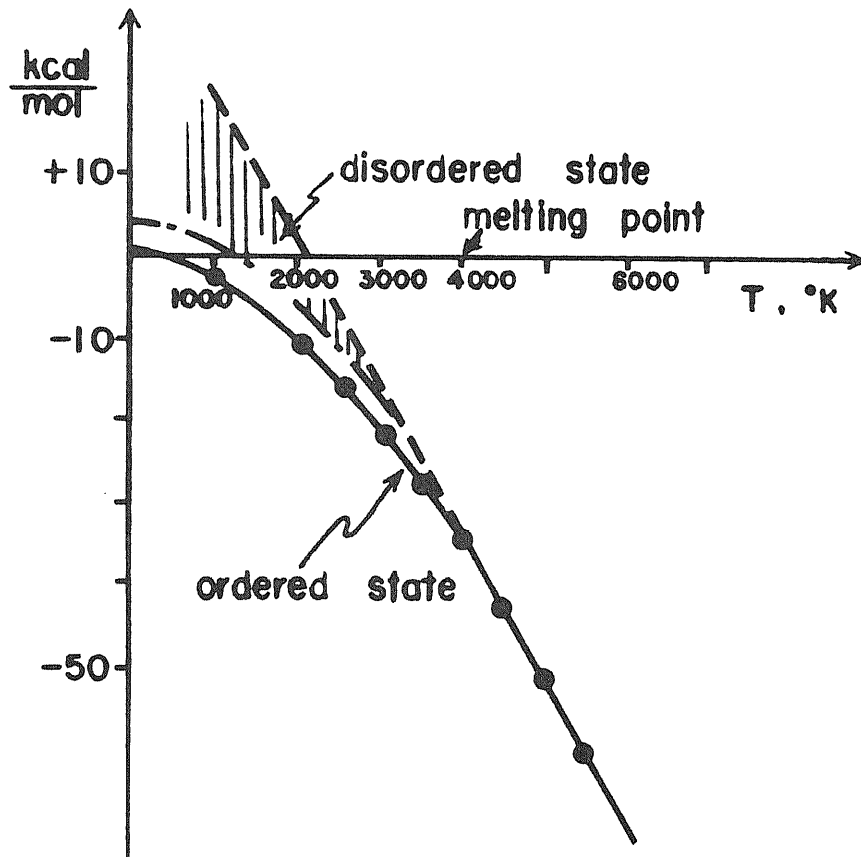


Fig.75 Free energy diagram of amorphous carbon and graphite



and by the reaction (5)

which reaction of Eqs. (5) and (6) proceeds mainly, depends upon whether or not the coexisting mineral react with carbon to form the carbide and the carbide reacts with carbon monoxide again to give the graphitic component under the experimental conditions.

b. Additional Effect of Surrounding Atmosphere on Formation of Graphitic Component.

There are principally three kinds of surrounding atmospheres to be taken into consideration in the present study.

The first is carbon dioxide caused by the decomposition of coexisting carbonate, such as limestone, calcium carbonate and sodium carbonate, and resulted from the oxidation of the carbon sample by included or absorbed oxygen. Carbon dioxide is considered to react with carbon sample according to Boudouard reaction.



Under the conditions of temperature and pressure used in the present study, the equilibrium of the reaction (7) should lean to the right hand side. In the pressure cell, therefore, most part of the surrounding atmosphere is to be carbon monoxide. Carbon monoxide is also produced by the reactions (5) and (6).

A relation between content of the graphitic component and ratio  $\text{C}^{13}/\text{C}^{12}$  of the carbon isotope in the carbon specimen heat-treated under 3.2kbar in the presence of limestone seemed to give certain informations on the effect of atmospheric carbon monoxide on graphitization of carbon. This measurements of the value of  $\delta\text{C}^{13}$  were performed by the same way as that described in Craig's paper<sup>11)</sup>. The results obtained is shown in Table 2.

Table 2. Measurement of Carbon Isotope.

Sample used	$C^{13}/O/100$	the content of the graphitic component
The original carbon sample (PV-7)	-0.66	-
Carbon specimen heat-treated at 1250°C in the presence of limestone	+1.20	34%
Carbon specimen heat-treated at 1100°C in the presence of limestone	±0.00	15%
Carbon contained as carbonate group in the limestone used	+20.14	-

where  $\delta C^{13}$  is

$$C^{13} \text{ in } \text{‰} = \frac{C^{13}/C^{12}_{\text{sample}} - C^{13}/C^{12}_{\text{standard}}}{C^{13}/C^{12}_{\text{standard}}} \times 1000$$

A negative value for  $\delta C^{13}$  means that the carbon sample is "lighter", that is, contains less  $C^{13}$  than the standard gas. Thus the values represent only the variations of relative abundance. Then the value  $x$  of  $\delta C^{13}$  for the graphitic component itself is estimated as follows;

for the carbon specimen heat-treated at 1250°C in the presence of limestone

$$0.34x + 0.66 (-0.66) = +1.20$$

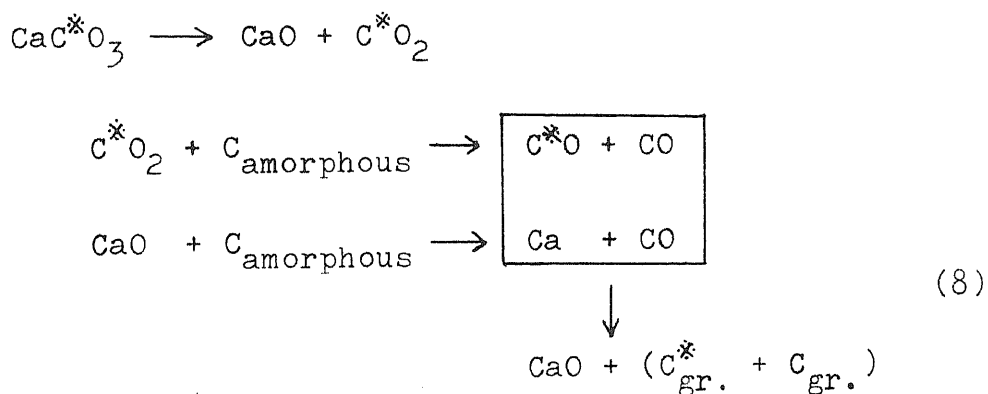
hence  $x = +4.71$  (‰),

for the carbon specimen heat-treated at 1100°C in the presence of limestone

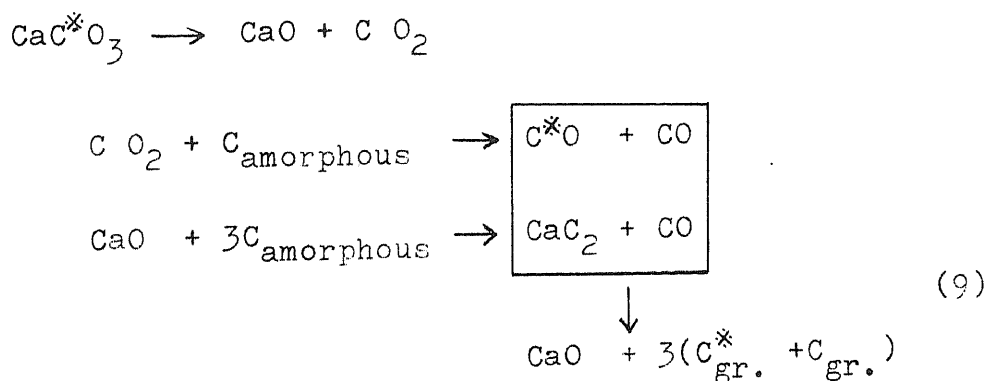
$$0.15x + 0.85 (-0.66) = \pm 0.00$$

hence  $x = +3.73$  (‰).

Thus it is assumed that the carbon specimen having a higher content of the graphitic component contains a larger amount of "heavier" carbon atoms. This assumption deduce the followings; carbon dioxide formed by the decomposition of the limestone might react with carbon sample according to the Boudouard reaction to produce carbon monoxide, and carbon monoxide thus produced might take part in the reaction between calcium oxide and carbon sample (Eqs. (1) to (4)). The proposed reactions (3) to (4) and (1) to (2) are rewritten as follows;



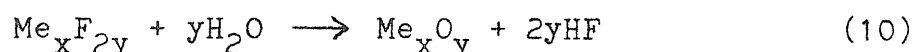
and



where  $\text{C}^*$  indicates the "heavier" carbon. The similar participation of carbon dioxide to the formation reactions of the graphitic component must be taken into consideration in the cases of other carbonates.

The second atmosphere which must be considered is water vapor caused by thermal decomposition of raw pyrophyllite

holder. In this case, water vapor seems to act on the co-existing mineral and also on the carbon sample. The typical example of the actions of water vapor on coexisting minerals is the case of the heat treatments of carbon under pressure in the presence of fluorides. In this case, fluorides reacts with water vapor to produce the corresponding oxides. Thus the mechanism of the accelerating effect of fluorides on graphitization is finally led to the same mechanism as that in the presence of the corresponding oxides.



On the other hand, the action of water vapor on the calcium carbonate (limestone) is considered to lower the dissociation temperature and consequently more reactive calcium oxide is formed.

On the action of water vapor on the carbon sample itself, it seems to be possible to say that the water-carbon reaction is unlikely to take place in the present work and consequently produce the graphitic component by the equilibrium among resultant gases, because no graphitic component could be found in the carbon specimen heat-treated up to 1500°C under 3.2kbar without any coexisting minerals when the pressure cell was constructed with raw pyrophyllite. The experiments on the effect of water vapor on graphitization of carbon were also performed by Kamiya and Inagaki<sup>89)</sup> under 5kbar. They found the accelerating effect of water vapor on graphitization in the case of heat treatments above 1500°C under 5kbar. Therefore, the effect of water vapor on the graphitization of carbon is negligible in the present study.

The third atmosphere which must be considered is nitrogen gas included when the assembly of the pressure cell is built in air. As discussed in chapter 7, the graphitic component is likely to be formed only when nitrogen reacts with carbide to form cyanamide or nitride. In the present work, however, any cyanamide and nitride could not be detected in the carbons heat-treated under pressure, because the amount of nitrogen gas included is small and traces of carbide could be observed

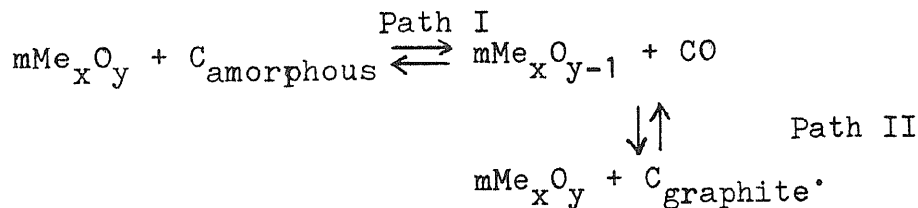
only in a few cases. Therefore the possibility that the graphitic component would be produced by the reaction of carbide with nitrogen seems to be excluded in the present study.

c. Effect of Pressure on Graphitization of Carbon in the Presence of Coexisting Minerals.

There seems to be mainly four kinds of effect of pressure on graphitization, concerning with the proposed mechanisms.

The first possible one is the change of the free energy of the reactions (5) and (6) with pressure. The change of Gibbs free energy with pressure at constant temperature is given by the integral of  $V \cdot dP$ . Thus, if there is an over-all volume change associated with a reaction, the equilibrium constant for the reaction may be shifted with pressure.

Consider the reaction (5) again,



The path I, in which gaseous product (carbon monoxide) is produced, will tend to be repressed by pressure. However, once the path I takes place, the path II may proceed simultaneously toward right hand side, because the path II leads to the decrease in over-all volume. Consequently the reaction may progress toward the right hand side to produce stable graphite. The oxide  $\text{Me}_x\text{O}_y$  reproduced by the reaction may react again with amorphous carbon. The same consideration can hold exactly in the reaction (6). Therefore the over-all free energy change with pressure should be taken into consideration as the driving force of each reaction. The change of the free energy with pressure can be given as follows;

$$\begin{aligned}
 \Delta G_T^\circ &= (\Delta G_{\text{Me}_x\text{O}_y\text{T}}^\circ + \Delta G_{\text{grT}}^\circ) - (\Delta G_{\text{Me}_x\text{O}_y\text{T}}^\circ + \Delta G_{\text{C}_{\text{amorphT}}}^\circ) \\
 &= \Delta G_{\text{grT}}^\circ - \Delta G_{\text{C}_{\text{amorphT}}}^\circ
 \end{aligned}$$

At any high pressure P,  $\Delta G_T^P$  is obtained from the following relation;

$$\left(\frac{\partial \Delta G}{\partial P}\right) = \Delta V \quad ,$$

where  $\Delta V$  is the difference in the volumes between graphite and amorphous carbon as a function of both T and P, that is,  $\Delta V = V_{gr}(P,T) - V_{amorph}(P,T)$ . Hence,

$$\Delta G_T^P = \Delta G_T^0 + \int_0^P \Delta V \cdot dP \quad .$$

In the free energy diagram Fig. 75,

$$\Delta G_T^0 < 0 \quad ,$$

and on the basis of the fact that the unit cell volume of graphite is smaller than that of amorphous carbon,

$$\Delta V = f(P,T) < 0 \quad ,$$

over the whole pressure and temperature. Therefore,

$$\Delta G_T^P < \Delta G_T^0 < 0 \quad .$$

This means that the application of pressure in the system is favourable to form the graphitic component.

Since the driving force to produce the graphitic component is the free energy difference  $\Delta G_T^P$ , it is not essential to go through the decomposition of carbide for the formation of the graphitic component. Thus only carbon monoxide and a reducing agent, such as metal or carbide, is found to be needed to form the graphitic component under pressure.

The second possible effect of pressure is the role of the enclosure of reaction products and consequently make the path II proceed easily. No graphitic component could be detected under an electron microscope in the carbon specimen heat-treated up to 1500°C in the flow of nitrogen in the

presence of magnesia, in spite of the occurrence of reaction between carbon and magnesia. In the case of the heat treatments under 3.2kbar, however, the graphitic particles were found in the carbon specimen heat-treated at 1400°C. These experimental facts seem to suggest the important role of enclosure of the reaction products in order to form the graphitic component. The similar reaction of  $Mg + CO \rightarrow MgO + C$  was also reported by Komarek et al.<sup>11)</sup>, and they could not get the graphitic component under normal pressure but amorphous carbon. This fact seems to demonstrate that some proper gas pressure of carbon monoxide is required to proceed the path II and to produce the graphitic component.

The third possible effect of pressure is the enhancement of the contact surface area of reactants. The path I in the reactions (5) and (6) is the solid-solid reaction between carbon sample and coexisting mineral. In such a reaction, the rate of the reaction depends greatly on the contact surface area between reactants. Therefore the pressure is expected to enhance the contact surface area and consequently increase the rate of the path I. For instance, Mukaibo and Yamanaka<sup>10)</sup> found that the higher the pressure for the moulding of lime and carbon was, the higher the rate of the reaction (3) became.

The fourth possible effect of pressure is the presence of the shearing stress in the carbon specimen. Generally speaking, shearing stress is known to increase the rate of solid-solid reaction. In the present study, pressure on the carbon sample is transmitted by solid medium of pyrophyllite in a simple piston-cylinder type pressure vessel so that the pressure is not hydrostatic but quasi-hydrostatic. Since liquidous metal and carbon monoxide gas are formed in the system, the deviation from the hydrostatic pressure may be reduced to certain extent. However, the effect of shearing stress on graphitization of carbon must be taken into consideration, but is not yet understood in detail. The further experiments should be carried out to evaluate of the effect of shearing stress on graphitization of carbon by using hydrothermal or hydrostatic pressure devices.

## 9. Summary.

The accelerating effect of coexisting minerals on graphitization of carbon under pressure was investigated in the present study.

Heat treatments of carbon in the presence of coexisting minerals were performed under 3.2kbar with a simple piston-cylinder type pressure vessel. The carbon sample used was the polyvinylchloride coke carbonized to 680°C and had a particle size in the range of 0.1 - 0.4mm. The carbon sample was sandwiched between two disks of coexisting minerals.

In the heat treatments under pressure, the real pressure on the small carbon specimen should be measured at first by using the same arrangement of the pressure cell as that in the heat treatment of carbon. The pressure in a simple piston-cylinder type vessel used was calibrated by means of a new method developed in the present study, which concerns with detecting volume change associated with polymorphic transformation of the standard specimen as the change of inductance of high frequency coil wound on the standard specimen. The flow of pressure transmitter of pyrophyllite during compression was also studied by the same method. Standard specimens used were  $\text{KNO}_3$  and  $\text{AgI}$ , which are known to have the transformation at a pressure of 3.6 and 3.0kbar at room temperature, respectively. The results obtained are summarized as follows: (1) The transformation points of the standard specimens were measured with good accuracy and reproducibility in spite of a small volume of specimen, about 8.7% of the total volume of pressure cell. (2) Loss of pressure in the present high pressure apparatus and the arrangement of pressure cell was as small as about 3%. This seemed to be caused from the reduction of friction between pistons and cylinder by using Myler and asbestos composite paper, and from the pressure multiplication by the steel disk used. (3) At the moment when pressure was reached 3kbar, the flow of pyrophyllite was found to be completed. At 1kbar, however,



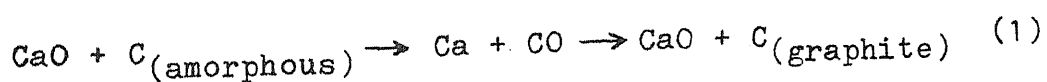
it required about 5min to complete the flow of pyrophyllite. The flow of pyrophyllite was greatly affected by the arrangement of pressure cell. The present method is expected to be used for detecting the transformation associated with the change in dielectric constant or magnetic susceptibility.

The X-ray diffraction profiles of the heat-treated carbon specimens were measured by using Ni-filtered  $\text{CuK}\alpha$  radiation. The observed diffraction intensity was corrected for the factors, such as Lorentz-polarization, atomic scattering and absorption factors, by a conventional method. The composite profiles of (002) and (004) diffraction lines were observed on some carbon specimens and were concluded to consist of two component profiles, one corresponding to the graphitic component  $G_M$  and the other to the turbostratic component  $A_M$ . The composite profiles observed were separated graphically into two component profiles. The content of the graphitic component  $G_M$  was obtained from the ratio of the area under the profile of the component  $G_M$  to the total area of the composite profile, after the correction for the preferred orientation of crystallites in the specimen used for the X-ray measurement. (chapter 2.)

In the presence of natural limestone and calcium carbonate, the graphitization of the carbon took place at about  $1050^\circ\text{C}$  under 3.2kbar and proceeded gradually with the increase in heat treatment temperature. In the presence of calcium hydroxide, the particles having the same diffraction pattern of six-fold symmetry as graphite single crystal were found, besides the particles having continuous diffraction ring for the turbostratic structure, under electron microscope in the carbon specimen heat-treated even at  $600^\circ\text{C}$  and the diffraction profile due to the graphitic component was observed in the carbon specimen heat-treated above  $800^\circ\text{C}$ . Under the same pressure and in the similar arrangement of pressure cell without any coexisting minerals, however, no graphitic component was found to occur up to  $1500^\circ\text{C}$ . Therefore, these low-temperature graphitization of the carbon was assumed to be attributed to the coexistence of calcium compounds. Phenomenally, a close relation seemed to present between the

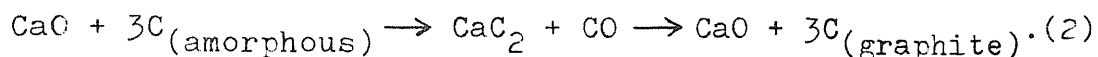
graphitization of carbon under pressure and the recrystallization of the coexisting calcium compounds. In these cases, however, a small amount of free calcium oxide was found in the heat-treated carbon specimen and this seemed to suggest a chemical theory of acceleration of graphitization. (chapter 3)

In order to study the effect of the reactivity of calcium oxide on the graphitization of carbon under 3.2kbar, the carbon sample was heat-treated under 3.2kbar in the presence of three kinds of calcium oxide which had different reactivities. The difference in the accelerating effect of these calcium oxides on graphitization of carbon was found to be remarkable. In the presence of the most reactive calcium oxide calcined at 920°C, the graphitization of the carbon began at almost the same temperature of 1100°C as in the cases of limestone and calcium carbonate, and the content of the graphitic component turned out to 100% at 1500°C for 60min. In this case, calcium carbide was detected in the specimen heat-treated above 1300°C. While in the presence of the least reactive calcium oxide calcined at 1470°C, any graphitic component, even hump on the profile of (002) diffraction line at the corresponding diffraction angle, could not be found in the specimens heat-treated up to 1500°C. The distributions of the graphitic component and calcium in the heat-treated carbon specimens were measured by X-ray diffraction method and an electron microprobe analyzer, respectively. It was found that a part having a larger content of calcium had a larger content of the graphitic component. The possible mechanisms of the accelerating effect of calcium compounds on the graphitization of carbon were considered to be chemical ones concerning with intermediate formation of metallic calcium and carbide. The formation of the graphitic component was suggested to proceed by the reactions;



below 1300°C

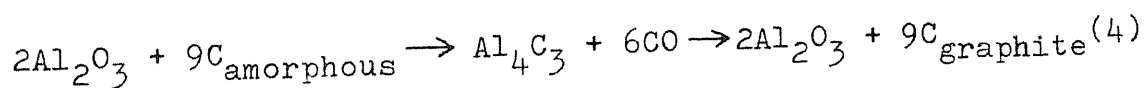
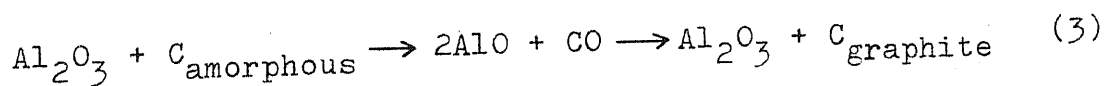
and, above 1300°C, mainly by the reactions;



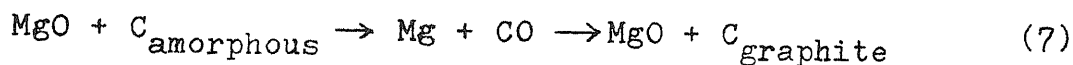
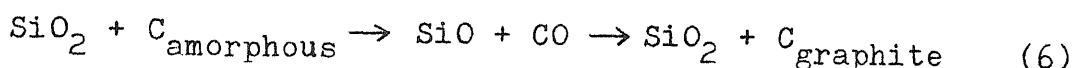
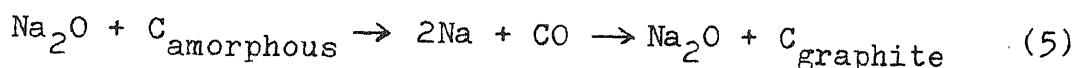
(chapter 4)

The same heat treatments were carried out in the presence of sodium carbonate, alumina, silica and magnesia so as to verify the mechanisms suggested. In the case of the presence of sodium carbonate which decomposes at the temperature of 600°C to form reactive sodium oxide, the particles having the graphitic structure were found in the specimen heat-treated at the temperature as low as 500°C. In the case of alumina, the graphitization took place above 1200°C and traces of aluminum carbide could be detected in the alumina disk at the part in contact with the carbon specimen heat-treated at 1500°C. In the case of silica, the graphitic component began to appear in the carbon specimen heat-treated at 1300°C, any carbide could not be identified. In the case of magnesia, though the reaction between the carbon sample and coexisting magnesia was found to occur above 1300°C, no graphitic component could be formed in the heat treatments of carbon in the flow of nitrogen. On the other hand, the particles having the graphitic structure were observed, besides the particles having the turbostratic structure in the carbon specimens heat-treated above 1400°C.

These experimental results were explained by the similar reactions to Eq. (1) and (2) as follows; the formation of the graphitic component in the presence of alumina proceeded through the similar process as that in the presence of calcium compounds,



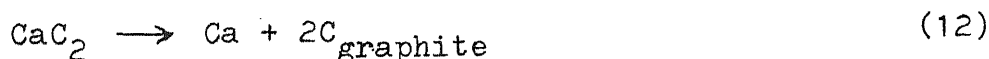
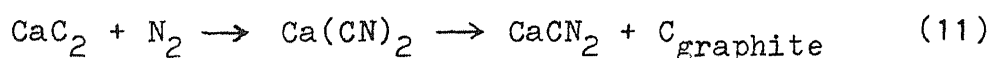
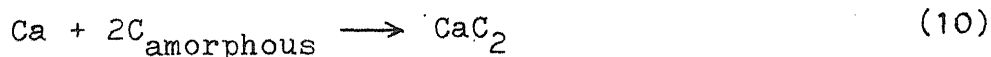
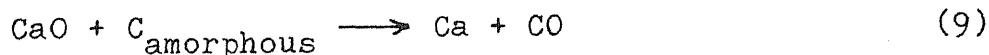
and in the presence of sodium carbonate, silica and magnesia, the graphitic component seemed to be formed through one of reactions,

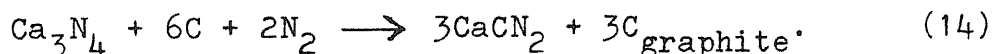


(chapter 5)

In the presence of calcium and magnesium fluorides, their accelerating effects on graphitization under pressure was considered to be attributed to the corresponding oxide produced by the reaction between fluorides and water vapor, which was resulted from decomposition of raw pyrophyllite used as pressure transmitter. On the other hand, water absorbed in calcium carbonate is known to depress its dissociation temperature and subsequently to make reactive calcium oxide at low temperature. In the present work, the graphitic component began to appear in the carbon specimen, heat-treated under 3.2kbar in the presence of calcium carbonate contained water, at 1000°C, 100°C lower than that in the case of dry calcium carbonate. (chapter 6)

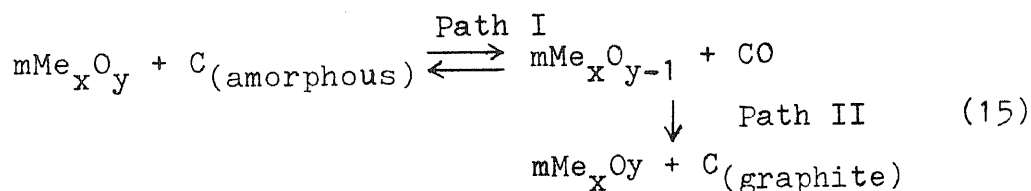
Nitrogen was also recognized to have a remarkable accelerating effect on graphitization of carbon in the presence of coexisting minerals. In the presence of calcium carbonate under the flow of nitrogen at one atmospheric pressure, the graphitic component began to appear at around 1700°C, about 200°C lower than under the flow of argon. This effect of nitrogen on graphitization of carbon in the presence of calcium carbonate was explained by the following reactions;



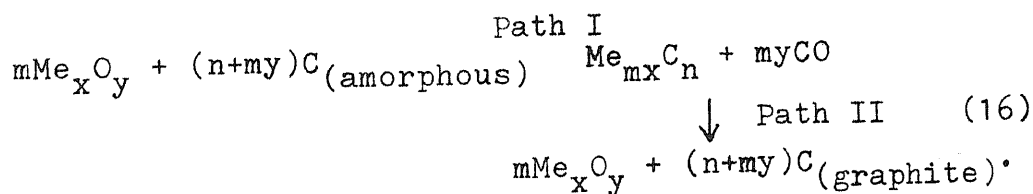


So, the graphitic component was formed through the formation of calcium cyanamide, the decomposition of calcium carbide, and the reaction among calcium nitride, carbon and nitrogen. However, it was possible to say that, because the amount of nitrogen was very small in the pressure cell and from the fact that any calcium cyanamide and nitride could not be detected in the specimens, this effect of nitrogen was hardly accepted as the mechanism for the formation of the graphitic component under pressure. (chapter 7)

On the basis of these experimental results, the possible mechanisms for the formation of the graphitic component under pressure at low temperature in the presence of coexisting minerals were discussed. The process for the formation of the graphitic component could be separated into two kinds of reactions depending upon whether or not carbide could be formed at the temperature under consideration, that is, at lower temperature



and at higher temperature



The reaction (15) seems to be also possible to take place at higher temperature.

The driving force of the formation of the graphitic component through the intermediate formation of reduced oxide

or carbide was considered to be the difference in the free energy between amorphous carbon and graphite. In these cases, pressure was assumed to increase the driving force, to act as a function of enclosure of the reaction products in the reaction system, and to increase the rate of path I of the solid-solid reaction due to the enhancement of the contact surface area between the coexisting mineral and the carbon sample. However, since pressure has also opposite effect, that is, to make the equilibrium of the path I lean to left hand side, one should determine the proper pressure under taking into account of these factors.

In the present study, sintered tablets of the carbon sample having the bulk density of  $1.6 - 1.7\text{g/cm}^3$  were obtained by the heat treatments under 3.2kbar at the temperature as low as around  $1000^\circ\text{C}$ . The graphitization was also taken place at low temperature which could not be expected in the case of heat treatments without any coexisting minerals under pressure as well as under normal pressure. Especially in the case of calcium fluoride, a good quality of sintered tablet was obtained by heat treatment of the carbon sample at  $1000^\circ\text{C}$  under 3.2kbar and the graphitization of carbon was completed at about  $1500^\circ\text{C}$ . Thus, it is expected from the results obtained in the present study that the carbon sample is possible to be sintered and also well-graphitized at extremely low temperature by the heat treatment of carbon under pressure in the presence of a proper coexisting mineral.

The results of the present study are also believed to give the substantial laboratory data for the formation mechanism of natural graphite, for example, in the beds of limestone and fluorite.

## References.

- 1) J. Bischoe and B.E. Warren; J. Appl. Phys., 13 364 (1942)
- 2) C.R. Houska and B.E. Warren; J. Appl. Phys., 25 1503 (1954)
- 3) R.E. Franklin; Acta Cryst., 4 253 (1951)
- 4) M. Mazza; J. Chim. Phys., 61 721 (1964)
- 5) M. Mazza, H. Gasparoux and J. Amell; J. Chim. Phys., 61 726 (1964)
- 6) M. Inagaki; Tanso No. 53, 61 (1968)
- 7) R.E. Franklin; Proc. Roy. Soc.(London) A209 196 (1951)
- 8) S. Mrozowski; Phys. Rev., 85 609 (1952)
- 9) S.B. Seeley; "Encyclopedia of Chemical Technology", John Wiley & Sons, Inc. Vol. 4, P.319 (1964)
- 10) Dana; System of Mineralogy, 1 152
- 11) H. Craig; Geochimica et Cosmochimica Acta, 3 53 (1953)
- 12) P.E. Rosenberg; Am. J. Sci., 261 683 (1963)
- 13) B.M. French and P.E. Rosenberg; Science, 147 1283 (1965)  
B.M. French and H.P. Eugster; Geol. Soc. Am. Spec. Papers, 73 155 (1962)
- 14) P.J. Wyllie and O.F. Tuttle; Nature; 183 770 (1959)
- 15) P.J. Wyllie and O.F. Tuttle; Am. Min., 44 453 (1959)
- 16) P.J. Wyllie and O.F. Tuttle; J. Petr., 1 1 (1960)
- 17) D.C. Gellatly; Min. Mag., 35 963 (1966)
- 18) A.A. Giardini, C.A. Salotti and J.F. Lakner; Science 159 317 (1968)
- 19) R.F. Müller and K.C. Condie; J. Geology, 70 400 (1964)
- 20) H. Ishikawa; Denki Hyoron, 19 493, 613, 690, 726, 824, 888 (1931)
- 21) H. Ishikawa; Denki Hyoron, 19 419 (1931)
- 22) L.M. Foster, G Long and H.C. Stumpf; Am. Min., 43 285 (1958)
- 23) T. Noda and M. Tanaka; Kogyo Kagaku Zasshi, 65 1329 (1962)
- 24) K. Taoka, M. Inagaki and T. Noda; private communication
- 25) T. Ishikawa, S. Kagi, Y. Mizutani and S. Yoshizawa; Tanso, No. 41, 8 (1965), No. 42, 7 (1965)
- 26) I. Yamada; Symposium on Carbon, Tokyo III-22 (1964)  
Tanso, No. 41, 18 (1965)
- 27) T. Sasaki and I. Komori; Kogyo Kagaku Zasshi, 63 37 (1960)
- 28) T. Ishii; Denki Kagaku Zasshi, 35 688 (1967)

- 29) D.V. Badami; Carbon, 3 53 (1965)
- 30) A.S. Schwartz and J.C. Bokros; Carbon, 5 325 (1967)
- 31) S.M. Irving and P.L. Walker, Jr.; Carbon, 5 399 (1967)
- 32) Y. Uchishima and S. Makishima; Kogyo Kagaku Zasshi, 71 86 (1968)
- 33) P.L. Walker, Jr., J.F. Rakszawski and G.R. Imperial; J. Phys. Chem., 63 133 (1959)
- 34) J.J. Trillat and S. Oketani; Comptes. Rend., 230 2203 (1950)
- 35) J.J. Trillat and S. Oketani; ibid 233 51 (1951)
- 36) B. Chatterjee and P.P. Das; Nature 173 1046 (1954)
- 37) G.A. Basset, J.W. Menter and D.W. Pashley; Proc. Roy. Soc., A246 345 (1958)
- 38) S.D. Robertson; Nature, 221 1044 (1969)
- 39) A.E.B. Presland and P.L. Walker, Jr.; Carbon 7 1 (1969)
- 40) T. Noda, Y. Sumiyoshi and N. Ito; Carbon 6 813 (1968)
- 41) H. Yoshida, M. Koyama and S. Matsuo; private communication
- 42) E. Fitzer and B. Kegel; Carbon, 6 433 (1968)
- 43) S.B. Austerman, S.M. Myron and J.W. Wagner; Carbon 5 549 (1967)
- 44) H.M. Strong and R.E. Hanneman; J. Chem. Phys., 46 3669 (1967)
- 45) A.C. Titus; Proc. of the Fourth Conference on Carbon, p.706, Pergamon Press, Oxford (1960)
- 46) B.J. Curtis; Carbon 4 483 (1966)
- 47) W.V. Kotlensky; Carbon, 5 409 (1967)
- 48) C.E. Lowell; J. Am. Chem. Soc., 50 142 (1967)
- 49) C. Yokogawa, K. Hosokawa and Y. Takegami; Carbon, 4 459 (1966)
- 50) J.J. Kipling, P.V. Shooter and R.N. Young; Carbon, 4 333 (1966)
- 51) T. Noda; J. Chim Phys. (n<sup>o</sup> special) p.151 (1969)
- 52) M.L. Pearce and E.A. Heintz; J. Phys. Chem., 70 1935 (1966)
- 53) A.W. Moore, A.R. Ubbelohde and D.A. Young; Proc. Roy. Soc., A280 153 (1964)
- 54) T. Noda and H. Kato; Carbon 3 289 (1965)
- 55) T. Noda, K. Kamiya and M. Inagaki; Bull. Chem. Soc. Japan, 41 485 (1968)
- 56) K. Kamiya; Thesis (March, 1969)



- 57) SKH-4A JIS G4403
- 58) R.H. Wentorf, Jr.; "Modern Very High Pressure Techniques", Butterworth, London p.18 (1962)
- 59) R.H. Wentorf, Jr.; *ibid* p.18
- 60) P.W. Montgomery; *Rev. Sci. Instr.*, 37 1526 (1966)
- 61) P.W. Bridgman; *Proc. Am. Acad. Arts Sci.*, 76 1 (1945)
- 62) L. Guengant et B. Voder; *C. R.* 239 431 (1959)
- 63) H.P. Klug and L.E. Alexandar; "X-ray Diffraction Procedures" John Willey, New York p.246 (1954)
- 64) D.T. Keating and B.E. Warren; *Rev. Sci. Instr.*, 23 519 (1952)
- 65) W.R. Ruston; *Fuel*, 32 53 (1953)
- 66) "Shigen Kobutsu Handbook" Asakura Shoten Co., p.339 (1965)
- 67) H.C. Fischer; *J. Am. Ceram. Soc.*, 38 245, 284 (1955)
- 68) Y. Ohno and T. Matsuoka; *Yogyo Kyokai Shi*, 59 284, 341 (1951)
- 69) T. Noda; *Kogyo Kagaku Zasshi*, 40 195, 196 (1937)
- 70) E.W. Guernsey and M.S. Sherman; *J. Am. Chem. Soc.*, 48 140 (1926)
- 71) K.L. Komarek, A. Coucoulas and N. Klenger; *J. Electrochem. Soc.*, 110 783 (1963)
- 72) L.M. Foster, G. Long and M.S. Hunter; *J. Am. Ceram. Soc.*, 39 1 (1956)
- 73) C.H. Prescott and W.B. Hincke; *J. Am. Chem. Soc.*, 49 2753 (1929)
- 74) W.A. Chupka; *J. Phys. Chem.*, 62 611 (1958)
- 75) V.R. Juza, A. Völling and H.U. Schuster; *Z. anor. all. chem.*, 352 89 (1967)
- 76) J.H. Swisher; *Trans. TMS-AIME*, 242 2033 (1968)
- 77) W.H.C. Rueggeberg; *J. Am. Chem. Soc.*, 65 602 (1943)
- 78) F.D. Richardson; *J. Iron and Steel Inst.*, Sept.1953 33 (1953)
- 79) E. Schlegel; *Ber. Dtsch. Keram. Ges.*, 45 520 (1968)
- 80) D.R. Messier; *J. Electrochem. Soc.*, 115 397 (1968)
- 81) D.M. Kerrick; *Am. J. Sci.*, 266 204 (1968)
- 82) D.R. Messier; *J. Am. Ceram. Soc.*, 48 452 (1965)
- 83) M. Inagaki, Y. Murase and T. Noda; *Tanso*, No.54, 80 (1968)

- 84) N. Kameyama and Y. Uraguchi; Kogyo Kagaku Zasshi, 45 1147  
(1943), 47 860 (1945), 48 57 (1946)
- 85) Briner and Kuhne; C.R., 156 621 (1913); J. Chim. Phys.,  
12 439 (1914)
- 86) Krase and Yee; J. Am. Chem. Soc., 46 1360 (1924)
- 87) N. Kameyama, Y. Ohta and Y. Inoue; Kogyo Kagaku Zasshi,  
44 929, 933 (1941)
- 88) Y. Mukaibo and Y. Yamanaka; Kogyo Kagaku Zasshi, 56 73,  
232 (1953)
- 89) K. Kamiya and M. Inagaki; private communication
- 90) T. Mukaibo and Y. Yamanaka; Kogyo Kagaku Zasshi, 56 313  
(1953)

The Papers published by the Author

- |  | places in<br>this thesis |
|--|--------------------------|
| 1) Detection of Pressure-Induced Transformations<br>by measuring the Change of Inductance<br>J. Ceram. Assoc. Japan, <u>76</u> 264 (1968)<br>M. Inagaki, S. Hirano and H. Saito          | chapter 2.               |
| 2) Heat Treatments of Carbon under 3kbar in the<br>Presence of Limestone<br>Bull. Chem. Soc. Japan, <u>41</u> 1245 (1968)<br>T. Noda, M. Inagaki, S. Hirano and<br>K. Amanuma            | chapter 3.               |
| 3) Accelerating Effect of Calcium Carbonate on<br>Graphitization of Carbon under Pressure<br>Kogyo Kagaku Zasshi, <u>72</u> 643 (1969)<br>T. Noda, M. Inagaki, S. Hirano and<br>H. Saito | chapter 3.               |
| 4) Accelerating Effect of Calcium Hydroxide<br>Bull. Chem. Soc. Japan, <u>42</u> 1738 (1969)<br>T. Noda, M. Inagaki, S. Hirano and<br>H. Saito   | chapter 3.               |
| 5) Accelerating Effect of Calcium Oxide<br>(submitted to Bull. Chem. Soc. Japan)<br>S. Hirano, H. Saito and M. Inagaki   | chapter 4.               |
| 6) Distribution of Calcium and Graphitic<br>Component in the Heat-Treated Specimens<br>(submitted to Bull. Chem. Soc. Japan)<br>S. Hirano, H. Saito and M. Inagaki                       | chapter 4.               |
| 7) Accelerating Effect of Some Oxides on<br>Graphitization<br>presented at 9th Biennial Conference<br>on Carbon, Boston (1969)<br>S. Hirano, H. Saito and M. Inagaki                     | chapter 5.               |

8) Accelerating Effect of Fluorides on  
Graphitization

chapter 6.

presented at 8th Biennial Conference on  
Carbon, Cleveland (1967)

S. Hirano, H. Saito and M. Inagaki